Aus dem Institut für Medizinische Genetik und Humangenetik
der Medizinischen Fakultät Charité – Universitätsmedizin Berlin

DISSERTATION

Identifizierung und Charakterisierung genetischer Ursachen von Skelettdysplasien

zur Erlangung des akademischen Grades
Doctor medicinae (Dr. med.)

Der Medizinischen Fakultät
Charité – Universitätsmedizin Berlin vorgelegt

von

Sevjidmaa Baasanjav
aus der Mongolei, Selenge Aimag

Datum der Promotion: 22.06.2014

Inhaltsverzeichnis

1. Zusammenfassung

1.1 Abstrakt

Identifizierung und Charakterisierung genetischer Ursachen von Skelettdysplasien

Einleitung: Die vorliegende Arbeit befasst sich mit der Suche nach krankheitsverursachenden Genen für verschiedene Skelettdysplasien und Bindegewebserkrankungen. Dabei stellen sich gerade die Skelettdysplasien als ausgesprochen heterogenes Krankheitsbild dar, an deren vielfältiger Ausprägung eine große Anzahl von Genen beteiligt ist, welche sich wiederum in unterschiedlichen Stoffwechselwegen auswirken. In dieser Arbeit wurden fünf Familien mit verschiedenen Skelettdysplasien untersucht.

Methodik: In einer Familie mit Skelettdysplasie (Familie 1) unbekannter genetischer Ursache wurde eine genomweite Kopplungsanalyse durchgeführt. Für die Einengung der Krankheitsregion wurden weitere Familienglieder einbezogen und zusätzliche Mikrosatellitenmarker typisiert. Innerhalb der resultierenden Region wurden positionelle und funktionelle Kandidatengene sequenziert. Für funktionelle Nachweise der Mutation wurden Expressionsanalysen an verschieden Mausgeweben (Leber, Knochen, Haut, Herz, Aorta, Osteoklast und Osteoblast) durchgeführt. Danach wurden Lokalisation und Enzymaktivität in Fibroblasten von Patienten und gesunden Kontrollen durch die Immunfluoreszenzmarkierung bestimmt.

Für Familien mit Skelettdysplasie (Familien 2-5) und eindeutiger klinischer Verdachtsdiagnose wurden die krankheitsrelevanten Gene (*EXT1, LEMD3* und *LBR*) sequenziert.

Ergebnisse: In Familie 1 konnte eine homozygote Mutation (c.830G>A, p.R277Q) im *B3GAT3*-Gen bei 5 Indexpatienten mit der Ausbildung eines komplexen Phäno-

typs mit Gelenkdislokationen und kongenitalem Herzdefekt in Verbindung gebracht werden. *B3GAT3* kodiert eine beta-1,3-glucuronyltransferase 3, welche Glykosaminoglykane mit spezifischen Proteinen bei der Biosynthese von Proteoglykanen verknüpft.

Desweiteren konnte im Exostosin-1 (*EXT1*) Gen eine bis dahin nicht in der Literatur beschriebene splice-site Mutation identifiziert werden, die in einer Familie (Familie 2) mit Osteopoikilosis und Exostose für die Ausprägung einer multiplen Exostose verantwortlich ist. *EXT1*, welches als Glycosyltransferase in der Heparansulfat-Biosynthese für eine Kettenverlängerung sorgt, ist ebenfalls in die Proteoglykansynthese involviert.

Neben diesen Mutationen wurden Mutationen in der Sterolreduktase-Domäne des *LBR*-Gens (Lamin B Rezeptor) identifiziert, welche gewöhnlich Zellkernfunktionsstörungen verursachen. Hier wird der Cholesterinstoffwechsel gestört, was mit einer weiteren Skelettdysplasie (Familien 3-5), der letalen Form der Greenberg-Dysplasie, einhergeht.

Schlussfolgerung: Mutationen in Genen der Proteoglykan-Synthese oder des Cholesterinstoffwechsels können nach unseren Daten Skelettdysplasien verursachen.

Identification and characterization of genetic causes of skeletal dysplasias

Introduction: The current work attends to the search for disease-causing genes of several skeletal dysplasias and connective tissue diseases. At this, the skeletal dysplasias show themselves as an entirely heterogeneous syndrome. Many genes, which have an impact on different metabolic pathways, are involved in its diverse form. In this work five families with different skeletal dysplasias were examined.

Methods: A genome-wide linkage analysis was performed in a family (family 1) with a skeletal dysplasias of unknown cause. More family members were integrated and additional microsatellite markers were used to narrow the disease region.

Within the resulting region, positional and functional candidate genes were sequenced. For functional proofs of the mutation, expressional analyses were performed in different mice tissues (liver, bones, skin, heart, aorta, osteoclast and osteoblast). Afterwards the localization and enzyme activity in fibroblasts of patients were determined by the immunofluorescence staining.

The disease relevant candidate genes *EXT1, LEMD3* and *LBR* were sequenced in the families (families 2-5) with skeletal dysplasias and a clinical suspected diagnosis.

Results: In five index patients of the first family, a homozygous mutation (c.830G>A, p.R277Q) in the *B3GAT3* gene was associated with the development of a complex phenotype with joint dislocations and congenital heart defect. The *B3GAT3* encodes a beta-1,3-glucoronyltranferase, which links glycosaminoglycans with specific proteins at the biosynthesis of proteoglycans.
In addition, a previously not described splice-site mutation was identified in the Exostosin-1 gene (*EXT1*). This mutation is responsible for the development of a mul-

tiple exostosis in a family, which is affected by osteopoikilosis and exostosis (family 2). The *EXT1*, which causes a chain extension as a glycosyltransferase in the heparansulfate biosynthesis, is also involved in the proteoglycansynthesis.

Furthermore mutations in the sterol reductase domain of the *LBR* gene (Lamin B receptor), which usually cause dysfunctions of the nucleus, were identified. In this case, another form of a skeletal dysplasia, the lethal form of the Greenberg-dysplasia, results from the disturbance of the cholesterine metabolism.

Conclusion: By reference to our results, mutations in genes of the proteoglycan-synthesis or in the cholesterine metabolism can cause skeletal dysplasias.

1.2 Einführung

Prinzipiell lässt sich der Prozess der Skelettentwicklung beim Menschen in drei Phasen unterteilen: Die Musterbildung, durch die die grundlegende Gestalt und die Zahl der einzelnen Elemente festgelegt wird, die Organogenese und die Wachstumsphase. Genetisch bedingte Störungen der Musterbildung führen zu Dysostosen, bei denen nur einzelne Elemente betroffen sind und der Prozess mit der Geburt abgeschlossen ist. Genetische Defekte, die die Organogenese oder die Wachstumsphase betreffen, resultieren in Dysplasien, die auch nach der Geburt noch Veränderungen unterliegen. Sie betreffen das Knorpel- und / oder das Knochengewebe, so dass generell das gesamte Skelett betroffen ist und regelmäßig Minderwuchs damit einhergeht. Grundsätzlich können in der Organogenese nach Anlage der zukünftigen Knochen zwei verschiedene Differenzierungsmechanismen unterschieden werden: Die enchondrale Ossifikation, bei der die knorpelige Anlage anschließend verknöchert wird und die desmale Ossifikation, bei der Knochen direkt aus den Vorläuferzellen entstehen [1, 2].

Zur Ausprägung einer Dysplasie kommt es hauptsächlich durch Störungen der Homöostase vom Knochenaufbau bzw. –abbau. Dabei kann sowohl ein Überschuss an Knochen (Osteopetrose) oder ein Mangel an Knochen auftreten (Osteoporose). Insgesamt sind viele Gene an der Bildung, dem Wachstum und der Homöostase des Skeletts beteiligt. Die klinische Manifestation der jeweiligen Gendefekte reicht von milden Symptomen bis hin zu intrauteriner Letalität [3].

In der Mehrzahl der Skelettdysplasien, insbesondere der monogen bedingten, handelt es sich um eher seltene Krankheiten. In der „Nosology and Classification of Genetic Skeletal Disorders“ aus dem Jahr 2010 wurden 456 Erkrankungen erfasst, die nach der Abgrenzung anhand biochemischer und / oder radiologischer Kriterien in 40 Gruppen unterteilt sind. Ursächlich konnten bislang für insgesamt 316 dieser Krankheiten Mutationen in einem oder mehreren von 226 Genen ge-

funden werden [4]. Aber auch bei dieser Einteilung ergeben sich eine Reihe von Überlappungen bezüglich der phänotypischen Ausprägung. Umgekehrt können aber auch Mutationen im gleichen Gen zu verschiedenen Krankheiten führen, die mitunter sogar einen unterschiedlichen Erbgang aufweisen. Ein Beispiel dafür ist das Larsen-Syndrom (MIM 150250), das durch spezielle Gesichtsmerkmale und multiple Gelenkdislokationen charakterisiert ist. Typische Gesichtsmerkmale des Larsen-Syndroms sind ein flacher Nasenrücken und Hypertelorismus in Verbindung mit Gaumen- und Lippenspalten. Häufig sind noch andere Bereiche des Bindegewebes betroffen. Es können Klumpfuß, Kyphoskoliose, zylindrische Finger und Kleinwuchs auftreten. Die klinische Ausprägung ist dabei durchaus variabel und geht mit Mutationen in zwei unterschiedlichen Genen einher. Zum einen betreffen diese Veränderungen das Filamin-B-Gen (*FLNB*), eines von 3 Aktin bindenen Filamin Proteinen, welche bei der Kommunikation zwischen Zellmembran und Zytoskelett eine bedeutende Rolle spielen. Diese Mutationen manifestieren sich autosomal-dominant [5]. Demgegenüber folgen Mutationen im *CHST3*-Gen (Chondroitin-6-sulfotransferase), einem autosomal rezessiven Erbgang und sind für die Ausprägung der Spondyloepiphysealen Dysplasie, Typ Omani (rezessive Form des Larsen-Syndroms), verantwortlich [6]. Bei dieser Form betrifft die Störung die Biosynthese von Chondroitin- und Heparansulfat.

Grundlage für die vorliegende Arbeit waren betroffene Patienten bzw. Feten aus 5 Familien, die alle Skelettdysplasien unterschiedlicher Ausprägung aufwiesen. Ziel war die Identifizierung der zugrunde liegenden Krankheitsgene. In vier Fällen konnten anhand der klinischen Verdachtsdiagnose in bereits bekannten Krankheitsgenen die Mutationen gefunden werden. In einem Fall wurde mittels genomweiter Kopplungsanalyse die Kandidatengenregion bestimmt. Daran schloss sich ein Mutationsscreening der relevanten Kandidatengene an. Dies führte zur Identifizierung eines neuen Krankheitsgens, wobei die pathogenetische Relevanz der Mutation durch einen funktionellen Assay überprüft wurde.

Abschließend sollte für alle identifizierten Mutationen eine Genotyp-Phänotyp Korrelation erstellt werden, um Hinweise auf einen Bezug zwischen der jeweiligen Mutation und dem klinischen Schweregrad der Erkrankung zu erhalten.

1.3 Methoden

1.3.1 Analyse von Mikrosatelliten-Markern

Mikrosatelliten-Marker sind hochpolymorphe DNA-Abschnitte, die aus hintereinander angeordneten, repetitiven Sequenzmotiven bestehen. Die einzelnen Allele unterscheiden sich in der Anzahl der Motivwiederholungen und werden nach den Mendelschen Regeln vererbt. Zur Genotypisierung von Mikrosatelliten-Markern (Short Tandem repeats, STR) wurden die gewählten DNA-Bereiche mittels PCR unter der Verwendung eines mit FAM- oder HEX-Fluorophoren markierten Primer amplifiziert. Anschließend erfolgte die elektrophoretische Auftrennung der amplifizierten Fragmente, die Detektion der Fluoreszenzdaten und die Datenauswertung auf einem ABI 3730 DNA Sequencer (Applied Biosystems, Life Technologies, Carlsbad, USA).

1.3.2 DNA-Sequenzierung

Die genomische DNA wurde aus EDTA-Blut entsprechend dem Protokoll des QIAamp DNA Blood Mini Kit (Qiagen, Hilden, Deutschland) isoliert. Die Exonbereiche der Kandidatengene wurden unter der Verwendung spezifischer Primer (s. Publikationen) mittels PCR amplifiziert und anschließend mit der Shrimp Alkaline Phosphatase (Affymetrix, Santa Clara, USA) enzymatisch gereinigt. Die Sequenzreaktion nach der Sanger-Methode wurde entsprechend dem Protokoll des BigDye^{tm} Terminator v3.0 Cycle Sequencing Kits (Applied Biosystems, Life Technologies, Carlsbad, USA) durchgeführt. Die Analyse der Sequenzierung erfolgte auf einem ABI 3730 Sequenzer. Abschließend wurden die erhaltenen Sequenzen mit Hilfe der Software SeqPilot und Seqman auf vorhandene Polymorphismen untersucht und ausgewertet.

1.3.3 Quantitative PCR (qPCR)

Für die quantitative Analyse der Genexpression wurde die gesamte RNA aus verschiedenen Geweben und Zelllinien isoliert. Dazu wurden die Zellen nach der Homogenisierung mit Trizol® aufgeschlossen und mittels Phenol/Chloroform-Extraktion die RNA isoliert. Danach wurde die RNA unter der Verwendung von RevertAidTM H Minus First Strand cDNA Synthesis Kit (Fermentas, Thermo Fisher Scientific, Hampton, USA) in cDNA transkribiert. Die qPCR wurde mittels genspezifischer Primer auf dem ABI Prism 7500 Thermocycler (Applied Biosystems, Life Technologies, Carlsbad, USA) unter der Verwendung von CyberGreen (Invitrogen, Life Technologies, Carlsbad, USA) durchgeführt. Die Auswertung erfolgte nach der ΔΔCt (CT=crossing time) Methode der relativen Quantifizierung als relative Expression, normalisiert gegen *GAPDH* als Referenzgen unter Verwendung des ABI Prism SDS Software-Pakets.

1.3.4 Immunfluoreszenz

Nach Kultivierung wurden die jeweiligen Zellen in PBS-Lösung gewaschen und in 4% Paraformaldehyd für 10 min bei 4°C fixiert. Zur Permeabilisierung wurden die Zellen für 10 min bei 4°C inkubiert (1x PBS, 3% BSA, 0,4% Triton-X-100). Der spezifische Proteinnachweis erfolgte mit polyklonalen Antikörpern (Maus-anti-B3GAT3, H00026229-B01P, Abnova, Taipei City, Taiwan). Zum Nachweis einer Co-Lokalisation mit Golgi-Proteinen wurden Schaf-anti-GM130, Kaninchen-Anti-Giantin (Covance, Princeton, USA) und Schaf-Anti-TGN46 (Serotec, Bio-Rad Laboratories, Hercules, USA) verwendet. Für den Fluoreszenznachweis wurde als Sekundärantikörper Anti-Maus IgG Alexa Fluor 555 (Invitrogen, Life Technologies, Carlsbad, USA) und ein „anti-sheep/rabbit IgG Alexa Fluor 488“ (Invitrogen, Life Technologies, Carlsbad, USA) genutzt. Die DNA wurde mit DAPI gegengefärbt, bevor die Zellen mit Fluoromount (Science Services, München, Deutschland) ein-

gedeckelt wurden. Die abschließende Dokumentation erfolgte mit einem LSM 510 META (Carl Zeiss, Göttingen, Deutschland) unter Verwendung eines Plan Apochromat Ölimmersionsobjektiv (x63).

1.4 Ergebnisse

1.4.1 Publikation 1: Mutation im *B3GAT3*-Gen verursacht Herz- und Gelenkdefekte

Die fünf betroffenen Kinder konsanguiner Eltern (Familie 1) wiesen multiple Gelenkdislokationen, Kleinwuchs und angeborene Herzfehler mit bikuspiden Aortenklappen auf. Die Verdachtsdiagnose betraf die rezessive Form des Larsen-Syndroms, Typ CHST3 (Abb. 1). Allerdings wich das klinische Bild in einigen Punkten davon ab, so dass zunächst eine genomweite Kopplungsanalyse durchgeführt wurde. Dadurch konnte die Kandidatengenregion mit einem signifikanten LOD score von 3,89 auf Chromosom 11q11-11q13 lokalisiert werden. Im Rahmen meiner Arbeit habe ich die Region durch Einbeziehung weiterer Familienangehöriger und zusätzlicher genetischer Marker auf einen Bereich von 7,3 cM zwischen den Markern D11S4191 und M11SB019 eingegrenzt.
Aus den ca. 360 Genen dieser Region habe ich 30 Kandidatengene ausgewählt und jeweils komplett sequenziert. Auf diese Weise gelang es, eine homozygote missense Mutation c.830G>A (p.Arg277Gln) im *B3GAT3*-Gen zu identifizieren. Diese Mutation betrifft eine evolutionär hoch konservierte Aminosäure in einer Substratbindungsstelle, was für eine funktionelle Relevanz spricht.

Durch Immunofluoreszenz konnte die Lokalisierung des Proteins im Golgi-Apparat bestätigt werden. Zudem konnten wir zeigen, dass durch die Mutation die Enzymaktivität dieser Glukuronyltransferase stark vermindert ist. Dementsprechend waren verschiedene Proteoglykane in Fibroblasten dieser Patienten deutlich vermindert.

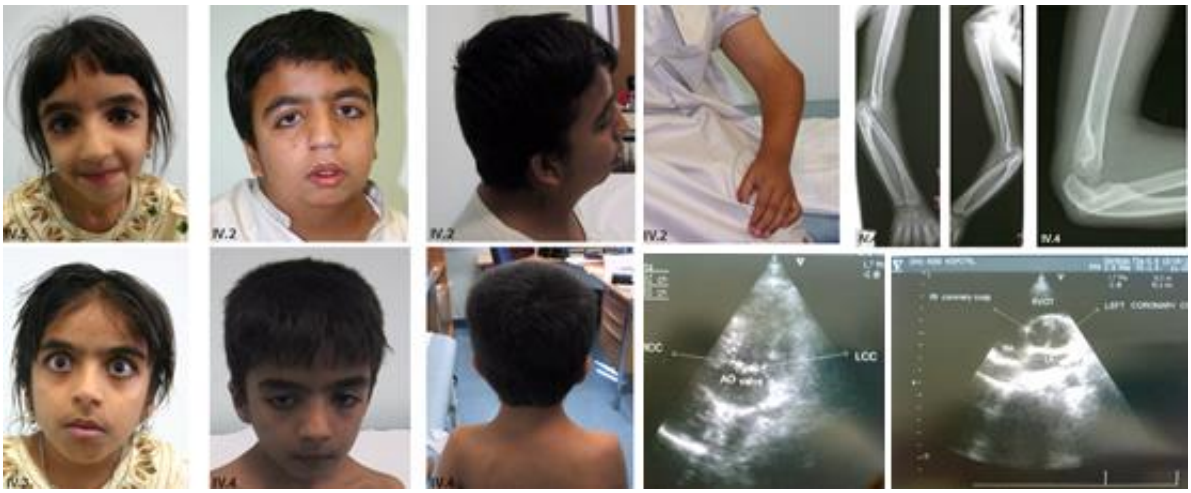

Abb. 1: Klinischer Phänotyp mit charakteristischem Gesicht (flaches Gesicht, flache Nase, Hypertelorismus, Gaumenspalte, Exophthalmus, kleiner Mund und kleine Mandibula), bilaterale Gelenkdislokationen der Ellenbogen und bikuspide Aortenklappen.

1.4.2 Publikation 2: Osteopoikilose und multiple Exostosen werden durch neue Mutationen in den *LEMD3* und *EXT1* Genen verursacht

In einer Familie mit Osteopoikilose (Familie 2) konnten radiologisch unregelmäßige, runde bis ovale Verdichtungszonen in der Spongiosa der Hand- und Fußknochen, im epiphysären Teil der langen Knochen, im Becken und im Kreuzbein der Betroffenen nachgewiesen werden (Abb. 2). Da als Hauptursache dieser klinischen Entität heterozygote Mutationen im *LEMD3*-Gen vorliegen, habe ich die kodierenden Bereiche des *LEMD3*-Gens sequenziert und auf diese Weise eine neue nonsense Mutation c.2203C>T (p.Arg735X) im Exon 9 identifiziert. Codon 735 kodiert gewöhnlich Arginin und wird nun zum vorzeitigen Stoppcodon.

Abweichend von dem klinischen Bild wurden bei einem Patienten der Familie zusätzlich multiple Exostosen vom Typ 1 diagnostiziert, so dass ich bei diesem Patienten zusätzlich eine Sequenzanalyse des dafür verantwortlichen Gens *EXT1* durchgeführt habe (Abb. 3). Ich wies eine bisher noch nicht beschriebene splice si-

te-Mutation im Intron 5 nach (c.1285-2A>G). Dies führt zu einer in frame-Deletion von 9 Basenpaaren, was drei evolutionär konservierte Aminosäuren betrifft. Im weiteren Verlauf der Arbeit konnten noch bei 3 von fünf an Osteopoikilose erkrankten Familienmitgliedern eine Basensubstitution G>A im *EXT1*-Gen auf der cDNA Position 1732 im Exon 9 (p.Ala578Thr) nachgewiesen werden. Die Konservierung der betroffenen Aminosäure ließ eine mögliche funktionelle Relevanz vermuten, allerdings wiesen diese Betroffenen neben der Osteopoikilose keine weiteren klinischen Auffälligkeiten auf. Da *LEMD3* ein Kernmembran Protein ist, führt die *LEMD3*-Mutation möglicherweise zu einer erhöhen Rate an Neumutationen.

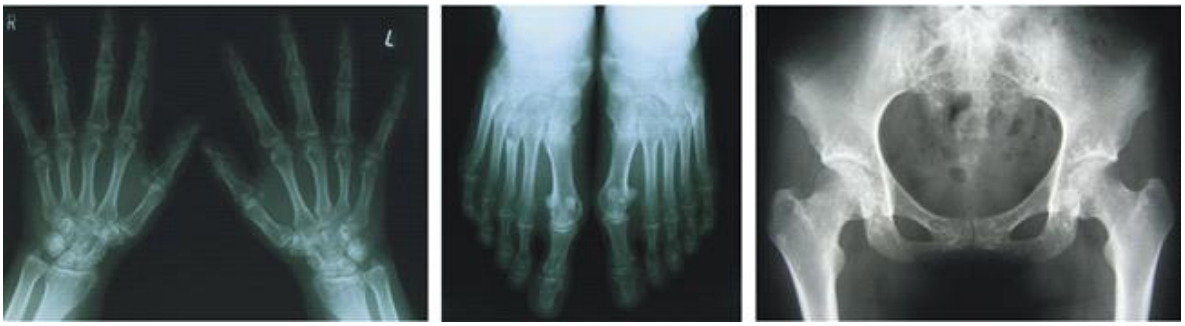

Abb. 2: Sklerotische Veränderungen in den Händen, Füßen und dem Becken der Osteopoikilose betroffenen Patienten mit der Mutation c.2203C>T (p.R735X) im Exon 9 des *LEMD3*-Gens. Hyperostotische Spots wurden in den Handwurzelknochen, Mittelhandknochen, sowie in dem Becken identifiziert.

Abb. 3: Das Röntgen Bild der rechten Hand des Probanden mit der Mutation c.1285-2A>G im Intron des *EXT1*-Gens, im Alter von 5 Jahren. Multiple Exostose im proximalen Teil des Oberarmknochens sowie das proximale und distale Ende der Ulna und der Radius sind mit Pfeilen gekennzeichnet.

1.4.3 Publikation 3: Mutationen des *LBR*-Gens, die ausschließlich die Sterolreduktasefunktion der Kernmembran, aber nicht die Kernfunktion beeinflussen

In dieser Arbeit untersuchten wir drei Feten (Familien 3-5), die alle die klinischen Kriterien der Greenberg-Dysplasie wie intrauterine Wachstumsretardierung, massive generalisierte Ödeme (Hydrops), extreme Verkürzungen der Röhrenknochen, ektopische Verkalkungen und einen schmalen Brustkorb aufwiesen. Für einen der Feten lagen Sterol-Analysen im Muskelgewebe vor, welche abnorme Sterol-Metaboliten 5α-Cholest-8,1-dien-3β-ol zeigten, die laut Literatur mit der Greenberg-Dysplasie assoziiert sind.

Da diese Greenberg-Dysplasie mit Mutationen im *LBR*-Gen assoziiert ist, wurden die Exons des Gens bei allen drei Feten sowie den jeweiligen Familien komplett sequenziert. Die Sequenzanalysen zeigten bei Fetus A eine homozygote Frameshift-Mutation c.1492delT (p.Y468TfsX475), Fetus B wies dagegen zwei verschiedene Mutationen, eine Deletion c.32delTGGT (p.V11EfsX24) sowie eine Basensubstitution c.1748G>A (p.Arg583Gln) auf. Die Deletion von 4 Basenpaaren verursacht eine Frameshift Mutation mit einem anschließenden vorzeitigen Stoppcodon nach weiteren 24 Codons (p.V11EfsX24). Die zweite Mutation c.1748G>A ist eine missense Mutation und führt zum Austausch von Arginin durch Glutamin an Position 583 (p.Arg583Gln). Beim dritten Fetus C konnte eine homozygote missense Mutation c.1639A>G (p.Asn547Asp) nachgewiesen werden. Diese Mutationen befinden sich in der Sterolreduktase-Domäne an einer evolutionär konservierten Aminosäure der Gensequenz. In folgenden Exprimenten konnten wir in Kooperation auch deren funktionelle Relevanz in Bezug auf die Sterolstruktur nachweisen.

1.5 Diskussion

Die in der vorliegenden Arbeit untersuchten Familien wiesen alle bisher klinisch und molekulargenetisch nicht aufgeklärte Skelettveränderungen auf. Aufgrund von molekulargenetischen und immunhistochemischen Untersuchungen konnten in allen Familien Mutationen identifiziert werden, die ursächlich an der Ausbildung der jeweiligen Phänotypen beteiligt sind (Tab. 1).

Familie	**1**	**2**	**3**	**4**	**5**
Erkrankung	Larsen like Syndrome, Typ B3GAT3	Osteopoikilose und Exostose	Greenberg-Dysplasie	Greenberg-Dysplasie	Greenberg-Dysplasie
Mutation	1. c.830G>A, p.R277Q im *B3GAT3*-Gen	1. c.2203C>T, p.R735X im *LEMD3*-Gen 2. c.1285-2A>G, im *EXT1*-Gen 3. c.1732G>A, p.A578T im *EXT1*-Gen	1. c.1492delT, p.Y468TfsX475 im *LBR*-Gen	1. c.32delTGGT , p.V11EfsX24 im *LBR*-Gen 2. c.1748G>A, p.R583Q im *LBR*-Gen	1. c.1639A>G, p.N547D im *LBR*-Gen
Publikation	1	2	3	3	3
Ergebnisteil	1.4.1	1.4.2	1.4.3	1.4.3	1.4.3

Tabelle 1. Übersicht der untersuchten Familien.

Darunter befand sich eine Familie (Familie 1) mit autosomal-rezessiver Vererbung, verschiedenen Skelettanomalien (Kleinwuchs, multiple Gelenkdislokationen) und variabler Mittelgesichtshypoplasie sowie Manifestationen am Herz und an der Aorta. Aufgrund dieses Krankheitsbildes, insbesondere multiplen Gelenkdislokationen, breiten Fingerspitzen und Hallux valgus, kam unter anderem das klassische Larsen-Syndrom (LRS [MIM150250]) als Diagnose in Frage, welches allerdings autosomal-dominant durch Mutationen des *FLNB*-Gens (MIM 603381) verursacht wird und auch leicht unterschiedliche Gesichtsmerkmale aufweist, wobei das Knochenalter eher verzögert als fortgeschritten ist [5]. Auch die autosomal rezessive Form des Larsen-Syndroms, Typ CHST3, weist ein abweichendes phänotypisches Spektrum auf, welches sich über humerospinale Dysostose, Chondrodysplasie,

multiple Dislokationen bis hin zur Spondylo-epiphysäre Dysplasie, Typ Omani, erstreckt [6]. Aus diesem Grund wurde eine genomweite Kopplungsanalyse durchgeführt, um weitere krankheitsassoziierte Loci einzugrenzen. Als Ergebnis konnte eine Mutation im *B3GAT3*-Gen, welche für eine Glucuronyltransferase (GlcAT-I) kodiert, identifiziert werden.

GlcAT-I ist ein Enzym mit Dimer-Struktur aus zwei Subdomänen und spezifischer Donor- und Acceptorspezifität [7]. Die hier identifizierte Mutation c.830G>A (p.Arg277Gln) liegt an einer Aminosäureposition, die von Ouzzine et al. mittels in-vitro-Mutagenese (Arg277Ala) untersucht wurde. Dabei wurde gezeigt, dass die Substratspezifität von GlcAT-I durch genau diese Aminosäure Arg277 definiert wird, die somit essentiell für die Funktion von GlcAT-I zu sein scheint [8]. Dies wird in unserer Familie bestätigt, da auch hier die missense Mutation p.Arg277Gln die GlcAT-I-Aktivität deutlich reduziert wird (in Kooperation durchgeführte Analysen in einem rekombinanten Zellsystem sowie in Patienten-Fibroblasten). Dabei zeigen die Fibroblasten der Patienten in vitro immer noch eine basale Restaktivität. Weiterhin wird durch die Reduktion der GlcAT-I-Aktivität die Synthese der Proteoglykane der extrazellulären Matrix verändert. Wir konnten zeigen, dass die Menge bestimmter Proteoglykane (Chondroitinsulfat und Heparansulfat) in Zellen mit der Mutation c.830G>A (p.Arg277Gln) deutlich reduziert ist. Die durchgeführte Immunhistochemie ergab, dass GlcAT-I im cis und cis-medialen Golgi-Apparat lokalisiert ist. Diese Lokalisation passt zur katalytischen Funktion von GlcAT-I bei der Glykolysierung, die im Golgi-Apparat stattfindet. Die Mutation führt zu einem Defekt in der Synthese der Tetrasaccharid-Linker-Region in der Proteoglykansynthese. Somit sind die bei den betroffenen Patienten auftretenden Symptome wie Gelenkdislokationen, kongenitale Herzdefekte und Kleinwuchs wahrscheinlich auf diese spezifische Störung der Proteoglykansynthese, speziell von Glukosaminoglykanen (GAG) zurückzuführen. Insbesondere ist auch auf die bei allen untersuchten Patienten vorliegenden angeborenen multiplen Herzfehler hinzuweisen (Mitralklappen-

prolaps, bikuspide Aortenklappe mit Aortenwurzelerweiterung, Ventrikelseptumdefekt und Vorhofseptumdefekt).

Unter den angeborenen Herzfehlern ist die bikuspide Aortenklappe mit einer Häufigkeit von 1-2% bei Neugeborenen die am häufigsten auftretende Fehlbildung [9]. Bikuspide Aortenklappen haben ein deutlich erhöhtes Risiko von lebensbedrohlichen Spätkomplikationen wie Aortenwurzelerweiterung, Aortendissektion und Stenose oder Insuffizienz der Aortenklappe. Mittlerweile sind eine ganze Reihe von Genen bekannt, die für die Ausbildung von Herzfehlern verantwortlich gemacht werden [9]. Allerdings ist unter denen mit *NOTCH1* (Neurogenic locus notch homolog protein 1, [MIM 190198]), bisher nur ein Gen, bei dem Mutationen mit bikuspiden Aortenklappen assoziiert sind [10]. In meiner Arbeit wurde mit *B3GAT3 (*beta-1,3-glucuronyltransferase 3, [MIM 606374]) ein weiteres Gen identifiziert, welches mit bikuspiden Aortenklappen assoziiert ist. Unsere Ergebnisse bestätigen, dass Mutationen in der Proteoglykansynthese Bindegewebserkrankungen und angeborene Herzdefekte wie bikuspide Aortenklappen verursachen. Das jetzt auch molekulargenetische charakterisierte Syndrom wurde als autosomal rezessives „Larsen Like Syndrom Typ B3GAT3“ benannt.

Bei einer weiteren Familie mit fünf Betroffenen (Familie 2) wurde klinisch der Verdacht auf eine Melorheostosis [MIM 155950] gestellt. Der Indexpatient wies jedoch zusätzlich multiple progressive Deformationen auf. Radiologisch wurde bei diesem Patienten ein Multiples Exostose-Syndrom festgestellt [MIM 133700]. Diese klinische Diagnose wurde anschließend durch die Sequenzanalyse des *EXT1*-Gens und die Identifikation einer bisher unbeschriebenen Splice-Site-Mutation (c.1285-2 A>G) bestätigt. Aufgrund dieses Befundes wurde das *EXT1*-Gen bei dem Rest der Familie ebenfalls sequenziert. Dabei zeigten drei der von Osteopoikilose betroffenen Patienten einen zusätzlichen Aminosäureaustausch (p.Ala578Thr) im *EXT1*-Gen. Das veränderte *EXT1*-Gen beeinflusst die Kettenverlängerung von Heparansulfat in der Proteoglykansynthese. Dies zeigt noch einmal deutlich, welche zentra-

le Rolle Proteoglykane als Bestandteile der extrazellulären Matrix sowohl bei der Signalfunktion der Zelle als auch bei der Gewebestabilisierung spielen.

Neben den Mutationen im *EXT1*-Gen wiesen wir bei den anderen Betroffenen (Familie 2, V.a. Melorheostosis) auch eine bisher nicht beschriebene, heterozygote Veränderung (p.Arg735Stop) im Exon 9 des *LEMD3*-Gens auf. Damit wurde bei den anderen Betroffenen molekulargenetisch eine Osteopoikilose bestätigt [MIM 166700]. Allerdings ist bisher unklar, wie Mutationen im *LEMD3*-Gen zur Bildung dieser Art von Knochenläsionen führen. In einem „knock-out" Mausmodell für *LEMD3* ist die homozygote Inaktivierung intrauterin letal, die heterozygoten Mäuse waren phänotypisch unauffällig und wiesen keine Knochenläsionen auf, die typisch für Osteopoikilose sind [11]. Somit konnten in dieser Familie mit komplexen Skelettveränderungen erstmalig Mutationen im *LEMD3*-Gen zusammen mit Mutationen in einem anderen Gen *EXT1* beschrieben werden. Ob die Funktion von *LEMD3* als Kernmembran Protein möglicherweise die Neumutationsrate erhöht und damit eventuell das Auftreten der de-novo *EXT1*-Mutation beim Indexpatienten beeinflusst hat, bleibt in weiteren Untersuchungen abzuklären.

In der dritten Arbeit wurden bei drei schweren Skelettveränderungen mit V.a. Greenberg-Dysplasie [MIM 215140] betroffenen Feten (Familien 3-5) sowohl Missense- als auch Nonsense-Mutationen im *LBR*-Gen identifiziert. Beide Missense-Mutationen betreffen dabei eine der beiden funktionellen Gruppen der Transmembrandomäne von *LBR.* Sie verändert evolutionär konservierte Aminosäuren der Sterolreduktase-Domäne. Funktionell konnte in Kooperation über ein Hefe-Rescue-Experiment die durch die Mutation veränderte Sterolreduktaseaktivität nachgewiesen werden. Der N-terminale Abschnitt von *LBR*, der etwa 200 Aminosäuren umfasst und mit Chromatin und anderen Kernkomponenten interagiert, wird durch diese missense Veränderungen nicht beeinflusst [12, 13]. Entsprechend unverändert waren auch die Kernform und Chromatinstruktur bei heterozygoten Trägern der missense Mutationen. Die Kombination von einem Enzymdefekt bei der

rezessiv vererbten Greenberg-Dysplasie und einer strukturellen Kernveränderung bei der dominanten Pelger-Anomalie in demselben Genprodukt ist unserem Wissen nach einzigartig.

1.6 Literatur

1. Mundlos S. Entwicklung und Wachstum des Skeletts – biologische Grundlagen. Medgen 2004;16:5-8.

2. Uwe Kornak, Stefan Mundlos. Genetic Disorders of the Skeleton: A Development Approach. Am J Hum Genet 2003; 73:447-474.

3. Superti-Furga A. Growing bone knowledge. Clin Genet 66 2004; 399-401.

4. Warman ML, Cormier-Daire V, Hall C, Krakow D, Lachman R, LeMerrer M, Mortier G, Mundlos S, Nishimura G, Rimoin DL, Robertson S, Savarirayan R, Sillence D, Spranger J, Unger S, Zabel B, Superti-Furga A. Nosology and Classification of Genetic skeletal Disorders: 2010 Revision. Am J Med Genet. Part A. 2011; 155:943-968.

5. Krakow D, Robertson SP, King LM, Morgan T, Sebald ET, Bertolotto C, Wachsmann-Hogiu S, Acuna D, Shapiro SS, Takafuta T, Aftimos S, Kim CA, Firth H, Steiner CE, Cormier-Daire V, Superti-Furga A, Bonafe L, Graham JM Jr, Grix A, Bacino CA, Allanson J, Bialer MG, Lachman RS, Rimoin DL, Cohn DH. Mutations in the gene encoding filamin B disrupt vertebral segmentation, joint formation and skeletogenesis. Nat Genet 36. 2004; 405 – 410.

6. Hermanns P, Unger S, Rossi A, Perez-Aytes A, Cortina H, Bonafe L, Boccone L, SetzuV, Dutoit M, Sangiorgi L, Pecora F, Reicherter K, Nishimura G, Spranger J, Zabel B, Superti-Furga A Congenital joint dislocations caused by carbohydrate sulfotransferase 3 deficiency in recessive Larsen syndrome and humero-spinal dysostosis. Am J Hum Genet 2008; 82:1368-1374.

7. Pedersen, L.C., Tsuchida, K., Kitagawa, H., Sugahara, K., Darden, T.A., and Negishi, M. Heparan/chondroitin sulfate biosynthesis. Structure and mechanism of human glucuronyltransferase I. J Biol Chem 2000; 275:34580-34585.

8. Ouzzine, M., Gulberti, S., Levoin, N., Netter, P., Magdalou, J., and Fournel-Gigleux, S. The donor substrate specificity of the human beta 1,3-glucuronosyltransferase I toward UDP-glucuronic acid is determined by two crucial histidine and arginine residues. J Biol Chem 2002; 277:25439–25445.

9. Bruneau, B.G. The developmental genetics of congenital heart disease. Nature 2008; 451(7181):p.943-948.

10. Garg, V., Muth, A.N., Ransom, J.F., Schluterman, M.K., Barnes, R., King, I.N.,Grossfeld, P.D., and Srivastava, D. Mutations in *NOTCH1* causeaorticvalvedisease. Nature 2005; 437:270–274.

11. Dheedene A, Deleye S, Hellemans J, Staelens S, Vandenberghe S. The Heterozygous Lemd3+/GT Mouse Is Not a Murine Model for Osteopoikilosis in Humans. Calcif Tissue Int 2009; 85(6):546-51.

12. Waterham HR, Koster J, Mooyer P, NoortGv G, Kelley RI, Wilcox WR, et al. Autosomal recessive HEM/Greenberg skeletal dysplasia is caused by 3 beta-hydroxysterol delta 14-reductase deficiency due to mutations in the lamin B receptor gene. Am J Hum Genet 2003; 72:1013-7.

13. Holmer L, Pezhman A, Worman HJ. The human lamin B receptor/sterol reductase multigene family. Genomics 1998; 54:469-76.

2. Anteilserklärung / Eidesstattliche Versicherung

2.1 Anteilserklärung

Sevjidmaa Baasanjav hatte folgenden Anteil an den folgenden Publikationen:

Publikation 1:

***Autoren*:** Sevjidmaa Baasanjav, Lihadh Al-Gazali, Taishi Hashiguchi, Shuji Mizumoto, Bjoern Fischer, Denise Horn, Dominik Seelow, Bassam R. Ali, Samir A.A. Aziz, Ruth Langer, Ahmed A.H. Saleh, Christian Becker, Gudrun Nürnberg, Vincent Cantagrel, Joseph G. Gleeson, Delphine Gomez, Jean-Baptiste Michel, Sigmar Stricker, Tom H. Lindner, Peter Nürnberg, Kazuyuki Sugahara, Stefan Mundlos, Katrin Hoffmann

***Titel*:** Faulty initiation of proteoglycan synthesis causes cardiac and joint defect

***Zeitschrift*:** Am J Hum Genet 89: 15-27, 2011 (Impact Factor: 11,680)

***Beitrag*:** Durchführung der Feinkartierung, Sequenzierung der Kandidatengene und der Analyse der Sequenzdaten. Auswertungen von Immunfluoreszenz, Westernblot und quantitativer PCR.

Publikation 2:

Autoren: Sevjidmaa Baasanjav, Aleksander Jamsheer, Mateusz Kolanczyk, Denise Horn, Tomasz Latos, Katrin Hoffmann, Anna Latos-Bielenska, Stefan Mundlos

***Titel*:** Osteopoikilosis and multiple exostoses caused by novel mutations in *LEMD3* and *EXT1* genes respectively-coincidence within one family.

Zeitschrift: BMC Med Genet 11: 110, 2010 (Impact Factor: 2,44)

Beitrag: Durchführung der Sequenzierung von *LEMD3* und der Exostose-Gene, Analyse der Sequenzdaten; cDNA-Synthese und cDNA-Sequenzierung. Erstellung wesentlicher Teile des Manuskripts (Tabellen und Abbildungen, Methoden und Ergebnisse)

Publikation 3:

Autoren: Peter Clayton, Björn Fischer, Anuska Mann, Sahar Mansour, Eva Rossier, Markus Veen, Christine Lang, Sevjidmaa Baasanjav, Moritz Kieslich, Katja Brossuleit, Sophia Gravemann, Nele Schnipper, Mohsen Karbasyian, Ilja Demuth, Monika Zwerger, Amparo Vaya, Gerd Utermann, Stefan Mundlos, Sigmar Stricker, Karl Sperling and Katrin Hoffmann

Titel: Mutations causing Greenberg dysplasia but not Pelger anomaly uncouple enzymatic from structural functions of a nuclear membrane protein.

Zeitschrift: Nucleus 1: 354-366, 2010 (Impact Factor: 6,643)

Beitrag: Durchführung der Sequenzierung des *LBR*-Gens, Analyse der Sequenzdaten und quantitative PCR.

Prof. Dr. med. S. Mundlos betreuender Hochschullehrer	Prof. Dr. med. K. Hoffmann betreuende Hochschullehrerin	S.Baasanjav Doktorandin

2.2 Eidesstattliche Versicherung

„Ich, Sevjidmaa Baasanjav, versichere an Eides statt durch meine eigenhändige Unterschrift, dass ich die vorgelegte Dissertation mit dem Thema: „Identifizierung und Charakterisierung genetischer Ursachen von Syndromen mit Skelettdysplasien und Herzdefekten“ selbständig und ohne nicht offengelegte Hilfe Dritter verfasst und keine anderen als die angegebenen Quellen und Hilfsmittel genutzt habe.

Alle Stellen, die wörtlich oder dem Sinne nach auf Publikationen oder Vorträgen anderer Autoren beruhen, sind als solche in korrekter Zitierung (siehe „Uniform Requirements for Manuscripts (URM)“ des ICMJE -*www.**icmje**.org*) kenntlich gemacht. Die Abschnitte zur Methodik (insbesondere praktische Arbeiten, Laborbestimmungen, statistische Aufarbeitung) und Resultaten (insbesondere Abbildungen, Graphiken und Tabellen) entsprechen den URM (s.o) und werden von mir verantwortet.

Meine Anteile an den ausgewählten Publikationen entsprechen denen, die in der untenstehenden gemeinsamen Erklärung mit der Betreuerin, angegeben sind. Sämtliche Publikationen, die aus dieser Dissertation hervorgegangen sind und bei denen ich Autor bin, entsprechen den URM (s.o) und werden von mir verantwortet.

Die Bedeutung dieser eidesstattlichen Versicherung und die strafrechtlichen Folgen einer unwahren eidesstattlichen Versicherung (§156,161 des Strafgesetzbuches) sind mir bekannt und bewusst.

Datum	Unterschrift

3. Druckexemplare der ausgewählten Publikationen

Publikation 1:

ARTICLE

Faulty Initiation of Proteoglycan Synthesis Causes Cardiac and Joint Defects

Sevjidmaa Baasanjav,[1,2,14] Lihadh Al-Gazali,[3,14] Taishi Hashiguchi,[4,14] Shuji Mizumoto,[4] Bjoern Fischer,[1] Denise Horn,[1] Dominik Seelow,[1] Bassam R. Ali,[5] Samir A.A. Aziz,[6] Ruth Langer,[7] Ahmed A.H. Saleh,[6] Christian Becker,[8] Gudrun Nürnberg,[8] Vincent Cantagrel,[9] Joseph G. Gleeson,[9] Delphine Gomez,[10] Jean-Baptiste Michel,[10] Sigmar Stricker,[11] Tom H. Lindner,[2] Peter Nürnberg,[8] Kazuyuki Sugahara,[4] Stefan Mundlos,[1,11,*] and Katrin Hoffmann[1,11,12,13,*]

Proteoglycans are a major component of extracellular matrix and contribute to normal embryonic and postnatal development by ensuring tissue stability and signaling functions. We studied five patients with recessive joint dislocations and congenital heart defects, including bicuspid aortic valve (BAV) and aortic root dilatation. We identified linkage to chromosome 11 and detected a mutation (c.830G>A, p.Arg277Gln) in *B3GAT3*, the gene coding for glucuronosyltransferase-I (GlcAT-I). The enzyme catalyzes an initial step in the synthesis of glycosaminoglycan side chains of proteoglycans. Patients' cells as well as recombinant mutant protein showed reduced glucuronyltransferase activity. Patient fibroblasts demonstrated decreased levels of dermatan sulfate, chondroitin sulfate, and heparan sulfate proteoglycans, indicating that the defect in linker synthesis affected all three lines of *O*-glycanated proteoglycans. Further studies demonstrated that GlcAT-I resides in the *cis* and *cis*-medial Golgi apparatus and is expressed in the affected tissues, i.e., heart, aorta, and bone. The study shows that reduced GlcAT-I activity impairs skeletal as well as heart development and results in variable combinations of heart malformations, including mitral valve prolapse, ventricular septal defect, and bicuspid aortic valve. The described family constitutes a syndrome characterized by heart defects and joint dislocations resulting from altered initiation of proteoglycan synthesis (Larsen-like syndrome, B3GAT3 type).

Introduction

Proteoglycans are a major component of connective tissue. They influence the mechanical properties and contribute to regulatory functions including cell proliferation, differentiation, and development.[1–9] The mechanical effect of glycosaminoglycans (GAG) is well understood. Their charge contributes to hydrophilic properties, and the accumulating water ensures an appropriate elastic tissue tonus. In this way, small proteoglycans such as biglycan and decorin help to form and modify collagen fibers in size and organization. Important functions for proteoglycans have been demonstrated for a number of organs including the cardiovascular system. For example, the growth of new blood vessels from pre-existing vasculature is influenced by proteoglycans through modulating the bioactivity of key angiogenic factors such as vascular endothelial growth factor (VEGF(165)) via affecting VEGF's diffusion, half-life, and interaction with its tyrosine kinase receptors.[10,11] Likewise, the differentiation of cardiomyocytes depends on changes in proteoglycan and hyaluronan concentration during differentiation, thereby governing the differentiation of precursor cells to mature functional cells.[12] The importance of these molecules is exemplified by mutations in human disorders such as Simpson-Golabi-Behmel syndrome (MIM 312870), a condition with overgrowth, coarse facies, and a high incidence of congenital heart defects.[13,14] In this case mutations in glypican 3 (*GPC3* [MIM 300037]), the gene encoding a heparan sulfate proteoglycan that binds to the exocytoplasmic surface of the plasma membrane through a covalent glycosylphosphatidylinositol (GPI) linkage, have been described. GPC3 is known to modify the WNT, hedgehog, fibroblast growth factor, and bone morphogenetic protein (BMP) signaling pathways.[14]

Proteoglycans consist of a core protein and glycosaminoglycan side chains. The glycosaminoglycans are attached to serine residues of the core protein via a tetrasaccharide linkage region.[5,15–17] This essential linker region always contains four saccharides (1× xylose [Xyl], 2× galactose [Gal], and 1× glucuronic acid [GlcA]). GAGs are polysaccharides

[1]Institute of Medical Genetics, Charité University Medicine, Augustenburger Platz 1, 13353 Berlin, Germany; [2]Division of Nephrology, Department of Internal Medicine, University Clinic Leipzig, Liebigstr. 20, 04103 Leipzig, Germany; [3]Department of Pediatrics, Faculty of Medicine and Health Sciences, United Arab Emirates University, P.O. Box 17666, Al Ain, United Arab Emirates; [4]Laboratory of Proteoglycan Signaling and Therapeutics, Faculty of Advanced Life Science, Graduate School of Life Science, Hokkaido University, Frontier Research Center for Post-Genomic Science and Technology, West-11, North-21, Kita-ku, Sapporo 001-0021, Japan; [5]Department of Pathology, Faculty of Medicine and Health Sciences, United Arab Emirates University, P.O. Box 17666, Al Ain, United Arab Emirates; [6]Department of Pediatrics, Saqr Hospital, P.O. Box 5450, Ras Al Khaimah, United Arab Emirates; [7]Department of Radiology, Faculty of Medicine and Health Sciences, United Arab Emirates University, P.O. Box 17666, Al Ain, United Arab Emirates; [8]Cologne Center for Genomics (CCG), University of Cologne, Weyertal 115b, 50931 Köln, Germany; [9]Neurogenetics Laboratory, Department of Neurosciences, University of California, San Diego, Leichtag 3A16, 9500 Gilman Drive, La Jolla, CA 92093, USA; [10]INSERM Unit 698, Cardiovascular remodeling, 46, rue Henri Huchard, 75018 Paris, France; [11]Max Planck Institute for Molecular Genetics, Development and Disease, Ihnestraße 63-73, 14195 Berlin, Germany; [12]The Berlin Aging Study II, Research Group on Geriatrics, Charité University Medicine, Reinickendorfer Str. 61, 13347 Berlin, Germany; [13]Institute of Human Genetics, Martin Luther University Halle-Wittenberg, Magdeburger Str. 2, 06112 Halle (Saale), Germany
[14]These authors contributed equally to this work
*Correspondence: stefan.mundlos@charite.de (S.M.), katrin.hoffmann@medizin.uni-halle.de (K.H.)
DOI 10.1016/j.ajhg.2011.05.021.

Table 1. Clinical Features of the Children in This Report

	Patient IV.2	Patient IV.3	Patient IV.4	Patient IV.5	Patient IV.7
Congenital Heart Defects					
Bicuspid aortic valve	-	+	+	+	-
Aortic root dilatation	-	+	+	+	-
Mitral valve prolapse	+	-	+	+	+
Atrial septal defect (ASD)/patent foramen ovale (PFO)	PFO	-	ASD (surgically closed)	PFO	PFO
VSD	-	+	-	-	+
Cranio-facial appearance					
Brachycephaly	+	+	+	+	+
Large prominent eyes	+	+	+	+	+
Downslant palpebral fissures	+	+	+	-	-
Depressed nasal bridge	-	+	+	+	+
Small mouth	+	-	-	+	+
Low set ears	+	-	+	-	-
Small/dysmorphic ears	+	+	+	-	-
Micrognathia/microretrognathia	+	-	+	+	+
Short/webbed neck	+	+	+	+	+
Skeletal Abnormalities					
Short stature	<P3[a]	<P3	<P3	P3	P3
Dislocated joints	elbow	elbow	shoulder, elbow, prox. radioulnar	elbow	elbow
Joint laxity (wrist and interphalangeal)	+	+	+	+	+
Elbow joint contractures	+	+	+	+	+
Broad ends of fingers and toes	+	+	+	+	+
Foot deformity (talipes varus, metatarsus varus, and flat feet)	+	+	+	+	+

All patients had heart and/or aortic disease as well as distinct skeletal abnormalities, including short stature and multiple joint dislocations together with variable degree of facial dysmorphic features.
[a] P percentile.

that are composed of repeating disaccharide units consisting of an amino sugar (*N*-acetylglucosamine [GlcNAc] or *N*-acetylgalactosamine [GalNAc]) and an uronic acid (GlcA or iduronic acid [IdoA]). The composition of the GAG chain defines the nature of the proteoglycan. Additional disaccharide repeat units of *N*-acetylglucosamine and glucuronic acid $[GlcNAc\text{-}GlcA]_n$ produce heparans, whereas repeats of *N*-acetylgalactosamine and glucuronic acid $[GalNAc\text{-}GlcA]_n$ produce chondroitins. Modifications such as sulfation and epimerization further increase the structural and functional diversity of proteoglycans (see Figure S1 available online). The synthesis of the proteoglycan linker region is a complex specialized process that involves several enzymatic steps (see Figure S1 for details).

Here we describe a family with a distinct recessive phenotype, consisting of small stature, joint dislocations, and congenital heart defects including bicuspid aortic valve and mitral valve prolapse. We identified mutations in *B3GAT3* (MIM 606374; ENA database AAH71961), the gene encoding glucuronyltransferase-I (GlcAT-I) that adds the last component of the linker region. The mutation causes a drastic reduction of GlcAT-I activity and results in the production of immature dermatan sulfate (DS) proteoglycans as well as in a reduced number of chondroitin sulfate (CS) and heparan sulfate (HS) chains. We describe a syndrome caused by impaired proteoglycan maturation, providing evidence that normal side chain synthesis is essential for the development of the heart, in particular its valves, and the skeleton. We suggest naming it Larsen-like syndrome, B3GAT3 type.

Material and Methods

Patients

We studied a consanguineous family with five affected children (Table 1, Figures 1 and 2, Figure S2). All members of the family

Figure 1. Mutations in *B3GAT3* Are Associated with a Specific Phenotype

(A) Facies appeared flattened with large eyes, hypertelorism, long and downslanting palpebral fissures, depressed nasal bridges, and micrognathia. Note dislocation of elbow, broad fingers and toes, and foot deformity.

(B) Radiographs show dislocation of shoulder, elbow, and proximal radio-ulnar joints. Mild shortening of metacarpal bone I, pseudoepiphysis at the second metacarpal bone, dissociation and retardation of the bone age, and mild irregularities at several metaphyses are shown.

(C) Echochardiography showing aortic dilation and bicuspid aortic valve.

Numbers in left lower corner indicate the patient's ID corresponding to the pedigree and Table 1.

were clinically assessed and individual organ systems studied to ascertain the full phenotype. The study has been approved by the Charité University medicine, United Arab Emirates University, and Hokkaido University ethics committees. The procedures followed were in accordance with the ethical standards of the responsible committees on human experimentation (institutional and national). Written, informed consent was obtained from all participants or their legal guardians.

Genomic and Molecular Analysis

Genotyping was performed with the 10 k Affymetrix SNP chip. The data were analyzed with ALLEGRO v1.2c, GENEHUNTER v2.1r5 under the graphical user-interface easyLINKAGE v5.08.[18,19] A recessive model with complete penetrance, disease allele frequency of 0.001, and equally distributed marker alleles was assumed. Fine mapping with microsatellites was done as previously described.[20] We included all available family members and reconstructed haplotypes by GENEHUNTER and manually.

We sequenced functional candidate genes within the linkage interval by standard sequencing procedures. Functional candidates were selected based on their expression potential function and/or previously reported skeletal and cardiac phenotypes in human or animal models, respectively, in the gene itself or associated pathway genes and interaction partners. Primer sequences of used microsatellite markers and sequenced genes are available upon request. The mutation was tested in controls (147 population-matched controls and 425 blood donors of European descent) and for correct segregation within the patient's family.

All coding sequences and flanking intron regions of *B3GAT3* (GlcAT-I, NM_012200.2, GI:12408653; NP_036332.2) were amplified and sequenced by standard protocols. Primer sequences are provided in Table S1.

Quantitative PCR

B3GAT3 mRNA levels were studied in different tissues and cell lines by quatitative PCR (qPCR). After cell lysis with Trizol and standard phenol/chloroform RNA extraction, total cDNA was transcribed by RevertAid H Minus First Strand cDNA Synthesis Kit (Fermentas, Burlington, Ontario, Canada). For qPCR on ABI Prism 7500 (Applied Biosystems, Foster City, CA), we mixed cDNA, SYBR Green (Invitrogen, Carlsbad, Ca), and primers (primer sequences in Table S1). We analyzed qPCR data with the ABI Prism SDS Software package (ΔΔCt method; normalization against *GAPDH*).

To determine the expression levels of decorin mRNA, total RNA was extracted from fibroblasts of each subject and cDNAs were synthesized with reverse transcriptase by standard protocols. The quantitative real-time RT-PCR was performed by Mx3005P (Stratagene, La Jolla, CA) with decorin-specific primer pairs (primer sequences in Table S1).

Molecular Modeling

The model used was the X-ray structure of the human GlcAT-I bound to UDP-GlcA. The Protein Data Bank code for this model is 1KWS and is available at the RCSC protein data bank. The result of the modeling was rendered with PyMol.

Glucuronyltransferase Activities of WT and Mutant GlcAT-I

UDP-[^{14}C]GlcA (180.3 mCi/mmol) was purchased from Perkin-Elmer Life and Analytical Sciences (Boston, MA). A human

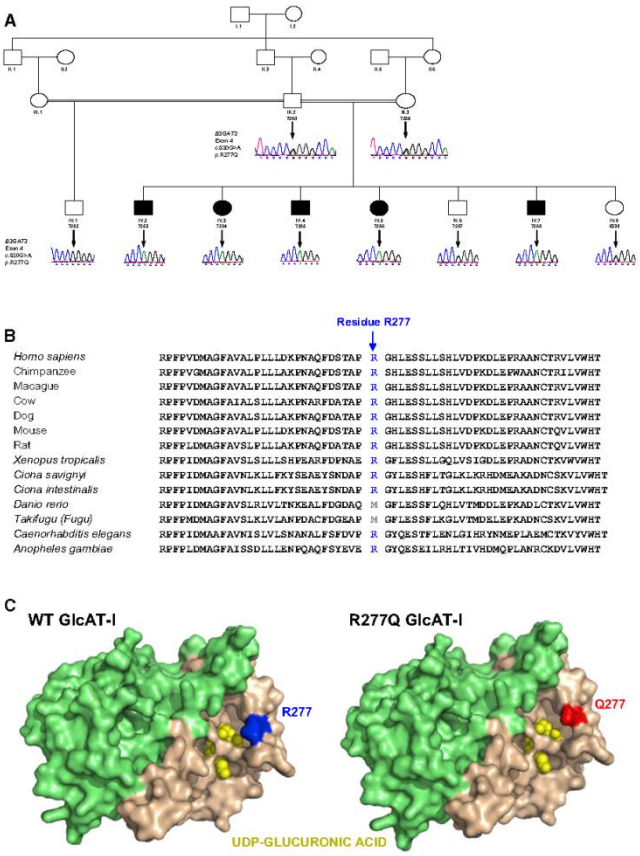

Figure 2. Molecular Analysis
(A) Pedigree of the family. All affected family members are homozygous for the mutation c.830G>A in exon 4 of the *B3GAT3* gene.
(B) Residue p.Arg277 (p.R277) is evolutionary conserved.
(C) *B3GAT3* encodes the glucuronyltransferase GlcAT-I that functions as a dimer (light green and light brown).[32,45] Residue p.Arg277 (p.R277, blue) is involved in substrate interaction and is critical for binding the substrate GlcA. Note that the side chain of p.Arg277 (p.R277) is close to the carboxyl group at the C-5 position of GlcA but is further away in the mutant p.Gln277 (p.Q277). (Modeling used Protein Data Bank file 1KWS for the crystal structure of GlcAT-I interacting with the substrate UDP-glucuronic acid [UDP-GlcA].)

GlcAT-I/pOTB7 vector (IMAGE Consortium cDNA clone, ID number 4299539) was purchased from Open Biosystems Inc (Huntsville, AL). Anti-FLAG M2 affinity resin, anti-FLAG Monoclonal antibody, Galβ1-3Galβ1-*O*-methyl, and p3XFLAG-CMV8 vector were purchased from Sigma (Saint Louis, MO). An ECL advance western blotting detection kit and Hybond-P membranes were purchased from GE Healthcare (Buckinghamshire, UK). FuGENE 6 transfection reagent was purchased from Roche Diagnostics (Basel, Switzerland). Restriction enzymes were purchased from New England Biolabs (Hitchin, UK). *KOD*-Plus DNA polymerase was purchased from Toyobo (Tokyo, Japan). AG 1-X8 resin (100–200 mesh) was purchased from Bio-Rad (Hercules, CA).

The expression vector of human GlcAT-I was constructed as described previously.[21,22] In brief, a truncated form of GlcAT-I (wild-type), lacking the first NH_2-terminal 43 amino acids of the GlcAT-I, was amplified by PCR with a 5′ primer containing an in-frame EcoRI site (5′-GCGAATTCACTACGGCAGAAGGAT-3′) and a 3′ primer containing a SalI site located 71 bp downstream of the stop codon (5′-GCGTCGACGAAAACCACATCCT-3′) and hGlcAT-I/pOBT7 as a template. We carried out two rounds of PCR for the construction of the amino acid-substituted mutant of GlcAT-I (p.Arg277Gln). The first PCR was performed with a 5′ primer containing an in-frame EcoRI site (5′-GCGAATTCACT ACGGCAGAAGGAT-3′) and a 3′ internal mutagenic oligonucleotide primer (5′-CA GGTGGCCCTGGGGAGCGGTGGA-3′), 5′ internal mutagenic oligonucleotide primer (5′-TCCACCGCTCCCCAGGGCCACCTG-3′), and 3′ primer containing a SalI site (5′-GCGTCGACGAAAACCACATCCT-3′) and hGlcAT-I/pOBT7 as a template (underlining indicates modified nucleotides). The second PCR was performed with a 5′ primer containing an EcoRI site (5′-GCGAATTCACTACGGCAGAAGGAT-3′), 3′ primer containing a SalI site located 71 bp downstream of the stop codon (5′-GCGTCGACGAAAACCACATCCT-3′), and the first PCR products as a template. PCR was carried out with *KOD*-Plus DNA polymerase by 30 cycles of 94°C for 30 s, 55°C for 42 s, and 68°C for 60 s. The amplified fragments were digested with EcoRI and SalI and inserted into p3XFLAG-CMV8.

The expression plasmid (6.7 μg) was transfected into COS-7 cells (Japan Health Sciences Foundation, Tokyo, Japan) on a 100 mm dish with FuGENE 6 according to the instructions provided by the manufacturer. Three days after transfection, 0.25 ml each of the culture medium was collected and incubated with 10 μl of anti-FLAG M2 affinity resin overnight at 4°C. The beads were recovered by centrifugation and washed with 1 ml of 50 mM Tris-HCl (pH 7.5) containing 150 mM NaCl, 0.05% Tween 20, and then resuspended in the assay buffer for enzyme activity.

The culture medium (0.2 ml) was incubated with 10 μl of anti-FLAG M2 affinity resin overnight at 4°C. The beads were recovered by centrifugation, washed with TBST, and then analyzed on a 12.5% sodium dodecyl sulfate (SDS)-polyacrylamide gel, transferred to a polyvinlidene difluoride (PVDF) membrane, and incubated for 1 hr with FLAG antibody. The bound antibody was

detected with anti-mouse IgG conjugated with horseradish peroxidase.

Enzyme Assay of the Recombinant WT and Mutant GlcAT-I

The glucuronyltransferase assay mixture contained 10 μl of the resuspended anti-FLAG affinity resins/50 mM 2-(*N*-morpholino) ethanesulfonic acid-NaOH (pH 6.5)/171 μM ATP/10 mM $MnCl_2$/14.3 μM UDP-[^{14}C]GlcA (1.77×10^5 dpm)/60 nmol Galβ1-3Galβ1-*O*-methyl as acceptor substrate in a total volume of 30 μl. The reaction mixture was incubated at 37°C for 1 hr. The ^{14}C-labeled products were isolated by applying the reaction mixture onto a tiny tip column packed with AG 1-X8 resin (a PO_4^{2-} form, 100–200 mesh) to remove excess UDP-[^{14}C] GlcA.[23] The isolated products were quantified in a liquid scintillation counter (LS6500, Beckman coulter).

Comparison of the GlcAT-I Activities of Fibroblast Homogenates from Patients and Age-Matched Controls

The following fibroblasts were used for the assay. Age-matched controls for patient A820 (male, 11 years old) were GM03348E (male, 10 years old) and AG16409 (male, 11 years old). Age-matched controls for patient A821 (male, 17 years old) were GM07492A (male, 17 years old) and GM07753 (male, 17 years old). The homogenates of the fibroblasts were assayed with Galβ1-3Galβ1-*O*-methyl as an acceptor (220 nmol) and UDP-[^{14}C]GlcA as a donor substrate, and then incubated for 4 hr at 30°C.

Immunofluorescence

For immunofluorescence analysis, the cells were washed three times in phosphate-buffered saline (PBS), fixed in 4% paraformaldehyde for 10 min at 4°C, and permeabilized in 3% BSA in 1× PBS with 0.4% Triton X-100 for 10 min at 4°C. GlcAT-I protein was detected by a mouse anti-GlcAT-I polyclonal antibody (Abnova, Taipei, Taiwan: H00026229-B01P). For testing the colocalization analysis with Golgi proteins, we used sheep anti-GM130 (kind gift by Francis A. Barr), rabbit anti-Giantin (Covance, Princeton, NJ), and sheep anti-TGN46 (Serotec, Oxford, UK). As secondary antibodies we applied anti-mouse IgG Alexa Fluor 555 (Invitrogen, Molecular Probes) and an anti-sheep/rabbit IgG Alexa Fluor 488 (Invitrogen, Molecular Probes) conjugates. We stained DNA by DAPI and mounted cells in Fluoromount (Scientific Services, Cornwall, UK). Images were collected with an LSM 510 meta (Carl Zeiss, Göttingen, Germany) with a x63 Plan Apochromat oil immersion objective.

Immunoblotting of Aortic Media Extracts

Normal walls of the ascending aorta and aortic arch were obtained in healthy subjects at the time of organ collection for heart/lung transplantation with the authorization from the French Biomedicine Agency. Protein extractions were performed directly from frozen aortic media (after the separation from intima and adventitia) and stored at −80°C. The media preparations were pulverized in liquid nitrogen, using a freezer mill (model 6750 SPEX SamplePrep, Metuchen, NJ), and subsequently homogenized in a hypotonic lysis buffer (50 mM Tris [pH 8], 150 mM NaCl, 1% Triton X-100, 1% sodium deoxycholate, 5 mM EDTA) containing a cocktail of protease and serine/threonine and tyrosine phosphatase inhibitors (Sigma). The protein concentration from each sample was determined and extracts were separated by 10% SDS-polyacrylamide gel electrophoresis. Proteins were transferred to a PVDF membrane, blocked with 5% BSA-TBS-T (Tris-buffered saline [pH 7.4]-0.1% Tween 20) for 1 hr. Membranes were then incubated overnight (4°C) with primary antibodies: polyclonal B3GAT3 (1 μg/ml, Abnova), monoclonal B3GAT3 (1 μg/mL, Abnova), or GAPDH (1.6 μg/ml, Biovalley, Freiburg, Germany). Membranes were then washed with TBS-T and incubated with anti-mouse IgG (Jackson Laboratories, Bar Harbor, ME) for 1 hr. The signal was detected with a chemiluminescence kit (ECL Plus kit; Amersham).

Analyses of Dermatan Sulfate, Chondroitin Sulfate, and Heparan Sulfate Proteoglycans in Patient and Control Fibroblasts

The serum-free conditioned medium of the cultured fibroblasts of control subjects and patients was collected and concentrated with Amicon Ultra-4 (Ultracel-30k, Millipore, Billerica, MA). An aliquot of the medium (5 μg as total protein) was digested with a highly purified (protease-free) chondroitinase (CSase) ABC (EC 4.2.2.20, Seikagaku Corp., Tokyo, Japan), and each digest was subjected to SDS-polyacrylamide gel electrophoresis. Western blotting was carried out with an anti-human decorin antibody (clone 115402, R&D Systems, Minneapolis, MN) and an ECL advance detection kit (GE healthcare).

For determination of the number of CS and HS chains, cultured fibroblasts from patients and control subjects (age and sex matched) were collected and washed with PBS. The cells were treated with CSase or a mixture of heparinases (HSases) -I (EC 4.2.2.7) and -III (EC 4.2.2.8) (IBEX Technologies, Montreal, Canada) at 37°C for 1 hr. After washing with PBS, CSase- or HSase-treated cells were individually incubated with the primary antibodies, anti-CS-stub (2B6) and anti-HS-stub (3G10) (Seikagaku Corp.), and subsequently the cells were incubated with the Alexa Fluor 488-labeled anti-mouse IgM secondary antibody (Molecular Probes, Eugene, OR). Incubation of the fibroblasts with the secondary antibody alone was also performed as a negative control experiment. Alexa Fluor 488-bound cells were analyzed by immunofluorescence flow cytometry in a BD FACSCanto (BD Biosciences, San Jose, CA).

Results

Patients' Phenotype Defines a Syndrome Characterized by Joint Dislocations and Congenital Heart Defects Including Bicuspid Aortic Valve

The parents were first cousins with five affected and two unaffected children (Figures 1 and 2, Figure S2, Table 1). All five patients had congenital heart defects in variable combinations (Figure 1C, Table 1). Bicuspid aortic valve with dilatation of the aortic root was present in three, mitral valve prolapse in four, patent foramen ovale in three, and ventricular septal defect in two of the patients. All affected children had short stature (height < 3%) and presented variable craniofacial dysmorphic features which included brachycephaly, thick eyebrows, large eyes with downslanting palpebral fissures, depressed nasal bridge, narrow mouth, and micrognathia or microretrognathia. The ears in some of them were small, low set with prominent antitragus, and slight uplift of the lobe. The neck was short (webbed in IV.2) with low posterior hair line. There was mild chest asymmetry.

In addition, all affected individuals had congenital dislocations and contractures of the elbow joint as well

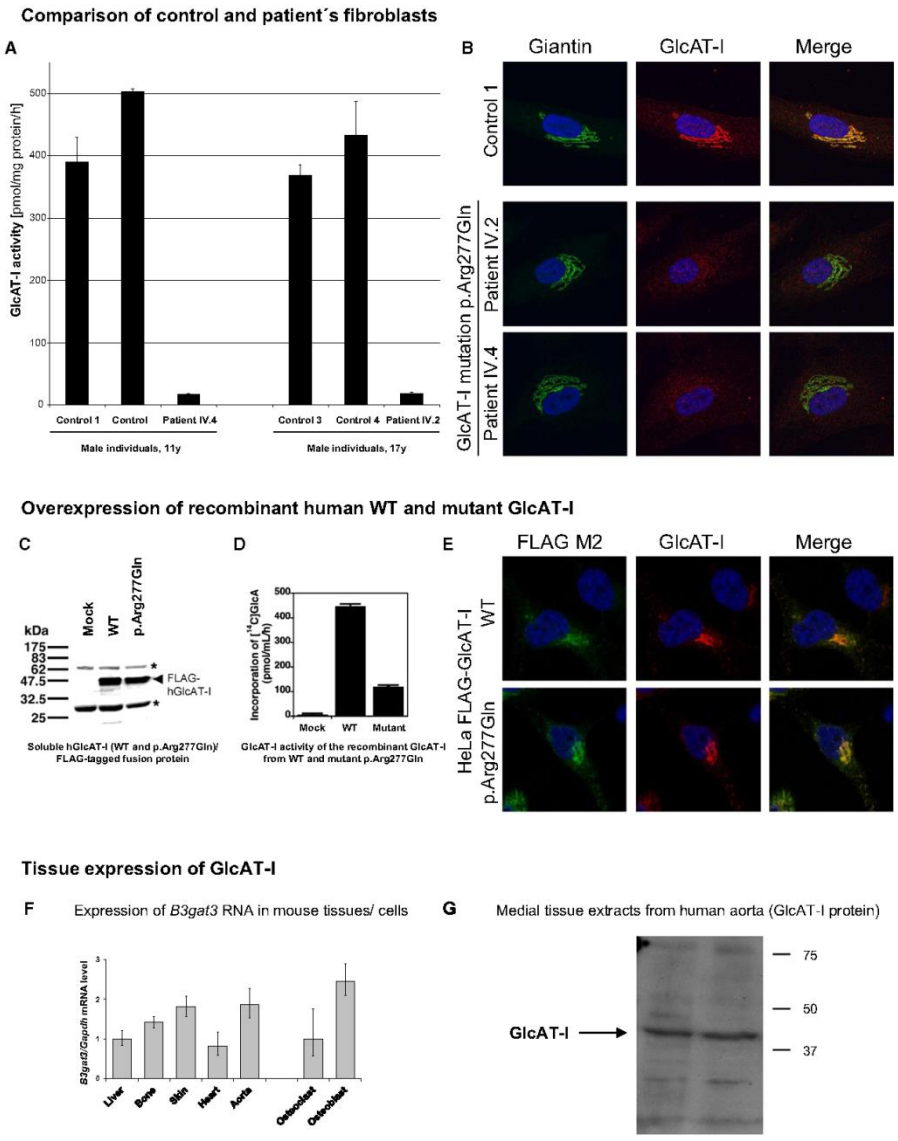

Figure 3. Expression and Activity of GlcAT-I

(A) GlcAT-I activity in fibroblasts is markedly reduced in patients compared to age-matched controls. The homogenates of the fibroblasts were assayed with Galβ1-3Galβ1-*O*-methyl as an acceptor (220 nmol) and UDP-[^{14}C]GlcA as a donor substrate, and then incubated for 4 hr at 30°C. The results are from duplicate experiments. Unit is pmol/mg protein/hr.

(B) Reduced amount of mutant GlcAT-I and loss of Golgi localization in patient's fibroblasts. By comparison, GlcAT-I (red) colocalizes with the *cis* and *cis*-medial Golgi marker GIANTIN (green) in wild-type fibroblasts.

(C and D) Glucuronyltransferase activities of the human recombinant GlcAT-I (WT and p.Arg277Gln) showed similar amounts of proteins (C) but reduced activity by mutation p.Arg277Gln (D).

as talipes equinovarus and/or metatarsus varus. Joint dislocations were also observed in the shoulders. Joint laxity was present in the wrists and interphalangeal joints. The finger tips and the hallux on both sides appeared wide. Radiographs showed dislocations of the shoulder, elbow, and proximal radial-ulnar joints (Figure 1), a mild shortening of the first metacarpal bone, delayed and dissociated bone age (~4 years at the chronological age of 8 years), mild dysplasia of the hip joints, and foot deformities. The vertebral column showed signs of osteopenia; several vertebrae were already flattened. The children had a normal mental and motor development.

Disease Mapping and Identification of the Disease-Causing Mutation in *B3GAT3*

We performed genome-wide linkage analyses and mapped the disease to chromosome 11q12 (multipoint LOD = 3.76; Figure S3A). Fine mapping narrowed the region to an 8 cM interval (final multipoint LOD = 3.89; Figure S3B) containing 262 genes. We sequenced 30 functional candidate genes within this region (Table S2). We identified the homozygous missense mutation c.830G>A in *B3GAT3*, the gene encoding the enzyme beta-1,3-glucuronyltransferase 3 (GlcAT-I), which resulted in the substitution of arginine at position 277 by glutamine (p.Arg277Gln). The mutation p.Arg277Gln segregated with the disease in the family (Figure 2A) and was present neither in 294 chromosomes from population-matched controls nor in 850 chromosomes from Berlin blood donors. Residue p.Arg277 is evolutionary highly conserved and alters a functionally important domain involved in substrate interaction, especially in binding the substrate GlcA (Figures 2B and 2C).

Reduced GlcAT-I Enzyme Activity in Patient Cells

The p.Arg277 residue has previously been shown to be essential for enzymatic activity in a mutagenesis experiment (p.Arg277Ala) by ensuring GlcAT-I substrate specificity.[24] We therefore reasoned that the mutation p.Arg277Gln might have a similar effect on GlcAT-I activity. Our studies in the homogenates from patient-derived fibroblasts demonstrated that the missense mutation p.Arg277Gln results in a significant reduction of glucuronyltransferase activity. GlcAT-I activity in patient fibroblasts (patients IV.2 and IV.4) was reduced to 3%–5% of age-matched control levels (Figure 3A). Thus, mutant cells showed a drastic reduction in GlcAT-I activity but still showed some basal activity, indicating that the mutation is hypomorphic.

By using immunofluorescence and colocalization with Golgi-marker proteins, we showed that GlcAT-I is located in the *cis* and *cis*-medial Golgi (Figure S4). In mutant cells the protein level is dramatically reduced (Figure 3B). We tested whether the antibody detects both the wild-type and the mutant protein and found that the mutation did not affect antibody binding (Figure S5), whereas mutation c.830G>A did not significantly reduce the level of *B3GAT3* mRNA (data not shown). These observations suggest that the mutant GlcAT-I protein might have been degraded or produced to a lesser extent as compared to the wild-type. As previously shown, artificially introduced missense mutations can reduce enzymatic activity and secondarily decreased stability of the mutant, dysfunctional enzyme by ER retention and subsequent proteasomal decay.[25]

To test whether the mutation p.Arg277Gln indeed reduces GlcAT-I activity by impaired enzymatic function and not by primary reduced protein level, we transfected cells with the human GlcAT-I wild-type and the mutated (p.Arg277Gln) vector. We found a marked reduction of GlcAT-I activity in the mutant despite similar amounts of the wild-type and mutant proteins (Figures 3C–3E), suggesting that the reduced enzymatic activity of GlcAT-I affects protein stability.

Expression of *GlcAT-I* in Heart, Aorta, and Bone

Individuals with the c.830G>A mutation showed heart defects, aortic root dilatation, and skeletal malformations. Reverse-transcriptase quantitative PCR on corresponding mouse tissues demonstrated that *B3GAT3* mRNA is expressed in heart, aorta, bone, and also in osteoblasts (Figure 3F). In addition, GlcAT-I protein was present in human aorta (Figure 3G).

GlcAT-I Mutations Are Associated with Immature DS Proteoglycans as well as with Reduced Amounts of CS and HS Chains in Patient Cells

We tested how the reduced enzyme activity affects the products of proteogylcan synthesis. The overall amount

(C) For western blotting, the purified recombinant FLAG-GlcAT-I (WT and p.Arg277Gln) was separated by 12.5% SDS-polyacrylamide gel electrophoresis and detected with the FLAG M2 antibody. The arrowhead and asterisks indicate the recombinant enzyme and the light and heavy chains of the antibody, which is derived from the anti-FLAG agarose resin used for purification, respectively.
(D) Catalytic GlcAT-I activity of the recombinant enzyme (p.Arg277Gln) was reduced compared to the wild-type. Activities represent the averages and standard error of two independent experiments, which were performed in duplicate. Mock indicates the glucuronyltransferase activity obtained with the conditioned medium transfected with an empty vector as a control. Experiments were performed at 37°C.
(E) The GlcAT-I antibody (Abnova) recognizes both the wild-type and the mutant recombinant GlcAT-I, thus excluding preferential antibody binding to the wild-type. (Western blotting in Figure S5.)
(F) RNA-expression of *B3gat3* in different disease relevant tissues (obtained from newborn black 6 mice [C57BL/6], postnatal day P4) as well as from osteoblast and osteoclast cell cultures. Data were obtained from three different experiments (error bars represent standard error of the mean [SEM]).
(G) Western blotting of GlcAT-I in human aorta. Western blotting shows presence of GlcAT-I in medial tissue extracts from human wild-type aorta.

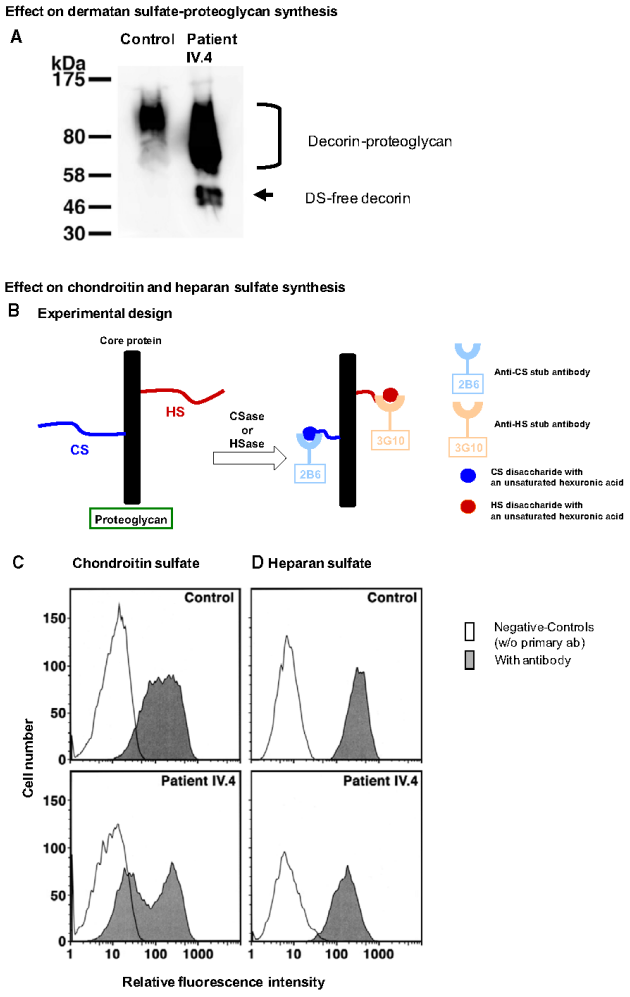

Figure 4. Effect of GlcAT-I Mutations on DS, CS, and HS Proteoglycan Synthesis

(A) DS-free decorin is detected in patient but not in control fibroblasts, indicating an insufficient dermatan sulfate synthesis. Western blotting of a DS-proteoglycan, decorin, produced by fibroblasts. The conditioned medium derived from wild-type fibroblasts showed a broad band of decorin-proteoglycan around 60–120 kDa. In contrast, the conditioned medium derived from the patient fibroblasts revealed two bands. The upper band represents decorin-proteoglycan with a DS chain. The lower band ~50 kDa is predicted to be decorin with only the linkage region trisaccharide (Gal-Gal-Xyl), without a DS chain. These observations suggest that the mutation p.Arg277Gln in GlcAT-I is associated with insufficient synthesis of dermatan sulfate proteoglycan.
Control: age-, sex-, and population-matched (male, 11 years old, AG16409); patient IV.4: male, 11 years old (mutation p.Arg277Gln in GlcAT-I, A820). The arrow indicates DS-free decorin.
(B) Experimental design for analyzing CS and HS synthesis. The unsaturated hexuronic acid containing CS and HS, which were generated by the treatment with CSase or HSase, are recognized by the anti-CS-stub and anti-HS-stub antibodies, respectively.
Anti-stub CS (2B6) and anti-stub HS (3G10) antibodies can recognize the unsaturated hexuronic acid-containing oligosaccharide that are generated by the treatment with bacterial CSase and HSase, respectively, whereas neither intact CS nor HS can be recognized. Therefore, these antibodies can be used as probes for investigating the *relative* number of CS and HS chains on the core proteins of proteoglycans. It should be noted that the truncated GAG-protein linkage trisaccharide Gal-Gal-Xyl- expressed on core proteins in the GlcAT-I mutant cells is not recognized by either antibody.
(C and D) Analysis of the relative number of CS and HS chains expressed on the cell surface of fibroblasts by flow cytometry. To examine the expression of CS and HS on the cell surface, the fibroblasts from the 11-year-old patient IV.4 and from controls (AG16409) were treated with CSase and then with anti-stub 2B6 antibodies (C) or HSase and then with anti-stub 3G10 antibodies (D), respectively. The binding of these antibodies to the epitopes on the cell surface was visualized by flow cytometry after incubating with Alexa Fluor 488-conjugated secondary antibody. The gray and white histograms show the intensity of the fluorescence with or without anti-stub antibody, respectively. Similar results were also obtained with those from the 17-year-old patient IV.2 (Figure S6B).

of GAGs in fibroblasts from patients did not show an obvious decrease compared to that of age-matched controls (data not shown). Next we analyzed the proteoglycan decorin in fibroblasts from patients by western blotting. Decorin is secreted by fibroblasts and has a single DS chain when proteoglycan synthesis is undisturbed. We detected DS-free decorin in the patients' cells but not in control fibroblasts (Figure 4A; Figure S6), suggesting that the mutation p.Arg277Gln in GlcAT-I results in the production of the immature DS-proteoglycan decorin.

We examined specifically decorin proteoglycan by western blotting by using the conditioned media from fibroblasts of patients IV.2 and IV.4. One broad-band of decorin-proteglycan (around 80 kDa) was detected in control fibroblasts. In contrast, we detected two bands in fibroblasts from both patients (Figure S6A, lanes 3 and 6). The upper band was decorin proteoglycan with a DS chain as

shown in the wild-types (Figure S6A, lanes 1, 2, 4, and 5), whereas the lower band (~50 kDa) is predicted to be DS-free decorin with the linkage region trisaccharide stub, Galβ1-3Galβ1-4Xyl, where Gal and Xyl stand for D-galactose and D-xylose, respectively. Furthermore, the lower band corresponded to the band observed for the conditioned medium treated with CSase ABC (Figure S6). Thus, the lower band in patients was most probably the signal of DS-free decorin. These observations suggest that the mutation of GlcAT-I (p.Arg277Gln) was responsible for the lack of a DS chain on the core protein.

Based on the result from western blotting of decorin, the amount of its core protein seemed to be upregulated. Therefore, we analyzed the expression level of decorin mRNA by quantitative RT-PCR. Interestingly, the mRNA levels of decorin were 3- to 4-fold increased in patients compared to control fibroblasts (Figure S7), indicating that decorin mRNA levels might be upregulated to compensate for the immature decorin.

Next we examined the synthesis of CS and HS chains on the surface of fibroblasts from patients and age- and sex-matched controls by flow cytometry with CS-stub and HS-stub antibodies (Figures 4B–4D; Figure S6B). The 2B6 antibody, which recognizes the oligosaccharides containing the unsaturated hexuronic acid after treatment with CSase, showed a markedly reduced binding to the epitopes on the patient cells relative to those of the control subject (Figure 4C), showing a bimodal distribution of the cells. To quantify the relative amounts of the CS chains, the mean fluorescence intensity (MFI) of the cell population stained with 2B6 was used. The MFI value for the patient IV.4 was 6.0 (65%) as compared with 9.2 of the age-matched control subject. The 3G10 antibody, which recognizes the oligosaccharides containing the unsaturated hexuronic acid after the treatment with HSase, also showed a reduced binding to the epitopes on the patient cells relative to those of the control subject (Figure 4D). The MFI value after staining with 3G10 was 21.4 (53%) for the patient IV.4 as compared with 40.3 for the age-matched control subject. Similar results were obtained for the fibroblasts from patient IV.2 (Figure S6B). These differences in the MFI values correspond to those of the numbers of the CS and HS chains at cell surface of the control and the patient cells. Namely, the number of the CS and HS chains was reduced to 65% and 53% of the control, respectively. The bimodal distribution of the cells from the 11-year-old male patient (Figure 4C) suggests two different cell populations, one with a reduced number of GAG polysaccharides most probably with a trisaccharide stub (Gal-Gal-Xyl), and the other with a larger number of GAG polysaccharides. Interestingly, the same seems to be true for the fibroblasts from the 17-year-old normal subject (Figure S6B). A possibility is the age-dependent bimodal cell population with a smaller and a larger number of GAG polysaccharides, which remains to be investigated.

These results suggest that the mutant GlcAT-I cannot transfer GlcA to a significant portion of the linker region trisaccharide Gal-Gal-Xyl, resulting in the partial deficiency of all three lines of *O*-glycanated proteoglycans (CS, HS, and DS proteoglycans).

Discussion

We describe a family with recessive inheritance of heart and/or aortic disease as well as of distinct skeletal abnormalities (short stature, multiple joint dislocations) and variable cranio-facial dysmorphic features (Larsen-like syndrome, B3GAT3 type).

There are some similarities to otopalatodigital syndrome type II (OPD2 [MIM 304120]), particularly the downslanting palpebral fissures, narrow mouth, contractures at the elbows, and broad fingertips and hallux. However, the radiological changes in OPD2 are different and the inheritance is X-linked recessive rather than autosomal recessive. Short stature, short webbed neck, and the facial appearance of the children in this report could also suggest Noonan syndrome. Nevertheless, the presence of joint dislocations and the recessive pattern of inheritance in this family made this diagnosis unlikely. Absence of the typical radiological changes seen in Desbuquois syndrome (DBQD [MIM 251450]) in this family ruled this diagnosis out. We also considered the classic Larsen syndrome (LRS [MIM 150250]) caused by dominant FLNB (MIM 603381) mutations particularly because there are multiple joint dislocations, broad fingertips, and hallux but the facial appearance is different, the bone age is delayed rather than advanced, and the inheritance is recessive in our family. There are also many similarities of the family in this report to the autosomal-recessive Larsen syndrome, CHST3 type. This disorder includes a spectrum of phenotypes ranging from Larsen syndrome, humerospinal dysostosis, chondrodysplasia multiple dislocations, and spondylo-epiphyseal dysplasia, Omani type.[26–28] Children present at birth with reduced length and multiple joint dislocations. During childhood, the dislocations improve and features of SED-OT appear. These features include intervertebral disc degeneration, rigid kyphoscoliosis, and trunk shortening. The bone age is also delayed. There are usually vertebral changes on lateral X-ray of the spine. These include superior and inferior notching reminiscent of a partial coronal cleft.[26] Involvement of the heart valves in this disorder has also been reported. There are no vertebral changes on radiological examination in our family and clinically the older children in our family (now 17, 14, and 13 years old) have no kyphoscoliosis or trunk shortening. However, differentiation between these two disorders is difficult in infancy and early childhood. The combination of brachycephaly, downslanting palpebral fissures, retrognathia, and abnormal ears with club feet, hypermobility of the joints of the hands, shoulders, and feet together with congenital heart disease raised the possibility of musculocontractural EDS (previously known as adducted thumb-clubfoot syndrome and EDS type VIB),

which is caused by mutations in *CHST14*.[29–31] However, the children in this report have normal build and skin with no delay in wound healing and no contractures of the fingers.

Here we describe that mutations in *B3GAT3*, the gene coding for GlcAT-I, result in a condition characterized by congenital dislocations, short stature, and heart defects including bicuspid aortic valve. GlcAT-I functions as a dimer of two subdomains with donor and acceptor specificity.[32] The active sites resides in a cleft between the two chains in which the new incoming saccharide is oriented, chemically reduced, and eventually fused to the already established trisaccharide linker.[32,33] Ouzzine et al. used in vitro mutagenesis to test which residues define the substrate specificity of GlcAT-I. They identified residue 277 (mutagenesis p.Arg277Ala) as important and concluded that the arginine at position 277 is essential for GlcAT-I substrate specificity.[24,34] Our studies in a recombinant cell system as well as in the homogenates from patient-derived fibroblasts demonstrated that the missense mutation p.Arg277Gln significantly reduces the glucuronyltransferase activity (GlcAT-I). Nevertheless, cells with mutant GlcAT-I had residual basal activity in the patient fibroblasts and in vitro, indicating that the mutated protein is still able to function.

We show that reduced GlcAT-I activity affects major components of the extracellular matrix, resulting in immature DS proteoglycans as well as in a reduced number of CS and HS chains in patient cells. The mutation affects the final step in the synthesis of the tetrasaccharide linker region, which is required for initiation of GAG side chain synthesis of proteoglycans. Our data demonstrate that GlcAT-I is located in the *cis* and *cis*-medial Golgi. This is consistent with the catalytic function in glycosylation of the Golgi apparatus and the identification of the GlcAT-I rat ortholog in an endoplasmic reticulum (ER)/Golgi proteomics screening perfomed in rat liver homogenates.[35]

We found that an impairment of GlcAT-I function affects the synthesis of CS, DS, and HS. DS-free decorin proteoglycans were present in the patient fibroblasts but not in controls. These results suggest that the GlcAT-I mutation p.Arg277Gln results in the synthesis of immature proteoglycans, i.e., GAG-free proteoglycans such as DS-free decorin. Interestingly, the synthesis of the decorin core protein was upregulated, probably to compensate for the dysfunctional decorin. In addition, mutant cells showed an apparent reduction in the relative number of CS and HS chains. This is consistent with the essential role of GlcAT-I in proteoglycan synthesis as the last step in linker synthesis before its division into CS, DS, and HS. Thus, any type of the affected GAG chains (CS, DS, or HS) may contribute to the characteristic symptoms of the patients.

Another step in linker synthesis, the addition of the second galactose residue, is affected in progeroid type Ehlers-Danlos syndrome (EDS progeroid form [MIM 130070]).[36–38] The phenotypic overlap with the family described here includes multiple joint dislocations, growth delay, skeletal malformations, and hypomineralization (osteopenia). Considerable overlap is also apparent with defects in another downstream enzyme which is essential for CS synthesis, chondroitin 6-*O*-sulfotransferase-1 (C6ST1 [MIM 603799]). Mutations in the gene carbohydrate sulfotransferase 3 (*CHST3* [MIM 603799]), coding for C6ST1, were shown to cause autosomal-recessive spondyloepiphyseal dysplasia with joint dislocations CHST3 type, a condition characterized by congenital joint dislocations (especially of the knee and elbow), club foot, vertebral changes (platyspondyly, intervertebral disc degeneration, scoliosis), short stature, arthritis, and heart defects (MIM 245600).[22,27,28] Mutations in chondroitin synthase 1 are associated with brachydactyly, mutations in the chondroitin beta-1,4-N-acetylgalactosaminyltransferase-1 with neuropathies.[39–41] A defect in the downstream enzyme in dermatan sulfate synthesis (dermatan 4-*O*-sulfotransferase 1, D4ST1, encoded by the gene carbohydrate sulfotransferase 14, *CHST14* [MIM 608429]) results in adducted thumb-clubfoot syndrome (ATCS [MIM 601776]), as well as a subtype of Ehlers-Danlos syndrome (EDS, musculocontractural type [MIM 601776]).[29,31] D4ST1 defects lead to a reduction in DS chains. Lack of DS chains was shown to impair the interaction with collagen to form collagen bundles.[31] Thus, proteoglycans devoid of DS chains may explain symptoms such as skin and joint laxity as well as tissue fragility. GlcAT-I defects also affect DS chains and accordingly symptoms of patients with GlcAT-I mutations overlap with these other clinical entities. However, defective linker synthesis additionally affects CS and HS proteoglycans.

We report a disease-causing mutation resulting in a defect terminal step of tetrasaccharide linkage region of proteoglycans synthesis. The phenotypes we observed in the affected individuals, namely joint dislocations, congenital heart defects, and short stature, overlap with symptoms seen in progeroid type EDS and in patients with spondyloepiphyseal dysplasia with congenital joint dislocations, CHST3 type. These findings suggest that proteoglycan synthesis pathway mutations may be responsible for atypical connective tissue disorders that feature joint dislocations, joint laxity, and congenital heart disease.

All patients described had congenital heart disease in various forms: mitral valve prolapse, bicuspid aortic valve with aortic root dilatation, ventricular septal defect, and atrial septal defect. Defects of heart valves are one of the most common inborn malformations. Among them, bicuspid aortic valve (BAV) is most frequent with a prevalence of 1%–2% in newborns.[42] Bicuspid aortic valves feature a significantly increased risk of life-threatening late complications such as aortic root dilatation, dissection of the aorta, and stenosis or insufficiency of the aortic valve with subsequent heart failure. In contrast to other congenital heart defects where already multiple genes were found to be involved, the genetic etiology of bicuspid

aortic valve remained mostly unresolved.[42,43] So far only one gene, *NOTCH1* (MIM 190198), was described for bicuspid aortic valve.[44] Thus, to the best of our knowledge, GlcAT-I defects appear to be the second gene pathogenetically related to this frequent and clinically relevant heart defect.

Our findings show that mutations affecting the proteoglycan linker region cause another subtype of connective tissue disorders and suggest pathogenetic relevance for a spectrum of congenital heart defects, including bicuspid aortic valves.

Supplemental Data

Supplemental Data include seven figures and two tables and can be found with this article online at http://www.cell.com/AJHG/.

Acknowledgments

We thank the family for their interest and participation. Friedrich Luft critically read the manuscript. S.B. received a scholarship from the Mongolian government and from the Charité Medical faculty. K.S. was supported by Grants-in-aid for Scientific Research B (20390019) and the Matching Program for Innovations in Future Drug Discovery and Medical Care from the Ministry of Education, Culture, Sports, Science, and Technology of Japan (MEXT). S.M. was supported by Grants-in-Aid for regional R&D Proposal-Based Program from Northern Advancement Center for Science & Technology of Hokkaido, and Grants-in-Aid for Young Scientists (B) 23790066 from Japan Society for the Promotion of Science, Japan. K.H. was supported by the Deutsche Forschungsgemeinschaft (DFG, SFB 577, project A4) and is a recipient of a Rahel Hirsch Fellowship, provided by the Charité Medical Faculty. S.B. dedicates this work to her father, Baasanjav Tseveen. S.B. genotyped the family for fine mapping and resequenced candidate genes. She and B.F. performed immunostaining, western blot, and quantitative PCR. L.A., B.R.A., S.A.A.A., and R.L. examined the patients. L.A., R.L., K.H., S.M., and D.H. compared phenotypes and analyzed the X-rays. C.B. and P.N. performed the Affymetrix SNP genotyping. Linkage analyses were run by K.H., T.H.L., and G.N. B.R.A. performed database searches identifying B3GAT3 as a candidate. Protein modeling was done by V.C., D.S., and J.G.G. T.H., S.M., and K.S. performed proteoglycan and GlcAT-I assays. K.H. supervised the project and wrote the manuscript. All authors edited and confirmed the manuscript.

Received: February 9, 2011
Revised: April 14, 2011
Accepted: May 16, 2011
Published online: July 14, 2011

Web Resources

The URLs for data presented herein are as follows:

Online Mendelian Inheritance in Man (OMIM), http://www.omim.org
PyMol, http://www.pymol.org
RCSC protein data bank, http://www.rcsb.org/pdb/home/home.do

References

1. Bulik, D.A., Wei, G., Toyoda, H., Kinoshita-Toyoda, A., Waldrip, W.R., Esko, J.D., Robbins, P.W., and Selleck, S.B. (2000). sqv-3, -7, and -8, a set of genes affecting morphogenesis in *Caenorhabditis elegans*, encode enzymes required for glycosaminoglycan biosynthesis. Proc. Natl. Acad. Sci. USA *97*, 10838–10843.
2. Sugahara, K., Mikami, T., Uyama, T., Mizuguchi, S., Nomura, K., and Kitagawa, H. (2003). Recent advances in the structural biology of chondroitin sulfate and dermatan sulfate. Curr. Opin. Struct. Biol. *13*, 612–620.
3. Haltiwanger, R.S., and Lowe, J.B. (2004). Role of glycosylation in development. Annu. Rev. Biochem. *73*, 491–537.
4. Häcker, U., Nybakken, K., and Perrimon, N. (2005). Heparan sulphate proteoglycans: The sweet side of development. Nat. Rev. Mol. Cell Biol. *6*, 530–541.
5. Berninsone, P.M. (2006). Carbohydrates and glycosylation. WormBook *18*, 1–22.
6. Franks, D.M., Izumikawa, T., Kitagawa, H., Sugahara, K., and Okkema, P.G. (2006). *C. elegans* pharyngeal morphogenesis requires both de novo synthesis of pyrimidines and synthesis of heparan sulfate proteoglycans. Dev. Biol. *296*, 409–420.
7. Bishop, J.R., Schuksz, M., and Esko, J.D. (2007). Heparan sulphate proteoglycans fine-tune mammalian physiology. Nature *446*, 1030–1037.
8. Sugahara, K., and Mikami, T. (2007). Chondroitin/dermatan sulfate in the central nervous system. Curr. Opin. Struct. Biol. *17*, 536–545.
9. Izumikawa, T., Kanagawa, N., Watamoto, Y., Okada, M., Saeki, M., Sakano, M., Sugahara, K., Sugihara, K., Asano, M., and Kitagawa, H. (2010). Impairment of embryonic cell division and glycosaminoglycan biosynthesis in glucuronyltransferase-I-deficient mice. J. Biol. Chem. *285*, 12190–12196.
10. Dai, J., and Rabie, A.B. (2007). VEGF: An essential mediator of both angiogenesis and endochondral ossification. J. Dent. Res. *86*, 937–950.
11. Stringer, S.E. (2006). The role of heparan sulphate proteoglycans in angiogenesis. Biochem. Soc. Trans. *34*, 451–453.
12. Chan, C.K., Rolle, M.W., Potter-Perigo, S., Braun, K.R., Van Biber, B.P., Laflamme, M.A., Murry, C.E., and Wight, T.N. (2010). Differentiation of cardiomyocytes from human embryonic stem cells is accompanied by changes in the extracellular matrix production of versican and hyaluronan. J. Cell. Biochem. *111*, 585–596.
13. Pilia, G., Hughes-Benzie, R.M., MacKenzie, A., Baybayan, P., Chen, E.Y., Huber, R., Neri, G., Cao, A., Forabosco, A., and Schlessinger, D. (1996). Mutations in *GPC3*, a glypican gene, cause the Simpson-Golabi-Behmel overgrowth syndrome. Nat. Genet. *12*, 241–247.
14. Capurro, M.I., Li, F., and Filmus, J. (2009). Overgrowth of a mouse model of Simpson-Golabi-Behmel syndrome is partly mediated by Indian hedgehog. EMBO Rep. *10*, 901–907.
15. Sugahara, K., and Kitagawa, H. (2000). Recent advances in the study of the biosynthesis and functions of sulfated glycosaminoglycans. Curr. Opin. Struct. Biol. *10*, 518–527.
16. Prydz, K., and Dalen, K.T. (2000). Synthesis and sorting of proteoglycans. J. Cell Sci. *113*, 193–205.
17. Guérardel, Y., Balanzino, L., Maes, E., Leroy, Y., Coddeville, B., Oriol, R., and Strecker, G. (2001). The nematode *Caenorhabditis elegans* synthesizes unusual O-linked glycans: Identification of glucose-substituted mucin-type O-glycans and short chondroitin-like oligosaccharides. Biochem. J. *357*, 167–182.

18. Hoffmann, K., and Lindner, T.H. (2005). easyLINKAGE-Plus—Automated linkage analyses using large-scale SNP data. Bioinformatics *21*, 3565–3567.
19. Lindner, T.H., and Hoffmann, K. (2005). easyLINKAGE: A PERL script for easy and automated two-/multi-point linkage analyses. Bioinformatics *21*, 405–407.
20. Hoffmann, K., Dreger, C.K., Olins, A.L., Olins, D.E., Shultz, L.D., Lucke, B., Karl, H., Kaps, R., Müller, D., Vayá, A., et al. (2002). Mutations in the gene encoding the lamin B receptor produce an altered nuclear morphology in granulocytes (Pelger-Huët anomaly). Nat. Genet. *31*, 410–414.
21. Kitagawa, H., Tone, Y., Tamura, J., Neumann, K.W., Ogawa, T., Oka, S., Kawasaki, T., and Sugahara, K. (1998). Molecular cloning and expression of glucuronyltransferase I involved in the biosynthesis of the glycosaminoglycan-protein linkage region of proteoglycans. J. Biol. Chem. *273*, 6615–6618.
22. van Roij, M.H., Mizumoto, S., Yamada, S., Morgan, T., Tan-Sindhunata, M.B., Meijers-Heijboer, H., Verbeke, J.I., Markie, D., Sugahara, K., and Robertson, S.P. (2008). Spondyloepiphyseal dysplasia, Omani type: further definition of the phenotype. Am. J. Med. Genet. A *146A*, 2376–2384.
23. Tone, Y., Kitagawa, H., Imiya, K., Oka, S., Kawasaki, T., and Sugahara, K. (1999). Characterization of recombinant human glucuronyltransferase I involved in the biosynthesis of the glycosaminoglycan-protein linkage region of proteoglycans. FEBS Lett. *459*, 415–420.
24. Ouzzine, M., Gulberti, S., Levoin, N., Netter, P., Magdalou, J., and Fournel-Gigleux, S. (2002). The donor substrate specificity of the human beta 1,3-glucuronosyltransferase I toward UDP-glucuronic acid is determined by two crucial histidine and arginine residues. J. Biol. Chem. *277*, 25439–25445.
25. Wei, G., Bai, X., and Esko, J.D. (2004). Temperature-sensitive glycosaminoglycan biosynthesis in a Chinese hamster ovary cell mutant containing a point mutation in glucuronyltransferase I. J. Biol. Chem. *279*, 5693–5698.
26. Unger, S., Lausch, E., Rossi, A., Mégarbané, A., Sillence, D., Alcausin, M., Aytes, A., Mendoza-Londono, R., Nampoothiri, S., Afroze, B., et al. (2010). Phenotypic features of carbohydrate sulfotransferase 3 (CHST3) deficiency in 24 patients: congenital dislocations and vertebral changes as principal diagnostic features. Am. J. Med. Genet. A. *152A*, 2543–2549.
27. Hermanns, P., Unger, S., Rossi, A., Perez-Aytes, A., Cortina, H., Bonafé, L., Boccone, L., Setzu, V., Dutoit, M., Sangiorgi, L., et al. (2008). Congenital joint dislocations caused by carbohydrate sulfotransferase 3 deficiency in recessive Larsen syndrome and humero-spinal dysostosis. Am. J. Hum. Genet. *82*, 1368–1374.
28. Thiele, H., Sakano, M., Kitagawa, H., Sugahara, K., Rajab, A., Höhne, W., Ritter, H., Leschik, G., Nürnberg, P., and Mundlos, S. (2004). Loss of chondroitin 6-*O*-sulfotransferase-1 function results in severe human chondrodysplasia with progressive spinal involvement. Proc. Natl. Acad. Sci. USA *101*, 10155–10160.
29. Dündar, M., Müller, T., Zhang, Q., Pan, J., Steinmann, B., Vodopiutz, J., Gruber, R., Sonoda, T., Krabichler, B., Utermann, G., et al. (2009). Loss of dermatan-4-sulfotransferase 1 function results in adducted thumb-clubfoot syndrome. Am. J. Hum. Genet. *85*, 873–882.
30. Malfait, F., Syx, D., Vlummens, P., Symoens, S., Nampoothiri, S., Hermanns-Lê, T., Van Laer, L., and De Paepe, A. (2010). Musculocontractural Ehlers-Danlos Syndrome (former EDS type VIB) and adducted thumb clubfoot syndrome (ATCS) represent a single clinical entity caused by mutations in the dermatan-4-sulfotransferase 1 encoding *CHST14* gene. Hum. Mutat. *31*, 1233–1239.
31. Miyake, N., Kosho, T., Mizumoto, S., Furuichi, T., Hatamochi, A., Nagashima, Y., Arai, E., Takahashi, K., Kawamura, R., Wakui, K., et al. (2010). Loss-of-function mutations of CHST14 in a new type of Ehlers-Danlos syndrome. Hum. Mutat. *31*, 966–974.
32. Pedersen, L.C., Tsuchida, K., Kitagawa, H., Sugahara, K., Darden, T.A., and Negishi, M. (2000). Heparan/chondroitin sulfate biosynthesis. Structure and mechanism of human glucuronyltransferase I. J. Biol. Chem. *275*, 34580–34585.
33. Negishi, M., Dong, J., Darden, T.A., Pedersen, L.G., and Pedersen, L.C. (2003). Glucosaminylglycan biosynthesis: What we can learn from the X-ray crystal structures of glycosyltransferases GlcAT1 and EXTL2. Biochem. Biophys. Res. Commun. *303*, 393–398.
34. Ouzzine, M., Antonio, L., Burchell, B., Netter, P., Fournel-Gigleux, S., and Magdalou, J. (2000). Importance of histidine residues for the function of the human liver UDP-glucuronosyltransferase UGT1A6: Evidence for the catalytic role of histidine 370. Mol. Pharmacol. *58*, 1609–1615.
35. Gilchrist, A., Au, C.E., Hiding, J., Bell, A.W., Fernandez-Rodriguez, J., Lesimple, S., Nagaya, H., Roy, L., Gosline, S.J., Hallett, M., et al. (2006). Quantitative proteomics analysis of the secretory pathway. Cell *127*, 1265–1281.
36. Kresse, H., Rosthøj, S., Quentin, E., Hollmann, J., Glössl, J., Okada, S., and Tønnesen, T. (1987). Glycosaminoglycan-free small proteoglycan core protein is secreted by fibroblasts from a patient with a syndrome resembling progeroid. Am. J. Hum. Genet. *41*, 436–453.
37. Okajima, T., Fukumoto, S., Furukawa, K., and Urano, T. (1999). Molecular basis for the progeroid variant of Ehlers-Danlos syndrome. Identification and characterization of two mutations in galactosyltransferase I gene. J. Biol. Chem. *274*, 28841–28844.
38. Faiyaz-Ul-Haque, M., Zaidi, S.H., Al-Ali, M., Al-Mureikhi, M.S., Kennedy, S., Al-Thani, G., Tsui, L.C., and Teebi, A.S. (2004). A novel missense mutation in the galactosyltransferase-I (*B4GALT7*) gene in a family exhibiting facioskeletal anomalies and Ehlers-Danlos syndrome resembling the progeroid type. Am. J. Med. Genet. A *128A*, 39–45.
39. Li, Y., Laue, K., Temtamy, S., Aglan, M., Kotan, L.D., Yigit, G., Canan, H., Pawlik, B., Nürnberg, G., Wakeling, E.L., et al. (2010). Temtamy preaxial brachydactyly syndrome is caused by loss-of-function mutations in chondroitin synthase 1, a potential target of BMP signaling. Am. J. Hum. Genet. *87*, 757–767.
40. Tian, J., Ling, L., Shboul, M., Lee, H., O'Connor, B., Merriman, B., Nelson, S.F., Cool, S., Ababneh, O.H., Al-Hadidy, A., et al. (2010). Loss of CHSY1, a secreted FRINGE enzyme, causes syndromic brachydactyly in humans via increased NOTCH signaling. Am. J. Hum. Genet. *87*, 768–778.
41. Saigoh, K., Izumikawa, T., Koike, T., Shimizu, J., Kitagawa, H., and Kusunoki, S. (2011). Chondroitin beta-1,4-*N*-acetylgalactosaminyltransferase-1 missense mutations are associated with neuropathies. J. Hum. Genet. *56*, 143–146.
42. Bruneau, B.G. (2008). The developmental genetics of congenital heart disease. Nature *451*, 943–948.

43. Leong, F.T., Freeman, L.J., and Keavney, B.D. (2009). Fresh fields and pathways new: Recent genetic insights into cardiac malformation. Heart *95*, 442–447.
44. Garg, V., Muth, A.N., Ransom, J.F., Schluterman, M.K., Barnes, R., King, I.N., Grossfeld, P.D., and Srivastava, D. (2005). Mutations in NOTCH1 cause aortic valve disease. Nature *437*, 270–274.
45. Tone, Y., Pedersen, L.C., Yamamoto, T., Izumikawa, T., Kitagawa, H., Nishihara, J., Tamura, J., Negishi, M., and Sugahara, K. (2008). 2-*o*-phosphorylation of xylose and 6-*o*-sulfation of galactose in the protein linkage region of glycosaminoglycans influence the glucuronyltransferase-I activity involved in the linkage region synthesis. J. Biol. Chem. *283*, 16801–16807.

Publikation 2:

Baasanjav *et al. BMC Medical Genetics* 2010, **11**:110
http://www.biomedcentral.com/1471-2350/11/110

BMC Medical Genetics

RESEARCH ARTICLE Open Access

Osteopoikilosis and multiple exostoses caused by novel mutations in *LEMD3* and *EXT1* genes respectively - coincidence within one family

Sevjidmaa Baasanjav[†1,6], Aleksander Jamsheer[†2,3], Mateusz Kolanczyk[*†1,4], Denise Horn[1], Tomasz Latos[5], Katrin Hoffmann[1,4], Anna Latos-Bielenska[2,3] and Stefan Mundlos[1,4]

Abstract

Background: Osteopoikilosis is a rare autosomal dominant genetic disorder, characterised by the occurrence of the hyperostotic spots preferentially localized in the epiphyses and metaphyses of the long bones, and in the carpal and tarsal bones [1]. Heterozygous *LEMD3* gene mutations were shown to be the primary cause of the disease [2]. Association of the primarily asymptomatic osteopokilosis with connective tissue nevi of the skin is categorized as Buschke-Ollendorff syndrome (BOS) [3]. Additionally, osteopoikilosis can coincide with melorheostosis (MRO), a more severe bone disease characterised by the ectopic bone formation on the periosteal and endosteal surface of the long bones [4-6]. However, not all MRO affected individuals carry germ-line *LEMD3* mutations [7]. Thus, the genetic cause of MRO remains unknown. Here we describe a familial case of osteopoikilosis in which a novel heterozygous *LEMD3* mutation coincides with a novel mutation in *EXT1*, a gene involved in aetiology of multiple exostosis syndrome. The patients affected with both *LEMD3* and *EXT1* gene mutations displayed typical features of the osteopoikilosis. There were no additional skeletal manifestations detected however, various non-skeletal pathologies coincided in this group.

Methods: We investigated *LEMD3* and *EXT1* in the three-generation family from Poland, with 5 patients affected with osteopoikilosis and one child affected with multiple exostoses.

Results: We found a novel c.2203C > T (p.R735X) mutation in exon 9 of *LEMD3*, resulting in a premature stop codon at amino acid position 735. The mutation co-segregates with the osteopoikilosis phenotype and was not found in 200 ethnically matched controls. Another new substitution G > A was found in *EXT1* gene at position 1732 (cDNA) in Exon 9 (p.A578T) in three out of five osteopoikilosis affected family members. Evolutionary conservation of the affected amino acid suggested possible functional relevance, however no additional skeletal manifestations were observed other then those specific for osteopoikilosis. Finally in one member of the family we found a splice site mutation in the *EXT1* gene intron 5 (IVS5-2 A > G) resulting in the deletion of 9 bp of cDNA encoding three evolutionarily conserved amino acid residues. This child patient suffered from a severe form of exostoses, thus a causal relationship can be postulated.

Conclusions: We identified a new mutation in *LEMD3* gene, accounting for the familial case of osteopoikilosis. In the same family we identified two novel *EXT1* gene mutations. One of them A598T co-incided with the *LEMD3* mutation. Co-incidence of *LEMD3* and *EXT1* gene mutations was not associated with a more severe skeletal phenotype in those patients.

Background

Osteopoikilosis is a rare and primarily benign autosomal dominant genetic entity caused by heterozygous mutations in the *LEMD3* gene. It is characterised by the occurrence of the hyperostotic spots throughout the skeleton, with most frequent localization in the epiphyses and metaphyses of the long bones, as well as in the carpal and tarsal bones [1]. The clinical features of osteopoikilosis are relatively mild, therefore the condition is usually diagnosed by chance or because of the association with other

* Correspondence: kolanshy@molgen.mpg.de
[1] Institute of Medical Genetics, Charité Berlin, Humboldt University, Augustenburger Platz 1, 13353 Berlin, Germany
† Contributed equally
Full list of author information is available at the end of the article

medical problems (fractures, joint dislocations, etc.). In addition to spotty bone changes, some patients affected by osteopoikilosis develop the superficial skin lesions (elastic-type nevi) and/or subcutaneous foci of dermatofibrosis. Such combination of clinical features is categorized as a separate condition named the Buschke-Ollendorff syndrome [3]. Osteopoikilosis has also been found in association with a more severe and detrimental bone disease called melorheostosis. Melorheostosis manifests with predominantly asymmetric depositions of dense compact bone on the periosteal and endosteal surface of the long bones, resembling a dripping wax of a candle. Bone deformations are often associated with the ossification of the soft tissue in the joint proximity, which can cause compression of the adjacent nerves, and result in pain. Heterozygous *LEMD3* gene mutations were detected in all such cases. In contrast, no germline *LEMD3* mutations were found in the isolated cases of melorheostosis [7,8]. Thus, genetic cause of isolated melorheostosis remains unknown. Melorheostosis belongs to a group of osteogenic lesions together with another disease called hereditary multiple exostoses (HME) [9]. Multiple exostoses (enchondromas) are caused by heterozygous mutations in *EXT1*, *EXT2* and/or *EXT3* genes. The EXT proteins function in the proteoglycan synthesis and play tumour suppressor roles. *EXT1* and *EXT2* have both been shown to encode a heparan sulphate polymerase with both D-glucuronyl (GlcA) and N-acetyl-D-glycosaminoglycan (GlcNAC) transferase activities and their functions are indispensable for heparin-sulphate biosynthesis [10]. The nature of the tumour suppressor effects of the heparan sulphate biosynthesis is not entirely clear, however the regulation of Ihh signalling was proposed to play an important role [11]. Here we describe a family with 5 patients affected by osteopoikilosis caused by novel mutation in the *LEMD3* gene. Interestingly, three of the patients affected with this new *LEMD3* mutation additionally carry a new mutation in the *EXT1* gene. We discuss possible implications.

Methods

Patients

We studied a two-branch family of Polish descent. The main branch comprised three generations with five individuals affected by osteopoikilosis. We also examined a more distant kindred affected by the severe deformational condition of the long bones. The local ethics committee approved the study and written, informed consent was obtained from all participants or their legal guardians for publication of this case report, including clinical data, pedigree and X-ray images. Copies of all written consents are available for review on request.

DNA sequencing

The *LEMD3* and *EXT1* genes were analyzed by bidirectional sequencing with primers listed in the see (Table 1). PCR amplification of *LEMD3* gene was performed in a 20 μl final volume, contained 1 U of Taq polymerase (FIRE Pol) with buffer supplemented with 1.5 mM Mg^{2+}, 0.4 mM dNTP, 8 pmol of each forward and reverse primer, and 30 ng of DNA. The exons were amplified as following: 5 min at 94°C, 35 cycles (30 sec 94°C, 30 sec 60°C, 30 sec 72°C) 10 min 72°C. PCR amplifications of *EXT1* gene were performed in a 20 μl final volume, contained 1 U of Taq polymerase (Invitek) with buffer supplemented with 2 mM Mg^{2+}, 0.4 mM dNTP, 8 pmol of each forward and reverse primer, and 30 ng of DNA. PCR conditions used were as in case of *LEMD3*, with exception of exon1-2 and exon 6 amplification, where annealing temperature varied from 55°C to 61°C (touchdown PCR). PCR products were sequenced with the DNA Sequencing Kit BigDye™ Terminator v3.0 Cycle Sequencing (Applied Biosystems) on an ABI 3730 automated sequencer. All exons were compared to genomic sequence (NM_014319.3 for *LEMD3* gene and NM_000127.2 for *EXT1* gene) and variations were numbered according to Ensembl ENSG00000174106 for *LEMD3* and ENSG00000182197 for *EXT1*. Healthy control subjects were screened for the identified mutations in the *LEMD3* and *EXT1* genes via sequence analysis. cDNA was synthesised using random hexamer primers as described below. PCR amplification of the *EXT1* cDNA fragments was done with primer pairs listed in (Table 2). The amplification conditions were like for the genomic DNA sequencing. PCR products were sequenced with the DNA Sequencing Kit BigDye™ Terminator v3.0 Cycle Sequencing (Applied Biosystems) on an ABI 3730 automated sequencer.

Isolation of the primary osteoblast cells

Surgically removed exostosis was placed in alphaMEM medium supplemented with 10% FCS, Penicilin-Streptomycin and Glutamine and transported to laboratory within 24 h. Bone was cleaned of any remaining connective tissue and 3 rounds of collagenase IV (2 mg/ml) digest 1× 5 min. and 2× 20 min. each at 37°C were performed. Cells from the first digestion were discarded whereas second and third digests were pooled and seeded in the alpha-MEM medium. Cells were cultured till confluent.

RNA isolation and cDNA synthesis

Total RNA was isolated with peqGOLD *TriFast*™ reagent (PeqLab) according to supplied protocol. cDNAs were synthesised from 1 μg total RNAs with SuperscriptII (Invitrogen) according to manufacturer's guidelines.

Table 1: Sequences of the primers used for *LEMD3* and *EXT1* gene amplification and sequencing.

Exon name	F Primer sequence 5'- 3'	R Primer sequence 5' - 3'
LEMD3_e1-1	CTCAGGTGAGCTCCTCCC	CGACTCGTCCGAGCTGAAG
LEMD3_e1-2	GCGACCTCTCCTACTTACGG	GTCGTCGTCGTCCTCTTCC
LEMD3_e1-3	AGGAGAGGGACCCGGAG	GGGGAGTCCACACTGAAGG
LEMD3_e1-4	AGGAGGGTGTGATCAAGTGG	GCGCAAATAGTCTTTCAGGG
LEMD3_e2	TTTAGCAAAGTACATGCTGGC	TTATACGACAGTTAGGGAATACTCAG
LEMD3_e3	TTCAGATTATGTGGCTTCTGTG	TTCACAAATATAACACTGGACTTGG
LEMD3_e4	TGTGGTTAATGTAATGGTAGTTGTTTG	GGAACAAGAGCGAAACTGTG
LEMD3_e5-6	TTGGAGTAGTGGGAAAATGC	GCTGTGACTTATGTGGCAACC
LEMD3_e7-8	GAAGGTTCATTCCGTTGTGG	AGTTGAGAAGGGTCACAGCTC
LEMD3_e9	CATCTAAATCTTCTTTGAACAAACTCC	CAGAACGAGAGAGTTTTGCC
LEMD3_e10	CTAACCAGGGGTCTGGCTC	TTTGCTTGGAATTTAATGAAAGAG
LEMD3_e11-12	TCTACCTCCTGTTAGTCAACAAGC	TGGTAAAAGACATATGAGCACAAAAC
LEMD3_e13	ATTGCATGGCTCTTGGTTTG	GCTGCCTCACTGCTAAATCC
EXT1_e1-1	TCTTTACAGGCGGGAAGATG	TGTTCCACAAGTGGAGACTCTG
EXT_e1-2	CCAGGTTCTACACCTCGGAC	CTCAGTTCCAGGCTCAAAGG
EXT1_e2	CTGGTGGCTTTCCCGAG	AAGGGAAACCACACCTTCTC
EXT1_e3	AAGCTTCCTTTCCTTCTGGC	CCATGACACAGGTAATTTTCTCC
EXT1_e4	TGCTAGAAGCCAAATGCTATG	TGGACCAATCACACATCCC
EXT1_e5	CTCTGACTGCCACCATCTTTC	AAGCAATCTTCAATGCAGGG
EXT1_e6	ATTTGCTCCAGCATGAGGC	TGAATGAAAGGGAGTAGCAGG
EXT1_e7	GCTGAGATTTCCAGCTCCTC	AACAGGGAGAAGATATCTAGGGC
EXT1_e8	AGATTCCTTCGGTGTTGAGG	CAAGGCACGGCTAAAAGAAG
EXT1_e9	CCGGATTTTGCATTATGAATTAG	ATCAGCAAAACTTAAGCGGG
EXT1_e10	GGGATTCAAAGAATGGGTATG	CTGGGTGGAACAGCTAGAGG
EXT1_e11	TGCTCATTTGCCTGACTCC	ACAATCTGGCTCTGCTGATG

Results

Clinical History

In the current study we identified a family with congenital osteopoikilosis (Figure 1). The affected family members suffered from moderate to intermittent pain in the hands and feet, with onset of the symptoms varying from 15 (Patient IV:17) to 26 years of age (Patient III:13). X-ray examination revealed disseminated sclerotic foci in the bones of the hands and feet, in the epiphyseal parts of the long bones as well as pelvis and sacrum (Figure 2). Clinical features observed in the affected family members are summarized in (Table 3), and involve several findings: dermatofibrosis, tetralogy of fallot (TOF), ovarian and sinus cysts, diabetes mellitus type 2, and vitiligo. Interestingly these various features were presented by the patients who carried both *LEMD3* and *EXT1* gene muta-

Table 2: Sequences of the primers used for *EXT1* cDNA amplification and sequencing.

PCR name	F Primer sequence 5'- 3'	R Primer sequence 5' - 3'
EXT1 cDNA1	GCTGCTCGCCCGCCCTGGGTG	GTGGTGCAAGCCATTCCTAC
EXT1 cDNA2	CTCAGCTGGCTCTTGTCTCG	CTCGGTGTAGTCAGGCCAAG
EXT1 cDNA3	CTTGTGGAACAATGGTAGG	CCTATGACGGCAGCTTGGTTC
EXT1 cDNA4	GTATGATTATCGGGAAATG	CTGGGCACAGTACTGGGACTTGG
EXT1 cDNA5	CTGGTCTCTCAGTCCCAGC	GTCCCATCATTGTCTCCTTATAC
EXT1 cDNA6	GCCTCCAATCAAAGTGACCC	CTCTGCTGATGAGTGGATCTGC

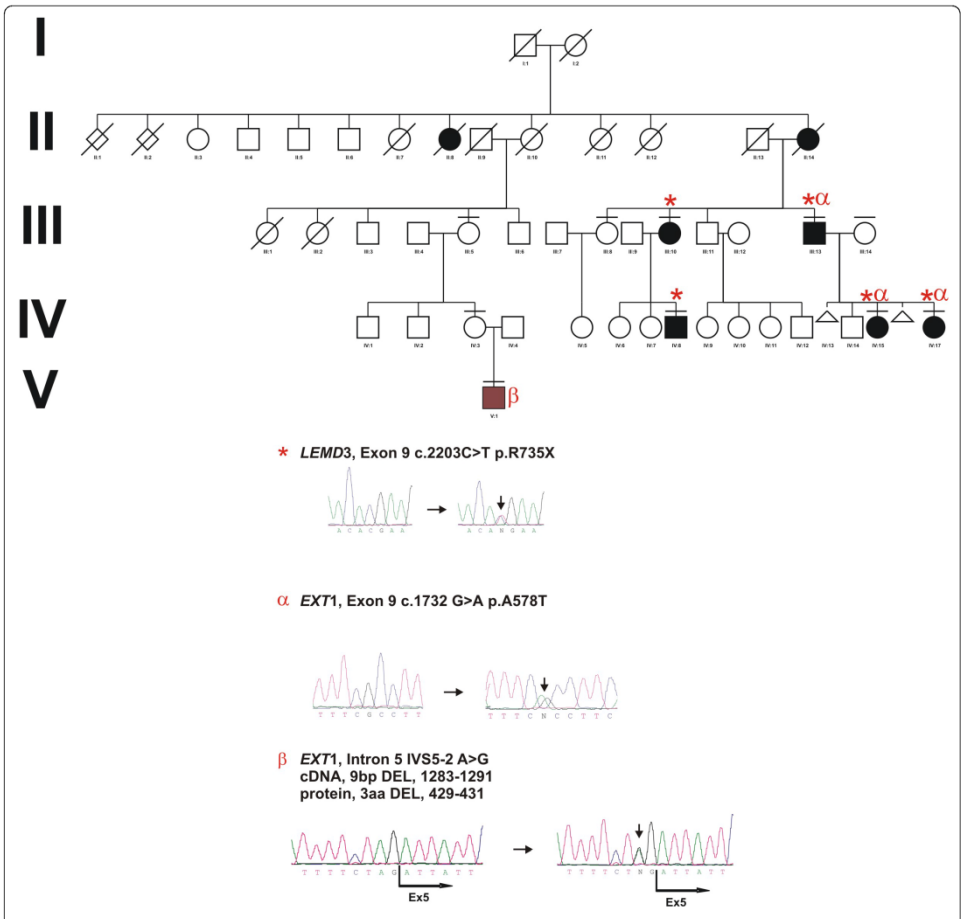

Figure 1 Co-occurrence of *LEMD3* and *EXT1* mutations. **(A)** Co-occurrence of *LEMD3* (*) and *EXT1* missense mutation (α) in the family affected with osteopoikilosis. A 9 bp deletion in *EXT1* gene (β) affecting patient suffering from multiple exostoses. **(B)** Representative electrophoregrams of the detected mutations. Osteopoikilosis phenotype is shown in black, whereas multiple exostoses syndrome is represented with brown colour. Horizontal bars over symbols mark patients who underwent clinical examination and molecular testing.

tions (with exception of dermatofibrosis which was presented by a patient affected with *LEMD3* mutation only).

We also consulted a more distant relative of this family (V:1), who was independently referred to a clinical geneticist at the age of 7 years. X-ray examination showed large multiple exostoses predominantly localized in the ends of the long bones (Figure 2). The boy was operated at the age of 7 years for a large exostosis affecting proximal part of the right humerus. Histopathological examination of the removed bone was suggestive of enchondromatosis.

Mutation Detection

Full coding sequence and exon-intron boundaries of the *LEMD3* gene were analyzed in the nine individuals. Patients (III:10, III:13, IV:8, IV:15, IV:17) were heterozygous for C-to-T transition in exon 9 (c.2203C > T) on genomic DNA. This mutation was predicted to change amino acid 735 from an arginine to a stop codon (p.R735X) (Figure 1, Figure 3A). Three out of these patients (III:13, IV:15, IV:17) additionally carried a heterozygous mutation in the *EXT1* gene. This mutation

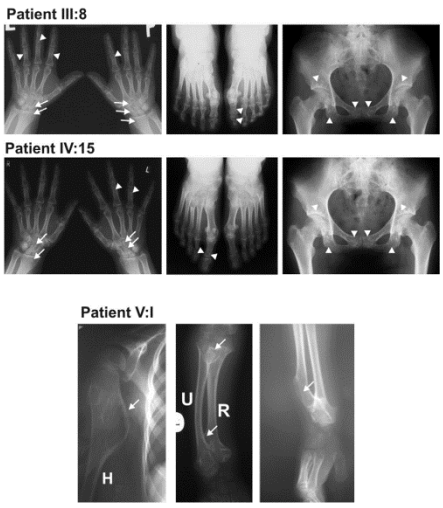

Figure 2 Sclerotic changes in the hands, feet, and pelvis of the osteopoikilosis affected patients positive for c.2203C > T (p.R735X) *LEMD3* mutation. (A) Hyperostotic spots are seen bilaterally in the distal parts of radius and carpal bones (arrows) as well as in the phalanges of hands and feet and in the pelvis (arrowheads). **(B)** Radiological appearance of the right hand of the proband (V:I - carrying intron 5 IVS5-2 A > G mutation) at the age of 5 years. Large exostoses in the proximal part of the humerus, as well as in the proximal and distal ends of the ulna and radius are demarcated with arrows.

altered G-to-A in exon 9 (c.1732G > A) on genomic DNA and predicted to change amino acid 578 from an alanine to a threonine (p.A578T). Presence of both *LEMD3* and *EXT1* variants was excluded among 81 and 247 healthy Polish and German controls respectively. Bioinformatic analysis of the EXT1 sequence with SIFT http://sift.jcvi.org and PolyPhen http://genetics.bwh.harvard.edu/pph/ software indicated a high probability of the mutation being deleterious for the protein function (PolyPhen - PSIC score difference for A578T: 1.688) - see (Figure 3B) for sequence conservation. However, affected patients did not exhibit exostoses and no additional skeletal manifestations beyond hyper-mineralized foci were detected. Interestingly, patients affected with both *LEMD3* and *EXT1* mutations presented spectrum of additional non-skeletal pathologies, which included: (IV:15) TOF and ovarian cysts, (IV:17) sinus cysts, and (III:13) diabetes melitus type 2 and vitiligo (Table 3).

A different mutation in *EXT1* gene was identified in the patient (V:1), diagnosed with multiple exostoses syndrome. The patient carried a heterozygotic splice site mutation in intron 5 (IVS5-2 A > G), as detected in blood lymphocytes and primary osteoblast progenitor cells obtained from the surgically removed exostoses. Sequencing of the exostoses derived cDNA (obtained from the cells isolated from the affected bone) showed that splice site mutation resulted in the in-frame deletion of 9 bp of the exon 5 leading to a deletion of three amino acids (pos. 429-431 - two conserved isoleucin residues and a conserved glutamic acid residue) (Figure 3B). Functional relevance of the deleted amino acids was predicted based on their evolutionary conservation.

Discussion

We identified a family with five members affected by osteopoikilosis caused by a novel nonsense heterozygous mutation (p.R735X) localised in exon 9 of the *LEMD3* gene. In other branch of this family we identified a boy affected by more severe bone deformations. The boy was initially suspected of the melorheostosis, but upon X-ray examination, the diagnosis was corrected to the multiple exostoses syndrome. Clinical diagnosis was subsequently confirmed by sequence analysis of the *EXT1* gene and identification of a previously undescribed splice site mutation (IVS5-2 A>G). This finding led us to sequence *EXT1* gene in the rest of the family. Surprisingly, three of the osteopoikilosis affected patients additionally to

Table 3: Clinical symptoms identified in the patients presenting with osteopoikilosis.

	Patient IV:15 (female; 26 years)	Patient IV:17 (female; 24 years)	Patient III:13 (male; 60 years)	Patient III:10 (female; 54 years)	Patient IV:8 (male; 19 years)
EXT1 mutation status	p.A578T	p.A578T	p.A578T	-	-
Painful hands and feet	+	+	+	+	+
Dermatofibrosis	-	-	-	+	-
Additional skin changes	-	-	Vitiligo	-	-
Other symptoms/disorders	TOF, Ovarian cyst	Sinus cyst	DM2	-	-
Laboratory tests (Ca, P, AP, ACP)	NE	NE	NE	Normal	NE

TOF - tetralogy of Fallot; DM2 - diabetes mellitus type 2; NE - not examined; Ca - calcium; P - phosphate; AP - alkaline phosphatase; ACP - acid phosphatase

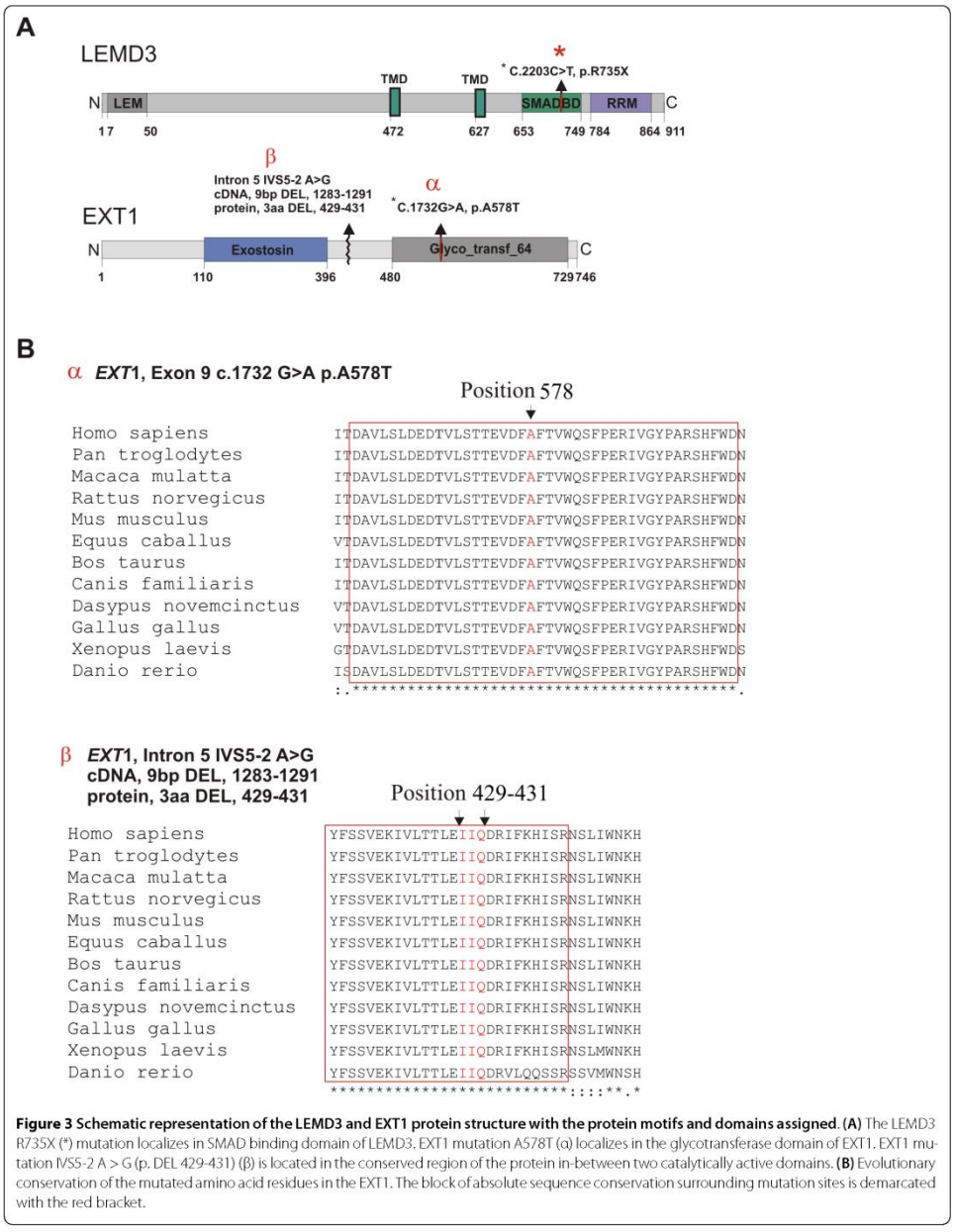

Figure 3 Schematic representation of the LEMD3 and EXT1 protein structure with the protein motifs and domains assigned. (A) The LEMD3 R735X (*) mutation localizes in SMAD binding domain of LEMD3. EXT1 mutation A578T (α) localizes in the glycotransferase domain of EXT1. EXT1 mutation IVS5-2 A > G (p. DEL 429-431) (β) is located in the conserved region of the protein in-between two catalytically active domains. **(B)** Evolutionary conservation of the mutated amino acid residues in the EXT1. The block of absolute sequence conservation surrounding mutation sites is demarcated with the red bracket.

LEMD3 mutation carried a yet unreported amino acid variant (p.A578T) in the *EXT1* gene. Of note was a wide spectrum of the clinical symptoms observed in these family members, which ranged from heart defect, diabetes mellitus, vitiligo to ovarian and sinus cyst formation. None of these pathologies was observed in the examined family members who carried *LEMD3* mutation only (patients III:10 and IV:8), nor in the family members who were free of mutations in both genes (patients III:5, III:8, III:14, IV:3). However, since we were unable to examine other unaffected family members, the relevance of this observation remains uncertain. The *EXT1* splice site mutation and other identified mutations must have occurred independently in the two branches of the family.

The exact mechanism by which *LEMD3* gene mutations lead to the formation of the bone lesions is not clear. *LEMD3* inactivation in mice was recently shown to result in the mid-gestation lethality [12]. However, heterozygous mice were healthy and no bone lesions reminiscent of osteopoikilosis could be detected, leaving question mark over patho-mechanism of the disease. Co-occurrence of the *LEMD3* gene mutation with the mutation in another gene has not yet been reported. Presented case constitutes first such report. Following considerations appear relevant based on the review of the available literature. It has been shown that LEM domain containing proteins interact with the barrier-to-autointegration factor (BAF) [13]. BAF is a component of the chromatin remodelling complex, which uses energy from ATP to dismantle DNA-histone complexes [14]. This is on one hand necessary for initiation of transcription, and it has been postulated that LEMD3, through BAF and SMAD interactions might regulate the expression of osteogenic genes [2]. On the other hand it is known that chromatin remodelling is necessary for the efficient DNA repair [15]. LEMD3 closely associates with the intranuclear lamina and mutations in other lamin interacting proteins are known to result in the DNA damage accumulation [16]. Indeed, it has been suggested that lamin complexes acts as assembly scaffolds for DNA repair machinery [17]. Thus, it seems legitimate to ask if inactivation of LEMD3 could also result in an increased mutational susceptibility and increased frequency of the post-zygotic second hit mutation occurrence. In this context it is interesting to note that osteopoikilosis was previously reported to coincide with other pathological entities, including various types of cancers: synovial chondromatosis [18], synoviosarcoma [19], chondrosarcoma [20], osteosarcoma [21], giant cell tumor [22], metastatic breast carcinoma [23], as well as developmental dysplasias: dental, facial abnormalities, coarctation of the aorta, double urether, mental retardation and other reviewed by Gunal et.al. [24].

Clearly, further research is needed to address possible association of the *LEMD3* loss of function with DNA mutation susceptibility. Presented study constitutes first example of the *LEMD3* gene mutation co-occurrence with additional genetic alteration, which could potentially modify and/or constitute the nature of the osteopoikilosis.

Conclusions

The presented case points to importance of the thorough clinical evaluation of the osteopoikilosis patients as phenotypic features of osteopoikilosis with melorheostosis might be confused with the co-occurrence of osteopoikilosis and multiple exostoses. The data encourage re-evaluation of the known osteopoikilosis families for the possible co-occurrence of other than Buschke-Ollendorff and melorheostosis disease entities and investigation of the possible LEMD3 function in the DNA repair.

Competing interests

The authors declare that they have no competing interests.

Authors' contributions

SV: performed sequencing and helped in manuscript preparation AJ: Consulted the family, collected and processed clinical material, conceived the manuscript. MK: coordinated sample processing, performed histological analysis of the surgically removed exostosis material, isolated primary cells from the exostoses tissue material and prepared DNA out of primary cells, and conceived the manuscript. DH: provided expert consultations critical in diagnosing multiple exostoses syndrome. KH: provided advice on sequencing, nuclear envelope proteins and helped in manuscript preparation. TL: Referred the family to a clinical geneticist. ALB: consulted the family, critically revised the manuscript. SM: critically revised the manuscript. All authors read and approved the final manuscript.

Acknowledgements

M.K. and N.K. were supported by the by the Young Investigator Award from Children Tumour Fundation - New York (Grant #2007-01-038) and Bundesministerium für Bildung und Forschung; Grant (NF1-01GM0844).
This work was also supported by the Sixth Framework of the European Commission (EuroGrow project LSHM-CT-2007-037471) and by a grant from the Polish Ministry of Science and Higher Education (495/N-NIEMCY/2009/0)
We thank Monika Osswald and Carola Dietrich for excellent technical assistance.

Author Details

[1]Institute of Medical Genetics, Charité Berlin, Humboldt University, Augustenburger Platz 1, 13353 Berlin, Germany, [2]Center for Medical Genetics in Poznań, ul. Grudzieniec 4, 60-601 Poznań, Poland, [3]Chair and Department of Medical Genetics, University of Medical Sciences in Poznań, ul. Grunwaldzka 55 paw.15, 60-352 Poznań, Poland, [4]Max Planck Institute for Molecular Genetics, Development and Disease, Ihnestraße 63-73, 14195 Berlin, Germany, [5]Department of Radiology and Diagnostic Imaging, Nicolaus Copernicus University, Collegium Medicum, Bydgoszcz, ul. Curie-Skłodowskiej 9, 85-094 Bydgoszcz, Poland and [6]Division of Nephrology, Department of Internal Medicine, University Clinic Leipzig, Philipp-Rosenthal-Str. 27, 04103 Leipzig, Germany

Received: 20 January 2010 Accepted: 9 July 2010
Published: 9 July 2010

References

1. Melnick JC: **Osteopathia condensans disseminata (osteopoikilosis); study of a family of 4 generations.** *Am J Roentgenol Radium Ther Nucl Med* 1959, **82(2):**229-238.

2. Hellemans J, Preobrazhenska O, Willaert A, Debeer P, Verdonk PC, Costa T, Janssens K, Menten B, Van Roy N, Vermeulen SJ, *et al.*: **Loss-of-function mutations in LEMD3 result in osteopoikilosis, Buschke-Ollendorff syndrome and melorheostosis.** *Nat Genet* 2004, **36(11):**1213-1218.
3. Ehrig T, Cockerell CJ: **Buschke-Ollendorff syndrome: report of a case and interpretation of the clinical phenotype as a type 2 segmental manifestation of an autosomal dominant skin disease.** *J Am Acad Dermatol* 2003, **49(6):**1163-1166.
4. Debeer P, Pykels E, Lammens J, Devriendt K, Fryns JP: **Melorheostosis in a family with autosomal dominant osteopoikilosis: report of a third family.** *Am J Med Genet A* 2003, **119A(2):**188-193.
5. Butkus CE, Michels VV, Lindor NM, Cooney WP: **Melorheostosis in a patient with familial osteopoikilosis.** *Am J Med Genet* 1997, **72(1):**43-46.
6. Nevin NC, Thomas PS, Davis RI, Cowie GH: **Melorheostosis in a family with autosomal dominant osteopoikilosis.** *Am J Med Genet* 1999, **82(5):**409-414.
7. Hellemans J, Debeer P, Wright M, Janecke A, Kjaer KW, Verdonk PC, Savarirayan R, Basel L, Moss C, Roth J, *et al.*: **Germline LEMD3 mutations are rare in sporadic patients with isolated melorheostosis.** *Hum Mutat* 2006, **27(3):**290.
8. Zhang Y, Castori M, Ferranti G, Paradisi M, Wordsworth BP: **Novel and recurrent germline LEMD3 mutations causing Buschke-Ollendorff syndrome and osteopoikilosis but not isolated melorheostosis.** *Clin Genet* 2009, **75(6):**556-561.
9. Bovee JV: **Multiple osteochondromas.** *Orphanet J Rare Dis* 2008, **3:**3.
10. Nadanaka S, Kitagawa H: **Heparan sulphate biosynthesis and disease.** *J Biochem* 2008, **144(1):**7-14.
11. Koziel L, Kunath M, Kelly OG, Vortkamp A: **Ext1-dependent heparan sulfate regulates the range of Ihh signaling during endochondral ossification.** *Dev Cell* 2004, **6(6):**801-813.
12. Dheedene A, Deleye S, Hellemans J, Staelens S, Vandenberghe S, Mortier G: **The Heterozygous Lemd3 (+/GT) Mouse Is Not a Murine Model for Osteopoikilosis in Humans.** *Calcif Tissue Int* 2009.
13. Margalit A, Brachner A, Gotzmann J, Foisner R, Gruenbaum Y: **Barrier-to-autointegration factor--a BAFfling little protein.** *Trends Cell Biol* 2007, **17(4):**202-208.
14. Lusser A, Kadonaga JT: **Chromatin remodeling by ATP-dependent molecular machines.** *Bioessays* 2003, **25(12):**1192-1200.
15. Zhang L, Zhang Q, Jones K, Patel M, Gong F: **The chromatin remodeling factor BRG1 stimulates nucleotide excision repair by facilitating recruitment of XPC to sites of DNA damage.** *Cell Cycle* 2009, **8(23):**.
16. Vlcek S, Foisner R: **Lamins and lamin-associated proteins in aging and disease.** *Curr Opin Cell Biol* 2007, **19(3):**298-304.
17. Manju K, Muralikrishna B, Parnaik VK: **Expression of disease-causing lamin A mutants impairs the formation of DNA repair foci.** *J Cell Sci* 2006, **119(Pt 13):**2704-2714.
18. Havitcioglu H, Gunal I, Gocen S: **Synovial chondromatosis associated with osteopoikilosis--a case report.** *Acta Orthop Scand* 1998, **69(6):**649-650.
19. Stadt J Van de, Thoua Y, Spiegl G, Rasquin C, Burny F: **Synoviosarcoma: presentation of a case and review of the literature.** *Rev Chir Orthop Reparatrice Appar Mot* 1984, **70(8):**643-648.
20. Grimer RJ, Davies AM, Starkie CM, Sneath RS: **Chondrosarcoma in a patient with osteopoikilosis. Apropos of a case.** *Rev Chir Orthop Reparatrice Appar Mot* 1989, **75(3):**188-190.
21. Mindell ER, Northup CS, Douglass HO Jr: **Osteosarcoma associated with osteopoikilosis.** *J Bone Joint Surg Am* 1978, **60(3):**406-408.
22. Ayling RM, Evans PE: **Giant cell tumor in a patient with osteopoikilosis.** *Acta Orthop Scand* 1988, **59(1):**74-76.
23. Kennedy JG, Donahue JR, Aydin H, Hoang BH, Huvos A, Morris C: **Metastatic breast carcinoma to bone disguised by osteopoikilosis.** *Skeletal Radiol* 2003, **32(4):**240-243.
24. Gunal I, Kiter E: **Disorders associated with osteopoikilosis: 5 different lesions in a family.** *Acta Orthop Scand* 2003, **74(4):**497-499.

Pre-publication history
The pre-publication history for this paper can be accessed here:
http://www.biomedcentral.com/1471-2350/11/110/prepub

doi: 10.1186/1471-2350-11-110
Cite this article as: Baasanjav *et al.*, Osteopoikilosis and multiple exostoses caused by novel mutations in *LEMD3* and *EXT1* genes respectively - coincidence within one family *BMC Medical Genetics* 2010, **11**:110

Publikation 3:

Nucleus 1:4, 354-366; July/August 2010 © 2010 Landes Bioscience

Mutations causing Greenberg dysplasia but not Pelger anomaly uncouple enzymatic from structural functions of a nuclear membrane protein

Peter Clayton,[1,†] Björn Fischer,[2,†] Anuska Mann,[1] Sahar Mansour,[3] Eva Rossier,[4] Markus Veen,[5] Christine Lang,[5] Sevjidmaa Baasanjav,[6,7] Moritz Kieslich,[7] Katja Brossuleit,[7] Sophia Gravemann,[7] Nele Schnipper,[7] Mohsen Karbasyian,[7] Ilja Demuth,[7] Monika Zwerger,[8] Amparo Vaya,[9] Gerd Utermann,[10] Stefan Mundlos,[2,11] Sigmar Stricker,[11] Karl Sperling[7] and Katrin Hoffmann[2,7,12,13,*]

[1]UCL Institute of Child Health with Great Ormond Street Hospital for ChildrenNHS Trust; London, UK; [2]Institute for Medical Genetics; Charité University Medicine; Berlin, Germany; [3]SW Thames Regional Genetics Service; St. George's Hospital Medical School; University of London; London, UK; [4]Humangenetik; Universitätsklinikum Tuebingen; Tuebingen, Germany; [5]Organobalance; Berlin, Germany; [6]Division of Nephrology; Department of Medicine, Neurology and Dermatology; University Hospital Leipzig; Leipzig, Germany; [7]Institute for Human Genetics; Charité University Medicine; Berlin, Germany; [8]B065 Functional Architecture of the Cell; German Cancer Research Center (DKFZ); Heidelberg, Germany; [9]Department of Clinical Pathology; La Fe University Hospital; Valencia, Spain; [10]Human Genetics; Department of Medical Genetics, Molecular and Clinical Pharmacology; Innsbruck, Austria; [11]Max Planck Institute for Molecular Genetics; Berlin, Germany; [12]Max Planck Institute for Human Development; Berlin, Germany; [13]The Berlin Aging Study II; Research Group on Geriatrics; Charité University Medicine; Berlin, Germany

[†]These authors contributed equally to this work.

Key words: Greenberg dysplasia, Pelger anomaly, lamin B receptor, sterol-metabolism, C14 sterol reductase

Abbreviations: LBR, lamin B receptor; ER, endoplasmatic reticulum; PHA, Pelger-Huët anomaly; HEM, hydrops, ectopic calcification and moth-eaten skeletal dysplasia (Greenberg dysplasia); gw, week of gestation; OC, in vitro differentiated osteoclast; HOS, human osteosarcoma cells; qPCR, quantitative PCR; SLOS, Smith-Lemli-Opitz syndrome; CHILD, congenital hemidysplasia with ichthyosiform erythroderma and limb defects; CDPX2, chondrodysplasia punctata X2; BLAST, basic local alignment search tool; FCS, fetal calf serum; PBS, phosphate buffered saline; BSA, bovine serum albumin; DAPI, 4',6-diamidin-2'-phenylindol-dihydrochlorid; SDS, sodium dodecyl sulfate; PVDF, polyvinylidenfluorid

The lamin B receptor (LBR) is an inner nuclear membrane protein with a structural function interacting with chromatin and lamins, and an enzymatic function as a sterol reductase. Heterozygous *LBR* mutations cause nuclear hyposegmentation in neutrophils (Pelger anomaly), while homozygous mutations cause prenatal death with skeletal defects and abnormal sterol metabolism (Greenberg dysplasia). It has remained unclear whether the lethality in Greenberg dysplasia is due to cholesterol defects or altered nuclear morphology.

To answer this question we characterized two LBR missense mutations and showed that they cause Greenberg dysplasia. Both mutations affect residues that are evolutionary conserved among sterol reductases. In contrast to wildtype LBR, both mutations failed to rescue C14 sterol reductase deficient yeast, indicating an enzymatic defect. We found no Pelger anomaly in the carrier parent excluding marked effects on nuclear structure. We studied Lbr in mouse embryos and demonstrate expression in skin and the developing skeletal system consistent with sites of histological changes in Greenberg dysplasia. Unexpectedly we found in disease-relevant cell types not only nuclear but also cytoplasmatic LBR localization. The cytoplasmatic LBR staining co-localized with ER-markers and is thus consistent with the sites of endogeneous sterol synthesis.

We conclude that LBR missense mutations can abolish sterol reductase activity, causing lethal Greenberg dysplasia but not Pelger anomaly. The findings separate the metabolic from the structural function and indicate that the sterol reductase activity is essential for human intrauterine development.

*Correspondence to: Katrin Hoffmann; Email: katrin.hoffmann.genetik@charite.de; khoffma@gmx.net
Submitted: 03/24/10; Revised: 05/21/10; Accepted: 05/21/10
Previously published online: www.landesbioscience.com/journals/nucleus/article/12435

Introduction

The lamin B receptor (LBR) is a multifunctional inner nuclear membrane protein with structural impact on nuclear shape and chromatin organization.[1] The nucleoplasmatic part directly and indirectly interacts with chromatin, lamins, heterochromatin proteins HP1α and γ, histones H3 and H4 and other nuclear components.[2,3] The transmembrane part belongs to the sterol reductase family and exhibits sterol reductase activity in vivo.[4-7]

LBR and lamins contribute to chromosome positioning, gene expression and distribution of nuclear pore complexes. Also, the lamin network has been shown to be involved in other essential cellular processes such as mitosis, meiosis and apoptosis. Laminopathies are diseases associated with lamin network proteins. Alterations of nuclear envelope components such as emerin or lamin A/C change nuclear shape and cause a variety of human diseases. Manifestations range from developmental to degenerative phenotypes, including cardiomyopathy, restrictive dermatopathy, lipodystrophy, mandibuloacral dysplasia, muscular dystrophy, peripheral neuropathy and premature ageing syndromes.[8-14] This demonstrates the essential cellular and clinical impact of the lamin network.

Lamin B receptor mutations cause human Pelger anomaly (Pelger-Huët anomaly, PHA [MIM 169400]), human lethal Greenberg dysplasia (HEM [MIM 215140]), and recessive ichthyosis in mice (ic/ic). We showed earlier that *LBR* mutations cause dose-dependent hyposegmentation of granulocyte nuclei in individuals with heterozygous or homozygous Pelger anomaly.[15] Heterozygous *LBR* mutations alter neutrophil morphology without causing disease, while homozygous *LBR* mutations cause a spectrum of systemic malformations ranging from cardiac defects, brachydactyly and mental retardation (as occurs in homozygous Pelger anomaly), to severe skin disease (modeled by ichthyotic ic/ic mice) and prenatal death, as found in Greenberg dysplasia.[15-18]

Greenberg dysplasia is also known as HEM skeletal dysplasia, an abbreviation derived from the characteristic features hydrops, ectopic calcification and moth-eaten skeletal dysplasia.[18-25] The disease is associated with an abnormal sterol metabolite, cholesta-8,14-dien-3β-ol. Defects in other sterol synthesis enzymes present with skeletal malformations, mental retardation, failure to thrive or even death, and are viewed as metabolic malformation syndromes.[26] Whereas some groups believe that in Greenberg dysplasia the sterol defect is causative,[18,26] others assume the primary problem in altered nuclear structure.[27]

So far, truncating mutations, namely nonsense, splice site and frameshift mutations, have been reported for Pelger anomaly.[15-17] For Greenberg dysplasia, one homozygous nonsense mutation and one homozygous missense mutation in the lamin B receptor gene were described.[18,28] In the family with Greenberg dysplasia due to homozygous missense mutation p.N547D, no sterol measurements or blood smears were available.[28] It thus remained unclear whether or not the lethal effect is due to altered sterol metabolism or due to altered nuclear structure.[28,29]

Results

We studied three fetuses that all fulfilled the clinical criteria of Greenberg dysplasia, namely intrauterine growth retardation, massive generalized edema (hydrops), extreme shortening of long bones (tetrabrachymelia) with a moth-eaten appearance of tubular bones, ectopic calcification centers and a narrow thorax (Fig. 1A, Suppl. Table 1). Detailed clinical examination was obtained from fetus A; fetus B has been described previously.[25] Sterol analyses were performed in muscle tissue of fetus B and revealed the abnormal sterol metabolite 5α-cholest-8,14-dien-3β-ol,[25] that was previously shown to be associated with Greenberg dysplasia.[18] Sterol analysis was not available for the other two fetuses.

Sequence analysis revealed frameshift and missense mutations in the LBR gene. We sequenced *LBR* and identified mutations in all three families (Fig. 1B, sequence traces and segregation in Suppl. Fig. 1A). Fetus A showed a homozygous frameshift mutation c.1492delT that is predicted to change residues 468 to 474 and to create a premature stop in codon 475 (p.Y468TfsX475). Fetus B revealed two different mutations, c.32delTGGT and c.1748G>A. The first is a deletion of 4 base pairs causing a frame shift with subsequent premature stop in codon 24 (p.V11EfsX24). The second is a missense mutation replacing arginine by glutamine at residue 583 (R583Q). Both parents of fetus C were carriers of the missense mutation p.N547D. Even though no material was available from fetus C to show homozygosity for mutation p.N547D, consanguinity of the parents and the presence of the same mutation in another fetus with Greenberg dysplasia[28] indicate that this mutation was causative. We proved that the nucleotide changes were not present in 150 controls, thereby making a polymorphism unlikely. For the missense mutations, we tested another 150 controls, to further reduce the possibility that they were rare variants.

The missense mutations reside in the sterol reductase domain and affect evolutionary conserved residues (Fig. 1B). We tested the potential relevance of the identified missense mutations by an interspecies comparison. The p.N547D and p.R583Q mutations both change residues that are evolutionary extremely conserved among LBR and other sterol reductases, indicating their functional relevance (Suppl. Fig. 1B). Sequencing of *DHCR7* and *TM7SF2* did not reveal alterations in any of the families, excluding a second hit in another gene of the C14 sterol reductase family.

LBR missense mutation did not alter nuclear shape in neutrophils. Since both missense mutations reside in the sterol reductase domain of the lamin B receptor, disruption of the sterol reductase function seemed likely. However, the position of these mutations made effects on the second function of the lamin B receptor, namely nuclear structure, less likely. Based on the assumption that the amino acid substitution does not affect essential regions for modification, transport, or lamin B receptor anchoring, we expected nuclear morphology to remain unchanged. To test this hypothesis, we obtained blood from the parents of fetus B. The blood smear of the father indeed showed apparently normal neutrophils with multisegmented nuclei, whereas the mother had an obvious heterozygous Pelger anomaly

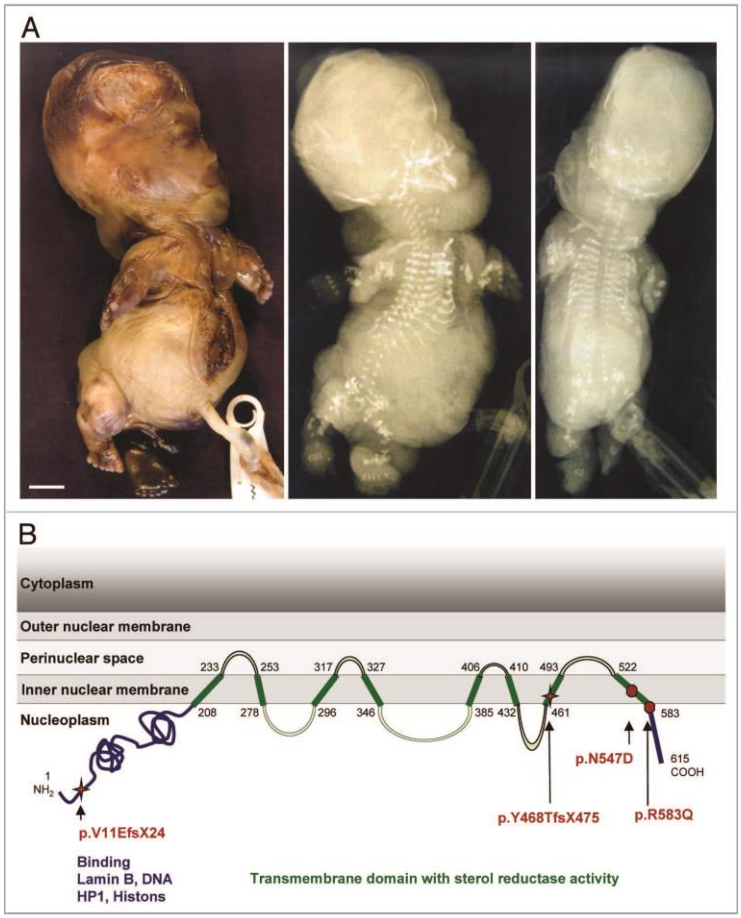

Figure 1. Phenotype and identified mutations. (A) Post mortem appearance of fetus A at 16 + 3 weeks pregnancy. Note the edema, extreme micromelia of all four limbs and roentgenographic moth-eaten appearance of tubular bones. The thorax is deformed and narrow. Note the large head with hygroma and the hexadactyly on hands and feet. Scale bar 1 cm. (B) Schematic view of the lamin B receptor as a protein of the inner nuclear membrane and identified mutations. The nucleoplasmatic part interacts directly and indirectly with lamins, chromatin and other nuclear proteins. The transmembrane domain belongs to the C14 sterol reductase family and displays sterol reductase activity. The missense mutations p.N547D and p.R583Q reside in the transmembrane domain (sterol reductase domain). The two frameshift mutations are predicted to create a premature stop codon and thus the RNA is likely to undergo nonsense mediated decay, abolishing both the structural and metabolic function. Missense mutation p.N547D was previously described.[28]

with nuclear hyposegmentation (**Fig. 2**). This state of affairs was confirmed by sequence analyses. The mother with the Pelger anomaly was the carrier of the nonsense mutation p.V11EfsX24. The father, with the normal neutrophils on blood smears, carried the heterozygous missense mutation p.R583Q, indicating that this mutation affects sterol metabolism but not nuclear shape. No blood smears from the parents of fetus A and C were available.

Both missense mutations failed to compensate for C14 sterol reductase deficiency in yeast. The human wildtype lamin B receptor can complement for the sterol reductase function in yeast.[5,30] LBR belongs to the C14 sterol reductase family as does yeast ERG24. The ERG24 deficient yeast has an altered sterol metabolism where the normal end product, ergosterol, is missing and the abnormal metabolite ignosterol is produced instead.

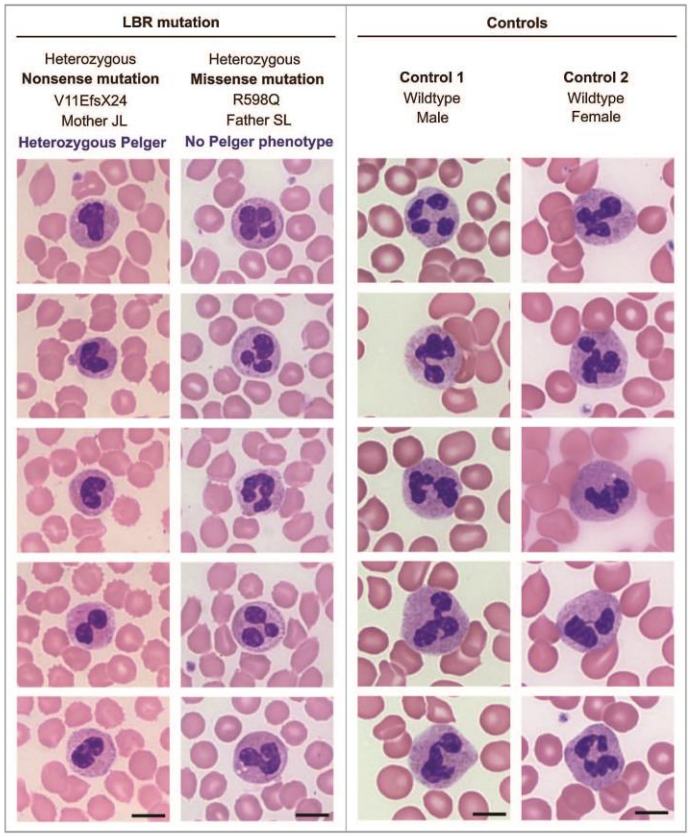

Figure 2. Neutrophils show normal nuclei with multiple segments in the father with heterozygous missense mutation p.R583Q and in controls, indicating that this mutation does not affect nuclear shape. In contrast, the mother is a heterozygous carrier of a nonsense mutation and shows Pelger anomaly with hypolobulated nuclei in blood smears. Five representative neutrophils per individual are shown. Scale bar 10 µm.

Since ergosterol is essential, ERG24 mutants show impaired growth (**Fig. 3A, Suppl. Fig. 2**).

We first demonstrated that wildtype human LBR and wildtype yeast ERG24 rescued the ERG24 deficient yeast phenotype in our system (data not shown). We then introduced the missense mutations p.N547D and p.R583Q, respectively, and transformed yeast with these mutant variants. We found that the mutants failed to rescue the yeast ergosterol phenotype (**Fig. 3B**). As expected, wildtype yeast showed metabolites of the normal pathway, lanosterol, fecosterol and ergosterol. The same applied for ERG24 deficient yeast rescued by transformation with the yeast ERG24 gene or by the human LBR wildtype gene. The human LBR mutant p.N547D also produced fecosterol and ergosterol in an amount similar to the wildtype rescue, indicating a partial compensation. However, p.N547D caused a significant accumulation of the abnormal metabolites 4-methylzymosterol and ignosterol. Human mutation p.R583Q failed to produce the normal end product ergosterol in significant amounts. Instead, we observed a huge accumulation of the abnormal end product ignosterol. Both mutations increased the total amount of pathway metabolites, probably to provide at least trace amounts of ergosterol that is necessary for a number of essential cellular functions in yeast. Analyses of growth pattern confirmed these results with p.N547D partially restoring growth and p.R583Q failing to do so (**Fig. 3C**).

In fibroblasts, LBR is not only located at the nuclear rim but also shows significant non-nuclear localization. The lamin B receptor is a protein of the inner nuclear membrane. Accordingly predominant localization was so far only reported in the nucleus. To test the hypothesis that malformations observed in Greenberg dysplasia result from effects other than nuclear sterol synthesis, we studied the cellular distribution of the protein. The abnormal sterol metabolite in Greenberg dysplasia was initially identified by growing Greenberg fetal fibroblasts in lipid-depleted serum.[18] We therefore reasoned that fibroblasts are a reasonable cell type to test this hypothesis and indeed found extensive localization of the lamin B receptor outside the nucleus (**Fig. 4A and B**). De-novo endogeneous sterol synthesis takes place in the endoplasmatic reticulum (ER). Accordingly, we found a co-localization of the non-nuclear LBR with calnexin as an ER membrane component (representative localization in **Fig. 4A**; more cells are shown in **Suppl. Fig. 3**). Further, we tested this in HeLa cells that have a higher growth rate and a higher expression level of LBR compared to fibroblasts. We found extensive cytoplasmic localization of LBR co-localizing with calnexin in immunostaining also in this cell type. Further, the western blot of fractionated HeLa cells revealed LBR in both the nuclear and cytoplasmic fraction whereas the nuclear marker lamin B was only present in the nuclear fraction (**Suppl. Fig. 4**).

LBR is expressed in human osteoclasts and osteoblast-like cells. The Greenberg phenotype manifests as hydrops and severe skeletal dysplasia with shortening of long bones and altered

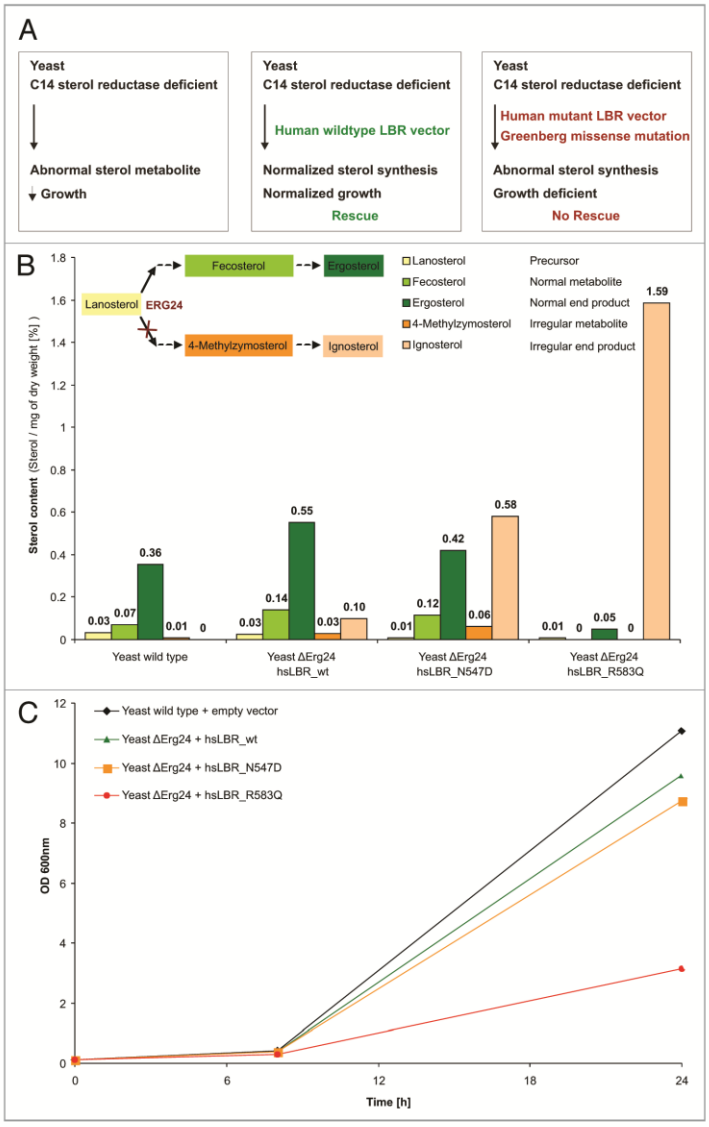

Figure 3. Design and results of the yeast rescue experiment. (A) Systematic view of the rescue experiment. (B) Analysis of human LBR constructs by GC/MS. hLBRwt is able to complement ERG24 deficiency in yeast. hLBR_N547D is partially able to complement ERG24 deficiency, visible in the production of the end product of the sterol pathway, ergosterol. However, providing this essential component happens on the cost of also producing large amounts of the abnormal metabolites 4-methylzymosterol and ignosterol. hLBR_R583Q is not able to complement ERG24 deficiency, seen in the insufficient production of the normal endproduct ergosterol and massive accumulation of the irregular product ignosterol. (C) Growth pattern. Mutation p.R583Q failed to normalize the growth of Erg24 deficient yeast. Mutation p.N547D partially compensated for Erg24 deficiency with respect to growth.

growth plates in early fetal development. Therefore, we analyzed RNA levels in potentially disease-relevant human cell lines. We found expression of *LBR* in fibroblasts, lymphoblastoid cells, and to a very high degree in human in vitro differentiated osteoclasts (OC) and human osteosarcoma cells (HOS) which are osteoblast-like (**Fig. 5A**).

LBR is strongly expressed in liver, skin, brain as well as in specific regions of the developing cartilage and bone in mouse embryos. To analyze Lbr expression in vivo we studied wildtype mouse embryos at developmental stages consistent with the earliest manifestations in human Greenberg fetuses which have been reported as early as in gw 13 by ultrasound. In situ hybridization in wildtype mouse embryos at embryonic day E12.5 (corresponding to human gw 8 + 2) and qPCR of mouse tissues at postnatal day P4 showed strong expression of *Lbr*-RNA in the liver, lung, midgut, skin, brain, as well as in developing cartilage (**Fig. 5B and C**). To further analyze Lbr expression in growth plate cartilage we performed immunohistochemistry on E15.5 mouse forelimb sections in comparison to the chondrogenic marker Sox9 (**Fig. 6A**). Lbr is expressed throughout growth plate cartilage, with weaker expression in hypertrophic chondrocytes. At the sites of trabecular bone formation Lbr expression was also seen in osteoblasts. In addition to the cartilage/bone expression, a signal for Lbr protein was also observed in muscle and in connective tissue fibroblasts. Consistent with the findings in human fibroblast cultures, we found, in addition to localization at the nuclear rim, a nonnuclear staining in connective tissue fibroblasts and also in Lbr-expressing cells of the developing cartilage and bone (**Fig. 6A** and magnification in **B**).

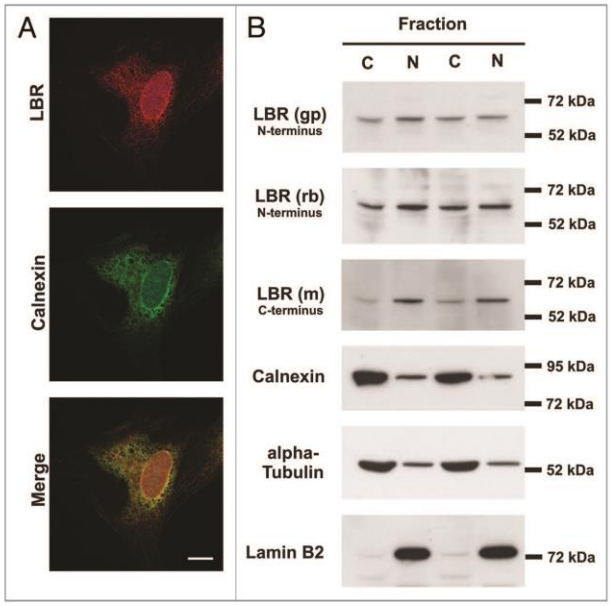

Figure 4. Localization of the lamin B receptor in human control fibroblasts. (A) Lamin B receptor staining (gp-anti-LBR_N-term) of the nuclear rim and in addition in the cytoplasm in control fibroblasts. The non-nuclear LBR showed a partial co-localization with the ER membrane protein calnexin (green), indicating a localization of LBR in this compartment. Scale bar 10 µm. (B) Nuclear (N) and cytoplasmatic (C) extracts from human control skin fibroblasts showed a strong LBR expression in both the nuclear and the cytoplasmatic fraction by three different LBR antibodies. The nuclear protein lamin B2 and the cytoplasmatic alpha tubulin confirmed separation of the nuclear and cytoplasmatic fractions.

Discussion

We studied three cases of Greenberg dysplasia in which *LBR* missense and nonsense mutations were identified. There was no phenotypic difference between fetuses with nonsense and missense mutations. Both missense mutations changed evolutionary conserved residues of the sterol reductase domain and failed to rescue sterol reductase deficient yeast. We showed that carrying a heterozygous missense mutation affecting the sterol reductase domain did not alter nuclear shape in neutrophils. We demonstrated LBR expression in cytoplasmatic compartments (ER) and in embryonic structures essential for bone development. Our findings uncouple the metabolic from the structural function of LBR and indicate that the developmentally essential enzymatic function may be exerted in the ER.

LBR is a hybrid protein, is likely to mediate separate functions and thus could also contribute to separate distinct diseases. LBR is the only sterol reductase that gained an additional 200 amino acids at the N-terminus which added new functions such as the localization to the nucleus and interaction with chromatin and other nuclear components.[1-7] The combination of an enzymopathy and a structural trait by mutations in the same gene product is, as to our knowledge, quite unique. We draw attention to the dominant structural effect in Pelger anomaly and the recessive enzymopathy in Greenberg dysplasia.

The N-terminal part mediates the interaction of the lamin B receptor with lamins, chromatin and heterochromatin proteins.[2,4,31] Nonsense mutations with subsequent loss of the encoded protein impair that structural function and result in hyposegmentation of neutrophil nuclei and altered chromatin structure, as seen in the Pelger blood phenotype in the mother with the heterozygous nonsense mutation p.V11EfsX24. In contrast, the nuclear structure of neutrophils was unaffected by missense mutation p.R583Q which affects a residue of the sterol reductase domain only. The father of fetus B was heterozygous for missense mutation p.R583Q and did not show any evidence for Pelger anomaly. We assume that the nuclear structure is also not markedly altered in other cell types since the nuclei of neutrophils are especially sensitive to loss of LBR. In addition, the position of this mutation within the membrane makes a marked structural effect on nuclear shape unlikely. The same applies for missense mutation p.N547D where no blood smears from the parents were available.

In contrast, both missense mutations failed to compensate for C14 sterol reductase deficiency in yeast, indicating severe enzymatic defects in sterol metabolism. We showed that both missense mutations affect evolutionary conserved residues of sterol reductases and experimentally proved that they both failed to compensate for sterol reductase deficiency in yeast. While p.R583Q completely failed to compensate, p.N547D could partially restore C14 sterol reduction, but produced a huge amount of abnormal metabolites. The relevant functional effect is underscored by the fact that mutations in homologous positions in another human sterol reductase, 7-dehydrocholesterol reductase [DHCR7 (MIM 602858)], cause Smith-Lemli-Opitz syndrome [SLOS (MIM 270400)].[6,32] Smith-Lemli-Opitz syndrome is a recessive disease with multiple malformations including skeletal and developmental defects, and mental retardation.[33,34] Notably, an abnormal sterol metabolite is also found in the same pathway where LBR is expected to function; whereas LBR acts in an earlier step in cholesterol synthesis, DHCR7 catalyzes the final conversion from 7-dehydrocholesterol to cholesterol (overview in **Fig. 7**, reviewed in ref. 26). The lamin B receptor mutation LBR. N547D corresponds to a mutation found in Smith-Lemli-Opitz syndrome affecting residue DHCR7.N407Y.[32] Mutation LBR. R583Q has a homolog DHCR7 mutation with even an identical amino acid exchange from arginine to glutamine (DHCR7. R443Q).[6] We excluded mutations in *DHCR7* and *TM7SF2* in all three of our families. Thus, both LBR missense mutations

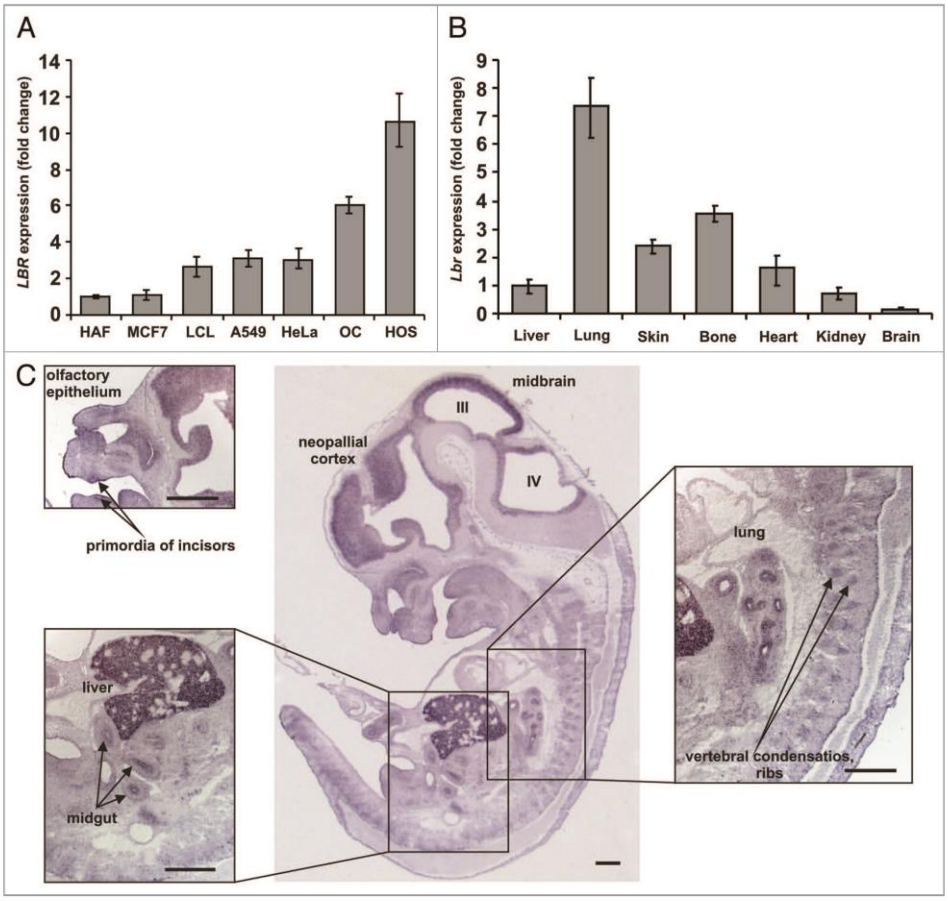

Figure 5. Expression of the lamin B receptor in different cell types and in development. (A) Relative LBR mRNA expression in different human cell lines, calibrated to fibroblasts. The highest expression is found in cell types associated with skeletal development, consistent with the most obvious manifestations in Greenberg dysplasia. Analyzed cell types: Skin fibroblasts (HAF), breast cancer cells (MCF-7), lymphoblastoid cells (LCL), lung cancer cells (A549), cervical cancer cells (HeLa), in-vitro differentiated osteoclasts (OC) and osteosarcoma cells (HOS). (B) Lbr expression in mouse tissues from developmental stage P4, calibrated to liver. Lung, skin and bone show the highest Lbr expression which is consistent with the main manifestation sites in patients with Greenberg dysplasia. (C) In-situ hybridization of Lbr in day 12.5 mouse embryos. Pronounced expression is found in liver, in several regions of the brain, in skin, developing incisors, in midgut epithelium, lung epithelium and in vertebral condensations. Mouse embryonic day E12.5 corresponds to human gestational week 8 + 2 (post menstruation). Scale bar 500 µm.

appear to result in functional null effects with respect to sterol metabolism.

The relevance of the metabolic function of LBR for Greenberg dysplasia is underscored by a phenotypic and pathogenic overlap with other diseases associated with cholesterol synthesis in humans. The congenital hemidysplasia with ichthyosiform erythroderma and limb defects [CHILD syndrome (MIM 308050)], chondrodysplasia punctata X2 [CDPX2 (MIM 302960)], lathosterolosis [MIM 607330], desmosterolosis [MIM 602398] and Smith-Lemli-Opitz syndrome all have defects in enzymes of the cholesterol synthesis pathway downstream of LBR (**Fig. 7**). Skeletal defects, complete or increased prenatal or perinatal lethality and dysmorphic facies are present in all these conditions (reviewed in ref. 26). The results presented here fit with the view that the enzymopathy in LBR deficiency is causative for Greenberg dysplasia and thus indeed belongs to

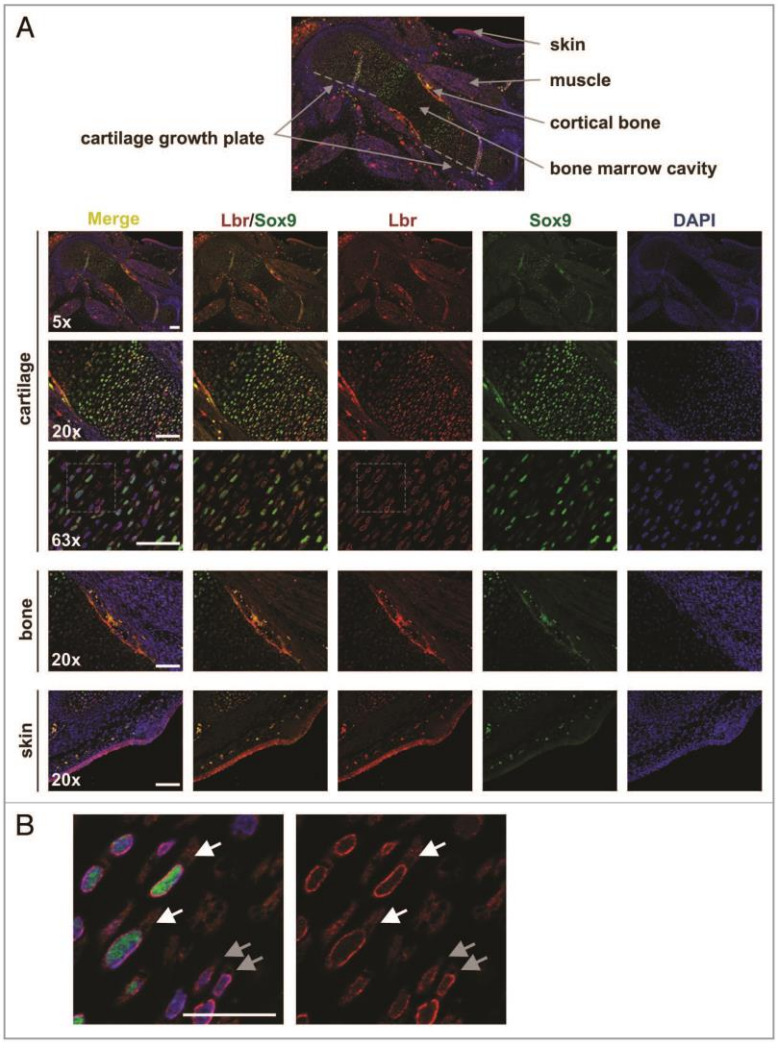

Figure 6. Expression analysis of Lbr protein in wildtype mouse fore limb on embryonic day E15.5. (A) Lbr (red) is strongly expressed in skin and in growth plate cartilage with exception of the hypertrophic zone. Immunostaining for the cartilage marker Sox9 (green) is shown for comparison. Positive staining is also detected in skin, muscle cells and connective tissue fibroblasts. In the region of the cortical bone, osteoblasts show a specific Lbr staining in higher magnification. DNA was stained by DAPI (blue). (Note that the bright Lbr and Sox9 staining at the diaphysic bone collar is an artifact due to unspecific antibody binding to the bone matrix). Scale bars: 5x and 20x 100 µm, 63x 50 µm. (B) Cytoplasmatic staining in chondrocytes and connective tissue fibroblasts. White arrowheads point to cytoplasmatic LBR staining in chondrocytes, grey in connective tissue fibroblasts. Magnification from (A) 63x cartilage. Scale bar 25 µm.

the metabolic malformation syndromes.[26] Detailed mechanistic information is not yet available how the loss of sterol reductase activity of the lamin B receptor causes Greenberg dysplasia. The abnormal metabolite, cholesta-8,14-dien-3β-ol, may mediate toxic effects. Alternatively, upstream or downstream intermediates in cholesterol metabolism that are altered in quantity or

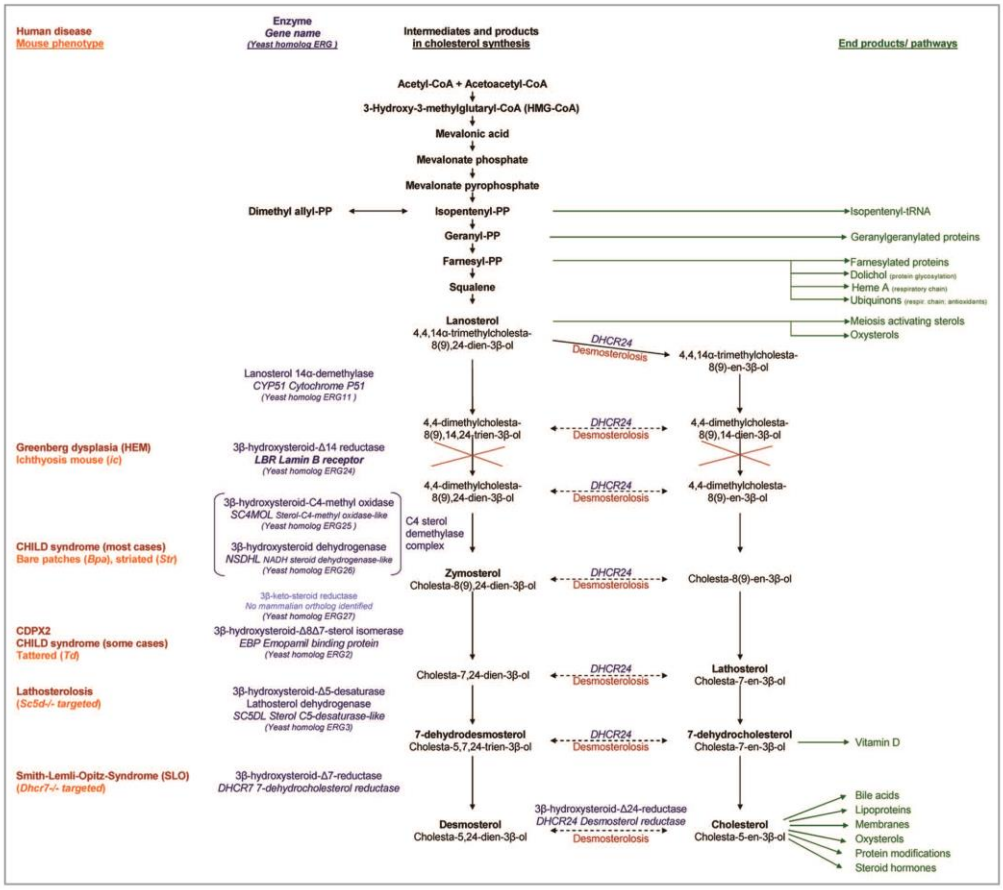

Figure 7. Cholesterol synthesis pathway, associated diseases and putative pathogenic mechanisms (reviewed in refs. 26, 49 and 50). Blockade of the C14 sterol step might lead to an accumulation of precursors with subsequent up or downregulation. This accumulation could affect important pathways such as farnesylation, heme and ubiquinone synthesis, or even the first hydroxyl methyl glutaryl CoA reduction step. Equally or more likely might be a deficiency in downstream products. LBR catalyzes an early step in post-squalene cholesterol synthesis. Failure in this step might subsequently result in different amounts or composition of derivates from intermediate steps, such as meiosis activating sterols, oxysterols, vitamin D, and finally of the end-product cholesterol and its derivates bile acids and steroid hormones.[26] Cholesterol is a major component of membranes and lipid rafts and is produced in significant amounts by the fetus itself.[51] Insufficient amounts and altered membrane composition could impair fetal development. Greenberg dysplasia could even feature a modified hedgehog pathway, as a result of cholesterol modification. Hedgehog proteins are modified by cholesterol.[52] Altered hedgehog signaling was shown in other diseases of the post-squalene pathway[35] and mutations in genes of the hedgehog pathway cause a number of skeletal defects. These defects include brachydactyly and polydactyly that are also seen in Greenberg dysplasia. Impaired vitamin D metabolism might be another potential effector in Greenberg dysplasia since LBR affects a step upstream of the vitamin D precursor 7-dehydrocholesterol. Vitamin D is essential for bone development. Vitamin D is produced in significant amounts in the placenta and the fetus itself. Though to our knowledge, whether or not there is de novo synthesis of vitamin D in the fetus is not entirely clear; however, at least locally such synthesis might be possible. There are overlapping pathophysiologic and histologic findings in Greenberg dysplasia, rickets in children, and osteomalacia in adults. Skeletal mineralization depends on the presence of sufficient amounts of calcium and phosphate at the sites of mineralization. Furthermore, chondrocytes, osteoblasts and collagen matrix must position and function properly. Mineralization occurs in chondrocytes. If osteoblasts produce more matrix than the chondrocytes can mineralize, rickets or osteomalacia can develop. Similar mechanisms could be operative in a very early stage of skeletal development in Greenberg dysplasia. The imbalance could either be due to absence or mal-position of calcium by vitamin D deficiency or by abnormal chondrocyte function. In addition, rickets show inadequate mineralization of the chondrocyte matrix in the growth plates. In both rickets and Greenberg dysplasia there is a disorganization or complete failure of chondrocytes to form chondrocyte columns. Epiphyses are stippled, growth of long bones is impaired in both conditions. Osteomalacia is also seen in neurofibromatosis and as a complication of anticonvulsive therapy.[53]

quality could affect farnesylation, oxysterols, steroid hormones, bile acids, vitamin D, hedgehog signaling, modification of other nuclear components as well as cytoplasmatic and nuclear lipid signaling.[26,35-37] These effects and alteration of the structural and metabolic function of cholesterol itself are all possible participants in the disease process.

The other sterol reductases of the postsqualene synthesis reside and act in the cytoplasm. We showed that the lamin B receptor is not only present in the nucleus but also exhibits an extensive presence in cytoplasmatic structures. The lamin B receptor has been so far viewed as a protein of the inner nuclear membrane. In contrast, fibroblasts showed in addition to the nuclear localization an extensive lamin B receptor staining in cytoplasmatic compartments (shown for three different LBR antibodies). This could either be due to a functional demand of cholesterol synthesis in certain cell types. Alternatively, cells with higher LBR expression levels might exceed the nuclear binding capacity for the lamin B receptor.[38] However, the abnormal sterol metabolite in Greenberg dysplasia was initially identified in fibroblasts that were grown in lipid depletion, forcing endogenous cholesterol synthesis.[18] Since fibroblasts show both this feature of sterol synthesis and this exceptional extranuclear localization of LBR, the lamin B receptor is likely to participate in cytoplasmatic cholesterol synthesis. Further, we demonstrated partial colocalization with the endoplasmatic reticulum membrane-protein calnexin. These findings are in agreement with the cytoplasmatic localization of other sterol reductases and the endogeneous cholesterol synthesis in the ER.[5] LBR localized to cytoplasmatic structures in significant amounts especially in certain cell types such as skin fibroblasts and bone-related cells, indicating the potential and probably the in vivo need for a de-novo endogeneous sterol synthesis.

We further showed that LBR is expressed in critical times and tissues of prenatal development in mice, corresponding to the predominant phenotypic defects skeletal dysplasia and edema seen in Greenberg fetuses. At mouse embryonic day 12.5 and 15.5 Lbr is present at RNA or protein level, respectively, in skin, epithelia of lung and midgut, liver as the organ of major fetal hematopoiesis but also in brain and distinct regions of skeletal development. Lbr expression in cartilage is pronounced in all growth plate chondrocytes and also present in osteoblasts forming the primary cortex. This is consistent with the histologic changes in bones from Greenberg fetuses such as disorganization or lack of chondrocyte columns, lack of growth plates, abrupt transition from cartilage to bone and premature excessive ossification of the diaphysic bone collar. These histologic changes were found, to our knowledge, in all histologically analyzed fetuses with Greenberg dysplasia,[18,19,21-25,28,39] and were also found in our fetuses. The expression pattern we document for the embryonic and postnatal mouse in combination with our finding that human osteoclasts and osteoblast-like cells (HOS) also strongly express *LBR*, indicate that the lamin B receptor is involved in cartilage and bone development in both human and mouse.

Complete loss or functional loss of LBR as a sterol reductase is developmentally lethal in humans whereas trace amounts might enable survival. We described a patient earlier with a homozygous *LBR* mutation, IVS12-5-10del, where the intronic deletion almost completely abolished normal splicing with subsequent skipping of exon 13, frameshift, and a premature stop codon.[15] However, the splicing defect was not complete. Trace amounts of normally spliced mRNA and normal protein could be shown. This patient clearly had homozygous Pelger manifestations with round neutrophil nuclei, indicating that there was an almost 100% penetrance of this mutation with respect to the structural function. However, with respect to sterol metabolism, even these tiny amounts of normal LBR seemed to have been sufficient to permit survival. This patient had mild mental retardation, brachydactyly due to shortened metacarpals, and a cardiac defect[15] all far less severe phenotypes than observed in Greenberg dysplasia. The findings in this Pelger patient and the presented Greenberg cases suggest that minimal amounts of functional LBR are essential for human fetal development and survival.

Complete loss of LBR is lethal in humans but not necessarily in mice. Lbr deficiency in mice (ic/ic) presents with severe skin alterations (alopecia and ichthyosis), a Pelger blood phenotype, growth deficit, increased perinatal death, variable syndactyly, and hydrocephalus.[7,17,40] Wassif et al. analyzed sterol metabolism in Lbr deficient mice bred on different backgrounds and identified a sterol defect only on specific backgrounds and at a defined point of development in the brain.[27] They concluded that the phenotype in Greenberg dysplasia and ichthyosis is more likely to be caused by altered nuclear structure than by sterol metabolism. Based on our finding that *LBR* missense mutations affected the sterol metabolism but not the nuclear morphology and that no additional mutation in *DHCR7* or *TM7SF2* were found, we conclude that in humans the sterol defect of the lamin B receptor is pathogenic for Greenberg dysplasia.

Manifestations in response to homozygous failure of the lamin B receptor differ between species. Complete lamin B receptor deficiency seems to be not compatible with life in humans, shows a severe phenotype in mice but is tolerated by Drosophila.[41] Drosophila Lbr is evolutionary not highly conserved and lacks sterol reductase activity,[41] probably because cholesterol is an essential nutrient in flies not requesting an endogenous cholesterol synthesis. There is no explanation yet for the different phenotypes of LBR deficiency in man and mice; hypotheses include variations in cholesterol synthesis, transport or placental transfer. Phenotypic differences between human and mice are also seen in defects of other components of cholesterol synthesis. Thus, 3β-hydroxysteroid dehydrogenase defects cause limb defects in humans (CHILD syndrome) but not in Bpa mice.[26]

In humans, the fetal deaths in Greenberg dysplasia and severe skeletal defects in other cholesterol synthesis disorders underscore the importance of normal sterol synthesis for intrauterine development. This is of relevance for considering potential teratogenic side effects of lipid lowering drugs but also of antimicrobial agents that often target sterol synthesis.[42-45]

We conclude that LBR missense mutations in the transmembrane domain can abolish sterol reductase activity, thereby causing lethal Greenberg dysplasia but not Pelger anomaly. This finding separates the metabolic from the structural function of

LBR and indicates that its sterol reductase function is essential for intrauterine development in humans.

Material and Methods

Patients. We studied three fetuses with the clinical diagnosis of Greenberg dysplasia. The Charité University Medicine ethics committee approved the study. Written, informed consent was obtained from all participants or their legal representatives. Sterol analyses for cholesta-8,14-dien-3β-ol was performed from fetal material (liver or muscle) as published in Offiah et al.[25]

Sequence analyses. We sequenced all exons including the flanking intron regions of the *LBR* gene (NM_002296.2) as described previously[15] in either the fetus or the parents as obligate heterozygous carriers. All mutations were tested for correct segregation in the patient's families (where available). We further analyzed 300 control chromosomes to exclude a previously undescribed polymorphism. To explore the functional effect of missense mutations, we proved the evolutionary conservation of the affected residues by BLAST alignment and interspecies comparison. We sequenced additionally all coding exons of the genes encoding the two other members of the C14 sterol reductases family, *DHCR7* (NM_001360.2) and *TM7SF2* (NM_003273.2), respectively. Primer sequences are available on request.

C14 deficient yeast complementation assay. C14 sterol reductase deficient yeast has a defect of ERG24, resulting in abnormal sterol metabolism and consequent failure to grow (Suppl. Fig. 2). ERG24 belongs to the same C14 sterol reductase family as the lamin B receptor. Human wildtype LBR rescues the ERG24 deficiency in yeast.[5,30] We therefore tested whether or not human LBR carrying the missense mutations rescued the yeast phenotype.

Vectors p1023 (hsLBR_wt) and p1032 (empty) were kindly donated by Gerard Loison. We introduced the missense mutations p.N547D and p.R583Q by mutagenesis following the manufacturer's instructions (QuikChange® XL Site-directed Mutagenesis Kit, Stratagene). ERG24, wild type LBR, LBR_N547D and LBR_R583Q were each cloned in the yeast expression vector pEMR1032. We performed all analyses under the control of two different promoters (*PGK1* and *TP1*) to ensure that the rescue deficit of mutants is not due to chance variations in vector insertion or promoter activity.

ERG24 deficient yeast *Saccharomyces cerevisiae* BY4742*erg24* (Y11164) and the corresponding reference strain *S. cerevisiae* BY4742 (Y10000) were obtained from Euroscarf (Frankfurt, Germany). Transformation, expression and sterol analysis in yeast were performed as previously described.[30,46] We replicated all measurements in at least two independent experiments and in 2 different colonies per transformation.

To confirm expression of LBR in the yeast transformants we prepared 1 ml from log phase cultures. We pelleted ~3 x 10^8 cells, resuspended in 100 µl distilled water, added 100 µl 0.2 M NaOH and vortexed for 5 min at room temperature. We pelleted the solution at 14,000 rpm for 2 min and resuspended in 50 µl 2x LDS buffer with 10% β-mercaptoethanol. After boiling for 3 min and pelleting, the samples were processed as previously described.[15] Human wildtype LBR and both mutants showed the same expression pattern in western blot indicating that transfection efficiency was comparable (data not shown).

Used LBR antibodies. The most widely used LBR antibody, the guinea pig polyclonal anti-LBR antibody (gp-anti-LBR_N-term) is directed to the first 210 aminoacids of LBR and was kindly provided by Harald Herrmann-Lerdon.[15] The specificity of this antibody was shown in Shultz and co-workers: Immunostaining and immunoblot of Lbr deficient cells showed no background staining by the LBR antibody.[17] The rabbit monoclonal anti-LBR antibody (rb-anti-LBR_N-term) is also directed against the N-terminus of human LBR (Epitomics, Burlingame, CA, catalogue number 1398-1). The mouse monoclonal anti-LBR antibody (mouse-anti-LBR_C-term) is directed against the C-terminal domain of LBR (klh-19, kindly provided by Harald Herrmann-Lerdon).

Immunostaining in human fibroblasts. Human dermal fibroblasts were cultivated in Dulbecco's Modified Eagle Medium (Lonza, Basel, Switzerland) with 10% fetal calf serum (FCS) and 2 mM L-glutamine. Cells were grown on coverslips, fixed in 4% paraformaldehyde in 1x phosphate buffered saline (PBS) for 10 min at 4°C, then blocked for 30 min with 10% bovine serum albumine (BSA) in PBS, incubated for 1 h with polyclonal gp-anti-LBR_N-term (1:100 dilution) followed by an 1 h incubation with the secondary antibody (Alexa 555-conjugated goat anti-guinea pig antibody, Molecular Probes, 1:1,000) and DAPI (Sigma, 1:1,000). Cells were mounted with Fluoromount G (Southern Biotech) and imaged using an LSM 510 meta microscope (Carl Zeiss, Göttingen, Germany) with a x63 Plan Apochromat oil immersion objective.

Nuclear extraction and immunoblotting. Nuclear and cytosolic fractions of whole cell lysates of skin fibroblasts were extracted by the Nuclear-Extraction Kit (Cayman Chemicals) and resolved by electrophoresis in SDS poly-acrylamide gels. The following antibodies were used for immunoblot analysis on PVDF membranes: as described above the polyclonal gp-anti-LBR_N-term, monoclonal rb-anti-LBR_N-term, monoclonal mouse-anti-LBR_C-term, further a rabbit polyclonal calnexin antibody (catalogue number GTX13504, Acris Antibodies, Herford, Germany), a mouse monoclonal alpha-tubulin antibody (ab7291, abcam, Cambridge, USA), and a mouse monoclonal anti-lamin B2 antibody (clone X223, catalogue number 65147C, Progen, Heidelberg, Germany). All immune reactions were carried out in 10 mM Tris-HCl, pH 8.0, 150 mM NaCl, 0.05% Tween-20 (TBST) with 5% dried milk at RT with washing steps in TBST.

Quantitative PCR (qPCR). We studied *LBR* mRNA levels in different human cell lines and mouse tissues from postnatal day four. Following lysis with Trizol® and standard phenol/chloroform RNA extraction, total cDNA was transcribed by RevertAid™ H Minus First Strand cDNA Synthesis Kit (Fermentas). For qPCR on ABI Prism 7500 (Applied Biosystems Foster City US) we mixed cDNA, CyberGreen (Invitrogen), and primers. We analyzed the data using the ABI Prism SDS Software package (ΔΔCt method, normalisation against GAPDH). Primer sequences are available on request.

In-situ hybridization. We generated probes for *Lbr* by RT-PCR from mouse E14.5 whole cDNA. Primer sequences are available on request. Antisense riboprobes were transcribed with SP6 or T7 polymerase using the Roche Dig-RNA labeling kit according to the manufacturer's instructions. Protocols for whole-mount in-situ hybridizations and in-situ hybridizations on paraffin sections have been previously described.[47,48]

Immunostaining in mouse embryos (paraffin sections). For immunostaining, paraffin sections were deparaffinized, rehydrated and boiled for 10 minutes in 0.01 M Sodium citrate pH 6.0. Sections were blocked in 10% goat serum for 1 h, primary antibodies (1:100 polyclonal guinea pig anti-LBR_N-term, generated by Monika Zwerger, initially described in;[40] 1:100 rabbit anti-Sox9, Santa Cruz) were applied in 5% goat serum at 4°C over night. Secondary antibodies (goat anti-guinea pig-Alexa Fluor 546, goat anti-rabbit Alexa Fluor 488, Molecular Probes, 1:1,000, together with DAPI, 1:2,000) were applied for 1 h at room temperature. Sections were analyzed using an Axiovert 200 (Zeiss) equipped with ApoTome optical section device and AxioVision software.

Web Resources

1. Basic Local Alignment Search Tool (BLAST), http://blast.ncbi.nlm.nih.gov/Blast.cgi
2. Ensembl Genome Browser, www.ensembl.org/
3. GenBank, www.ncbi.nlm.nih.gov/Genbank/
4. Online Mendelian Inheritance in Man (OMIM), www.ncbi.nlm.nih.gov/Omim/
5. National Center for Biotechnology Information (NCBI), www.ncbi.nlm.nih.gov

Acknowledgements

We thank the patients and their families. We thank Gerard Loison and Georg Krohne for providing LBR vectors. We appreciate the technical assistance provided by Catrin Janetzki and Dominik Seelow. Friedrich C. Luft, Tom H. Lindner, Ada Olins, Don Olins and Eddy Rubin critically read the manuscript. The Deutsche Forschungsgemeinschaft (DFG, SFB 577, project A4) supported K.H., who also received a Rahel Hirsch fellowship from the Charité Medical Faculty.

This paper is dedicated to Prof. Dr. Dietmar Müller on the occasion of his "retirement" and in recognition of his significant contribution to the identification of the PHA gene.

Note

Supplementary materials can be found at: www.landesbioscience.com/supplement/ClaytonNUC1-4-Sup.pdf

References

1. Courvalin JC, Segil N, Blobel G, Worman HJ. The lamin B receptor of the inner nuclear membrane undergoes mitosis-specific phosphorylation and is a substrate for p34cdc2-type protein kinase. J Biol Chem 1992; 267:19035-8.
2. Ye Q, Callebaut I, Pezhman A, Courvalin JC, Worman HJ. Domain-specific interactions of human HP1-type chromodomain proteins and inner nuclear membrane protein LBR. J Biol Chem 1997; 272:14983-9.
3. Mattout-Drubezki A, Gruenbaum Y. Dynamic interactions of nuclear lamina proteins with chromatin and transcriptional machinery. Cell Mol Life Sci 2003; 60:2053-63.
4. Schuler E, Lin F, Worman HJ. Characterization of the human gene encoding LBR, an integral protein of the nuclear envelope inner membrane. J Biol Chem 1994; 269:11312-7.
5. Holmer L, Pezhman A, Worman HJ. The human lamin B receptor/sterol reductase multigene family. Genomics 1998; 54:469-76.
6. Witsch-Baumgartner M, Loffler J, Utermann G. Mutations in the human DHCR7 gene. Hum Mutat 2001; 17:172-82.
7. Bennati AM, Castelli M, Della Fazia MA, Beccari T, Caruso D, Servillo G, et al. Sterol dependent regulation of human TM7SF2 gene expression: role of the encoded 3beta-hydroxysterol Delta14-reductase in human cholesterol biosynthesis. Biochim Biophys Acta 2006; 1761:677-85.
8. Burke B, Stewart CL. Life at the edge: the nuclear envelope and human disease. Nat Rev Mol Cell Biol 2002; 3:575-85.
9. Eriksson M, Brown WT, Gordon LB, Glynn MW, Singer J, Scott L, et al. Recurrent de novo point mutations in lamin A cause Hutchinson-Gilford progeria syndrome. Nature 2003; 423:293-8.
10. Mounkes LC, Kozlov S, Hernandez L, Sullivan T, Stewart CL. A progeroid syndrome in mice is caused by defects in A-type lamins. Nature 2003; 423:298-301.
11. Gruenbaum Y, Margalit A, Goldman RD, Shumaker DK, Wilson KL. The nuclear lamina comes of age. Nat Rev Mol Cell Biol 2005; 6:21-31.
12. Shumaker DK, Dechat T, Kohlmaier A, Adam SA, Bozovsky MR, Erdos MR, et al. Mutant nuclear lamin A leads to progressive alterations of epigenetic control in premature aging. Proc Natl Acad Sci USA 2006; 103:8703-8.
13. Capell BC, Collins FS. Human laminopathies: nuclei gone genetically awry. Nat Rev Genet 2006; 7:940-52.
14. Worman HJ, Bonne G. "Laminopathies": a wide spectrum of human diseases. Exp Cell Res 2007; 313:2121-33.
15. Hoffmann K, Dreger CK, Olins AL, Olins DE, Shultz LD, Lucke B, et al. Mutations in the gene encoding the lamin B receptor produce an altered nuclear morphology in granulocytes (Pelger-Huet anomaly). Nat Genet 2002; 31:410-4.
16. Hoffmann K, Sperling K, Olins AL, Olins DE. The granulocyte nucleus and lamin B receptor: avoiding the ovoid. Chromosoma 2007; 116:227-35.
17. Shultz LD, Lyons BL, Burzenski LM, Gott B, Samuels R, Schweitzer PA, et al. Mutations at the mouse ichthyosis locus are within the lamin B receptor gene: a single gene model for human Pelger-Huet anomaly. Hum Mol Genet 2003; 12:61-9.
18. Waterham HR, Koster J, Mooyer P, Noort Gv G, Kelley RI, Wilcox WR, et al. Autosomal recessive HEM/Greenberg skeletal dysplasia is caused by 3 beta-hydroxysterol delta 14-reductase deficiency due to mutations in the lamin B receptor gene. Am J Hum Genet 2003; 72:1013-7.
19. Greenberg CR, Rimoin DL, Gruber HE, DeSa DJ, Reed M, Lachman RS. A new autosomal recessive lethal chondrodystrophy with congenital hydrops. Am J Med Genet 1988; 29:623-32.
20. Spranger J, Maroteaux P. The lethal osteochondrodysplasias. Adv Hum Genet 1990; 19:1-103.
21. Chitayat D, Gruber H, Mullen BJ, Pauzner D, Costa T, Lachman R, et al. Hydrops-ectopic calcification-moth-eaten skeletal dysplasia (Greenberg dysplasia): prenatal diagnosis and further delineation of a rare genetic disorder. Am J Med Genet 1993; 47:272-7.
22. Horn LC, Faber R, Meiner A, Piskazeck U, Spranger J. Greenberg dysplasia: first reported case with additional non-skeletal malformations and without consanguinity. Prenat Diagn 2000; 20:1008-11.
23. Trajkovski Z, Vrcakovski M, Saveski J, Gucev ZS. Greenberg dysplasia (hydrops-ectopic calcification-moth-eaten skeletal dysplasia): prenatal ultrasound diagnosis and review of literature. Am J Med Genet 2002; 111:415-9.
24. Oosterwijk JC, Mansour S, van Noort G, Waterham HR, Hall CM, Hennekam RC. Congenital abnormalities reported in Pelger-Huet homozygosity as compared to Greenberg/HEM dysplasia: highly variable expression of allelic phenotypes. J Med Genet 2003; 40:937-41.
25. Offiah AC, Mansour S, Jeffrey I, Nash R, Whittock N, Pyper R, et al. Greenberg dysplasia (HEM) and lethal X linked dominant Conradi-Hunermann chondrodysplasia punctata (CDPX2): presentation of two cases with overlapping phenotype. J Med Genet 2003; 40:129.
26. Herman GE. Disorders of cholesterol biosynthesis: prototypic metabolic malformation syndromes. Hum Mol Genet 2003; 12:75-88.
27. Wassif CA, Brownson KE, Sterner AL, Forlino A, Zerfas PM, Wilson WK, et al. HEM dysplasia and ichthyosis are likely laminopathies and not due to 3beta-hydroxysterol Delta14-reductase deficiency. Hum Mol Genet 2007; 16:1176-87.
28. Konstantinidou A, Karadimas C, Waterham HR, Superti-Furga A, Kaminopetros P, Grigoriadou M, et al. Pathologic, radiographic and molecular findings in three fetuses diagnosed with HEM/Greenberg skeletal dysplasia. Prenat Diagn 2008; 28:309-12.
29. Worman HJ, Courvalin JC. Nuclear envelope, nuclear lamina and inherited disease. Int Rev Cytol 2005; 246:231-79.
30. Silve S, Dupuy PH, Ferrara P, Loison G. Human lamin B receptor exhibits sterol C14-reductase activity in *Saccharomyces cerevisiae*. Biochim Biophys Acta 1998; 1392:233-44.
31. Ma Y, Cai S, Lv Q, Jiang Q, Zhang Q, Sodmergen, et al. Lamin B receptor plays a role in stimulating nuclear envelope production and targeting membrane vesicles to chromatin during nuclear envelope assembly through direct interaction with importin beta. J Cell Sci 2007; 120:520-30.

32. De Brasi D, Esposito T, Rossi M, Parenti G, Sperandeo MP, Zuppaldi A, et al. Smith-Lemli-Opitz syndrome: evidence of T93M as a common mutation of delta7-sterol reductase in Italy and report of three novel mutations. Eur J Hum Genet 1999; 7:937-40.
33. Fitzky BU, Witsch-Baumgartner M, Erdel M, Lee JN, Paik YK, Glossmann H, et al. Mutations in the Delta7-sterol reductase gene in patients with the Smith-Lemli-Opitz syndrome. Proc Natl Acad Sci USA 1998; 95:8181-6.
34. Wassif CA, Maden C, Kachilele-Linjewile S, Lin D, Linck LM, Connor WE, et al. Mutations in the human sterol delta7-reductase gene at 11q12-13 cause Smith-Lemli-Opitz syndrome. Am J Hum Genet 1998; 63:55-62.
35. Cooper MK, Wassif CA, Krakowiak PA, Taipale J, Gong R, Kelley RI, et al. A defective response to Hedgehog signaling in disorders of cholesterol biosynthesis. Nat Genet 2003; 33:508-13.
36. Chamoun Z, Mann RK, Nellen D, von Kessler DP, Bellotto M, Beachy PA, et al. Skinny hedgehog, an acyltransferase required for palmitoylation and activity of the hedgehog signal. Science 2001; 293:2080-4.
37. Gondre-Lewis MC, Petrache HI, Wassif CA, Harries D, Parsegian A, Porter FD, et al. Abnormal sterols in cholesterol-deficiency diseases cause secretory granule malformation and decreased membrane curvature. J Cell Sci 2006; 119:1876-85.
38. Soullam B, Worman HJ. The amino-terminal domain of the lamin B receptor is a nuclear envelope targeting signal. J Cell Biol 1993; 120:1093-100.
39. Madazli R, Aksoy F, Ocak V, Atasu T. Detailed ultrasonographic findings in Greenberg dysplasia. Prenat Diagn 2001; 21:65-7.
40. Cohen TV, Klarmann KD, Sakchaisri K, Cooper JP, Kuhns D, Anver M, et al. The lamin B receptor under transcriptional control of C/EBPepsilon is required for morphological but not functional maturation of neutrophils. Hum Mol Gen 2008; 17:2921-33.
41. Wagner N, Weber D, Seitz S, Krohne G. The lamin B receptor of *Drosophila melanogaster*. J Cell Sci 2004; 117:2015-28.
42. Kolf-Clauw M, Chevy F, Ponsart C. Abnormal cholesterol biosynthesis as in Smith-Lemli-Opitz syndrome disrupts normal skeletal development in the rat. J Lab Clin Med 1998; 131:222-7.
43. Roux C, Wolf C, Mulliez N, Gaoua W, Cormier V, Chevy F, et al. Role of cholesterol in embryonic development. Am J Clin Nutr 2000; 71:1270-9.
44. Lorand T, Kocsis B. Recent advances in antifungal agents. Mini Rev Med Chem 2007; 7:900-11.
45. Parker JE, Merkamm M, Manning NJ, Pompon D, Kelly SL, Kelly DE. Differential azole antifungal efficacies contrasted using a *Saccharomyces cerevisiae* strain humanized for sterol 14 alpha-demethylase at the homologous locus. Antimicrob Agents Chemother 2008; 52:3597-603.
46. Veen M, Stahl U, Lang C. Combined overexpression of genes of the ergosterol biosynthetic pathway leads to accumulation of sterols in *Saccharomyces cerevisiae*. FEMS Yeast Res 2003; 4:87-95.
47. Hoffmann K, Muller JS, Stricker S, Megarbane A, Rajab A, Lindner TH, et al. Escobar syndrome is a prenatal myasthenia caused by disruption of the acetylcholine receptor fetal gamma subunit. Am J Hum Genet 2006; 79:303-12.
48. Stricker S, Verhey van Wijk N, Witte F, Brieske N, Seidel K, Mundlos S. Cloning and expression pattern of chicken Ror2 and functional characterization of truncating mutations in Brachydactyly type B and Robinow syndrome. Dev Dyn 2006; 235:3456-65.
49. Moebius FF, Fitzky BU, Glossmann H. Genetic defects in postsqualene cholesterol biosynthesis. Trends Endocrinol Metab 2000; 11:106-14.
50. Waterham HR. Defects of cholesterol biosynthesis. FEBS Lett 2006; 580:5442-9.
51. McConihay JA, Horn PS, Woollett LA. Effect of maternal hypercholesterolemia on fetal sterol metabolism in the Golden Syrian hamster. J Lipid Res 2001; 42:1111-9.
52. Porter JA, Young KE, Beachy PA. Cholesterol modification of hedgehog signaling proteins in animal development. Science 1996; 274:255-9.
53. Fauci AS, Kasper DL, Braunwald E, Hauser SL, Longo DL, Jameson JL, et al. Harrison's Principles of Internal Medicine. McGraw-Hill Professional 2008.

Mein Lebenslauf wird aus datenschutzrechtlichen Gründen in der elektronischen Version meiner Arbeit nicht veröffentlicht.

5. Publikationsliste

1. **Baasanjav S**, Al-Gazali L, Hashiguchi T, Mizumoto S, Fischer B, Horn D, Seelow D, Ali BR, Aziz S A.A, Langer R,. Saleh A A.H, Becker C, Nürnberg G, Cantagrel V, Gleeson JG, Gomez D, Michel JB, Stricker S, Lindner TH, Nürnberg P, Sugahara K, Mundlos S, Hoffmann K. Faulty initiation of proteoglycan synthesis causes cardiac and joint defects. Am J Hum Genet 89: 1-13, 2011

2. **Baasanjav S**, Jamsheer A, Kolanczyk M, Horn D, Latos T, Hoffmann K, Latos-Bielenska A, Mundlos S. Osteopoikilosis and multiple exostoses caused by novel mutations in *LEMD3* and *EXT1* genes respectively--coincidence within one family. BMC Med Genet 11: 110, 2010

3. Clayton P, Fischer B, Mann A, Mansour S, Rossier E, Veen M, Lang C, **Baasanjav S**, Kieslich M, Brossuleit K, Gravemann S, Schnipper N, Karbasy-ian M, Demuth I, Zwerger M, Vaya A, Utermann G, Mundlos S, Stricker S, Sperling K and Hoffmann K. Mutations causing Greenberg dysplasia but not Pelger anomaly uncouple enzymatic from structural functions of a nuclear membrane protein. Nucleus 1:4, 354-366, 2010

4. Lindner TH, **Baasanjav S**, Kollert A, Amann K, Mihatsch MJ, Eckardt KU and n Hoffmann K. An unknown form of autosomal−dominant glomerulocystic kidney disease with a unique phenotype, TH−PO065, Annual Meeting of the American Society of Nephrology, ASN 2008 (Poster)

5. Graul-Neumann LM, Kienitz T, Robinson PN, **Baasanjav S**, Karow B, Gillessen-Kaesbach G, Fahsold R, Schmidt H, Hoffmann K and Passarge E. Marfan Syndrome with Neonatal Progeroid Syndrome-Like Lipodystrophy Associated with a Novel Frameshift Mutation at the 3` Terminus of the FBN1-Gene. Am J Med Genet Part A 152A:2749-2755, 2010

6. Danksagung

Am Zustandekommen dieser Dissertation bzw. der ihr zugrunde liegenden Publikationen waren zahlreiche Kolleginnen und Kollegen beteiligt. Unter Ihnen möchte ich folgende Personen besonders hervorheben:

Herrn Prof. Dr. med. Stefan Mundlos und Frau Prof. Dr. med. Katrin Hoffmann möchte ich für die Vergabe des Dissertationsthemas und für die hervorragende wissenschaftliche Betreuung der Arbeit, ohne welche die Erstellung dieser Dissertation nicht möglich gewesen wäre, herzlich danken. Mein großer Dank gilt ihren wertvollen Anregungen und ihrer Bereitschaft, Fragestellungen zu diskutieren und zu kommentieren.

Bjoern Fischer, Mateusz Kolanczyk, Dominik Seelow und allen meinen Kollegen vom Institut für Medizinische Genetik und Humangenetik an der Charité möchte ich meinen besonderen Dank für die unermüdliche Unterstützung und die geduldige Anleitung bei den Experimenten aussprechen.